SUPPLEMENTARY MATERIALS

The Draft Genome of the Globally Widespread and Invasive Argentine ant (*Linepithema humile*)

Table of Contents

AFFILIATIONS & ROLES IN PROJECT

Christopher D. Smith[a*], Aleksey Zimin[b], Carson Holt[c], Ehab Abouheif[d], Richard Benton[e], Elizabeth Cash[f], Vincent Croset[e], Cameron R. Currie[g,h], Eran Elhaik[i], Christine G. Elsik[j], Marie-Julie Fave[d], Vilaiwan Fernandez[d], Jürgen Gadau[f], Joshua D. Gibson[f], Dan Graur[k], Kirk J. Grubbs[f], Darren E. Hagen[j], Martin Helmkampf[f], Jo-Anne Holley[l], , Hao Hu[c], Ana Sofia Ibarraran Viniegra[d], Brian R. Johnson[m], Reed M. Johnson[l], Abderrahman Khila[d], Jay W. Kim[a], Joseph Laird[l], Kaitlyn A. Mathis[m], Joseph A. Moeller[g,h], Monica C. Munoz-Torres[j], Marguerite C. Murphy[n], Rin Nakamura[a], Surabhi Nigam[n], Rick P. Overson[f], Jennifer E. Placek[a], Rajendhran Rajakumar[d], Justin T. Reese[j], Hugh M. Robertson[l,o], Chris R. Smith[p], Andrew V. Suarez[l,o], Garret Suen[g,h], Elissa L. Suhr[l], Shu Tao[j], Candice W. Torres[m], Ellen van Wilgenburg[m], Lumi Viljakainen[q], Kimberly K. O. Walden[l], Alexander L. Wild[l], Mark D. Yandell[c], James A. Yorke[r], Neil D. Tsutsui[m*]

[a]Department of Biology, San Francisco State University, San Francisco, CA 94132; [b]Institute for Physical Science and Technology, University of Maryland, College Park, MD 20742; [c]Department of Human Genetics, Eccles Institute of Human Genetics, University Utah and School of Medicine, Salt Lake City, UT 84112; [d]McGill University, Department of Biology, 1205 Avenue Dr. Penfield, Montreal, Quebec, Canada, H3A 1B1; [e]Center for Integrative Genomics, Genopode Bldg., University of Lausanne, CH-1015 Lausanne, Switzerland; [f]School of Life Sciences, Arizona State University, Tempe, AZ 85287; [g]Department of Bacteriology, University of Wisconsin-Madison, Madison WI 53706; ; [h]DOE Great Lakes Bioenergy Research Center, University of Wisconsin-Madison, Madison, WI 53706; [i]The Johns Hopkins University School of Medicine, Baltimore, MD 21205; [j]Department of Biology, Georgetown University, Washington, DC 20057; [k]Department of Biology and Biochemistry, University of Houston, Houston, Texas 77204; [l]Department of Entomology, University of Illinois at Urbana-Champaign, Urbana, IL 61801; [m]Department of Environmental Science, Policy and Management, UC Berkeley, Berkeley, CA 94720-3114; [n]Department of Computer Science, San Francisco State University, San Francisco, CA 94132; [o]Institute of Genomic Biology, University of Illinois, Urbana 61801; [p]Department of Biology, Earlham College, Richmond, IN 47374; [q]Department of Molecular Biology and Genetics, Cornell University, NY; [r]Department of Mathematics, University of Maryland, College Park, MD 20742.

Project Coordination and Writing of Main Text:

Christopher D. Smith[a], Neil D. Tsutsui[m]

Sample Handling, Transcriptome & Genomic DNA Sequencing:

Hugh M. Robertson[l,o], Christopher D. Smith[a], Neil D. Tsutsui[m]

Assembly:

James A. Yorke[r], Aleksey Zimin[b], Christopher D. Smith[a]

Automated Annotation:

Mark Yandell[c], Carson Holt[c], Hao Hu[c]

Gene Ontology, Inteproscan, & KEGG Analyses:

Jennifer E. Placek[a], Christopher D. Smith[a]

Cytoplasmic Ribosomal Protein Genes:

Martin Helmkampf[f]

Oxidative Phosphorylation Genes:

Joshua D. Gibson[d]

Repetitive Elements:

Jay W. Kim[a], Christopher D. Smith[a]

Chemoreceptor Genes:

Hugh Robertson[l,o] Jo-Anne Holley[l], Elisssa L. Suhr[l], Andrew V. Suarez[l,o] Kimberly K. O. Walden[l], Alexander L. Wild[l], Vincent Croset[e], Richard Benton[e]

P450 Genes:

Reed Johnson[l]

Olfactory Learning and Memory:

Kaitlyn Mathis[m], Brian R. Johnson[m], Candice W. Torres[m]

Opsins and Circadian Genes:

Neil D. Tsutsui[m]

Immune Genes:

Lumi Viljakainen[q], Kirk J. Grubbs[f]

Behavior and Aggression Genes:

Candice W. Torres[m], Rin Nakamura[a]

Hox Genes:

Monica C. Munoz-Torres[j], Darren Hagen[j], Christine G. Elsik[j]

Global Compositional Analysis:

Eran Elhaik[i], Justin T. Reese[j], Dan Graur[k], Christine G. Elsik[j]

DNA Methylation Toolkit:

Chris R. Smith[p]

RNAi Pathway Genes:

Shu Tao[j], Monica C. Munoz-Torres[j], Jennifer E. Placek[a], Christopher D. Smith[a], Christine G. Elsik[j]

MicroRNAs:

Darren E. Hagen[j], Christine G. Elsik[j]

Wing Polyphenism and Reproductive Division of Labor:

Ehab Abouheif[d], Marie-Julie Fave[d], Vilaiwan Fernandes[d], Rajendhran Rajakumar[d], Ana Sofia Ibarraran Viniegra[d], Abderrahman Khila[d]

Candidate Caste Determination Genes:

Chris R. Smith[p], Rajendhran Rajakumar[d], Martin Helmkampf[f], Garret Suen[g,h], Cameron Currie[g,h]

Yellow / Major Royal Jelly Protein Genes:

Rick P. Overson[f], Martin Helmkampf[f]

Desaturase Genes:

Elizabeth Cash[f], Martin Helmkampf[f]

Evolutionary Rate Analysis:

Carson Holt[c], Christopher D. Smith[a]

Earlham College Evolutionary Genomics Class Annotation:

Chris R. Smith[p] et al.

Mitochondrial Genome Assembly:

Joshua D. Gibson[f], Chris R. Smith[p]

SNP Analysis:

Surabhi Nigam[n], Marguerite C. Murphy[n], Christopher D. Smith[a]

Cuticular Hydrocarbon Analysis, Microsatellite genotyping, Behavioral assays:

Ellen van Wilgenburg[m]

Insulin Pathway Genes:

Rajendhran Rajakumar[d], Joseph A. Moeller[g,h], Garret Suen[g,h], Cameron R. Currie[g,h]

SUPPLEMENTARY INFORMATION

Source material

We collected an Argentine ant colony fragment (hereafter "Saratoga") from a residential orchard in Saratoga, Santa Clara County, California, USA (N37º 15' 23.5"; W122º 00' 55.2").

Several lines of evidence confirmed that these ants are members of the large supercolony that dominates California. First, we conducted a genetic analysis of 12 workers at 13 microsatellite loci and estimated the genetic distances to 9 other *L. humile* populations (1). We genotyped 12 workers from the Saratoga at 13 polymorphic microsatellite loci (GenBank Accession numbers AF173164, AF093514, AF093515, AF093517, AF093520, AF093521, AF093522, AF093524, AF093525, AF093526, AF093527, AF093531, and AF093533) (2-4) and estimated the genetic distances of this population to nine other *L. humile* populations (1) according to Nei (5) using the computer program GenAlEx (www.anu.edu.au/BoZo/GenAlEx/) (Table S14). The Saratoga population was genetically most similar to ants in Berkeley, California (Nei distance=0.037) that is part of the large Californian supercolony. Other genetically similar populations were those in Melbourne, Australia and the largest supercolony in Hawaii (Nei distances <0.1). The Saratoga ants were least similar to one of the smaller supercolonies in Hawaii, a supercolony in South Africa and a smaller supercolony from Lake Hodges, La Mesa, California (Nei distances all >0.26).

Table S1. The number and types of sequencing runs performed. The runs using DNA from a single diploid queen pupae and ~100 diploid workers from a single colony in the invasive range. Workers were pooled for a single DNA extraction. The same 3kb and 8kb paired end libraries were used for the 454 and Illumina sequencing.

# runs	Sequencing platform	Paired-end?	Source material
7	454FLX Titanium	No	Single queen pupa
1	454FLX Titanium	Yes; 3kb	~100 workers
1	454FLX Titanium	Yes; 8kb	~100 workers
1	Illumina 84 cycle	No	~100 workers
1	Illumina	Yes; 3kb	~100 workers
1	Illumina	Yes; 8kb	~100 workers
1	454FLX - transcriptome	No	Mixed caste, age, location

Table S14. Genetic comparison (Nei genetic distance) between the sequenced *L. humile* population (Saratoga, CA) and nine other introduced populations.

Pairwise population matrix of Nei Genetic Distance

	SAR	AU	B	F	HB	HR	J	LH	NZ	SA
SAR	0.000									
AU	0.071	0.000								
B	0.037	0.093	0.000							
F	0.110	0.115	0.051	0.000						
HB	0.094	0.150	0.161	0.206	0.000					
HR	0.424	0.423	0.452	0.482	0.356	0.000				
J	0.249	0.136	0.279	0.228	0.203	0.407	0.000			
LH	0.262	0.266	0.312	0.375	0.220	0.081	0.361	0.000		
NZ	0.118	0.094	0.132	0.137	0.164	0.372	0.108	0.280	0.000	
SA	0.314	0.267	0.341	0.442	0.411	0.412	0.454	0.335	0.372	0.000

LEGEND

California, USA

Saratoga (SAR)	37° 15' 24" N	122° 00' 55" W
Berkeley (B)	37° 52' 22" N	122° 15' 52" W
Lake Hodges (LH), La Mesa	33° 3' 45" N	117° 7' 8" W

France

Marseille (F)	43° 29' 80" N	05° 37' 41" W

Australia

Melbourne (AU)	37° 47' 53" N	144° 57' 32" W

New Zealand

Wellington (NZ)	41° 28' 00" N	174° 76' 00" W

Japan

Iwakuni City, Yamaguchi (J)	34°06'15"N	132°12'01"E

Hawaii, USA

Kipuka Nene (HB)	19° 13' 21" N	155° 38' 04" W
KMC (HR)	19° 26' 01" N	155° 16' 25" W

South Africa

Stellenbosch (SA)	33° 3' 45" N	117° 7' 8" W

Second, we performed standard aggression assays (1) to assay the colonymate recognition behavior of the Saratoga ants. We collected *L. humile* workers from three Californian populations; Saratoga, Berkeley (which is part of the large supercolony that dominates California), and Lake Hodges (one of the smaller Californian supercolonies). Live ants were transported to the laboratory and maintained on a diet of sugar water, chicken egg and protein solution (modified LB broth). We performed standard behavioral assays to test for aggression between Saratoga and the other two populations. We observed the behavior of the ants for three minutes and scored the assay as aggressive if the ants showed one or more of the following behaviors; flaring of mandibles, recoil behavior, biting, or grabbing. These assays revealed no aggression between workers of the Saratoga population and the population in Berkeley (0 out of 20 trials). We did, however, find high levels of aggression between the Saratoga population and workers of the smaller supercolony from Lake Hodges, La Mesa, California (17 out of 20 trials).

Finally, we compared the cuticular hydrocarbon profiles of the Saratoga population to the Berkeley population and the smaller Lake Hodges colony (Fig. S17). Cuticular hydrocarbons are substances that are used by Argentine ants to distinguish colonymates from ants that belong to foreign colonies. We extracted cuticular hydrocarbons from individual workers from each of the populations used for the behavioral assays by immersing each ant in 45 mL of hexane for 10 minutes. Each worker's profile was analyzed separately, using gas chromatography and mass spectrometry (GC–MS). To detect quantitative differences in the hydrocarbon patterns of our samples, we injected 1 mL of each sample into an Agilent 7890 GC equipped with a 190915-433 capillary column (30 m X 250 mm X 0.25 X m, Agilent Technologies). We used helium as carrier gas at 1 mL/min, the injector in splitless mode (1 min), and a temperature program of 2 min at 80 °C, to 270 °C at 20 °C/min, then to 310 °C at 3 °C/min (6). Injector temperature was set at 250°C. Electron

Figure S17. Cuticular hydrocarbon profiles of Argentine ant workers from the source location for this genome sequencing project (Saratoga, CA) and two other sites in the location for this genome sequencing project (Saratoga, CA) and two other sites in the introduced California range. Argentine ants at the Berkeley, CA site belong to the large supercolony that occupies the vast majority of the introduced range, whereas the Lake Hodges, CA population is spatially much smaller and is genetically, behaviorally and chemically distinct.

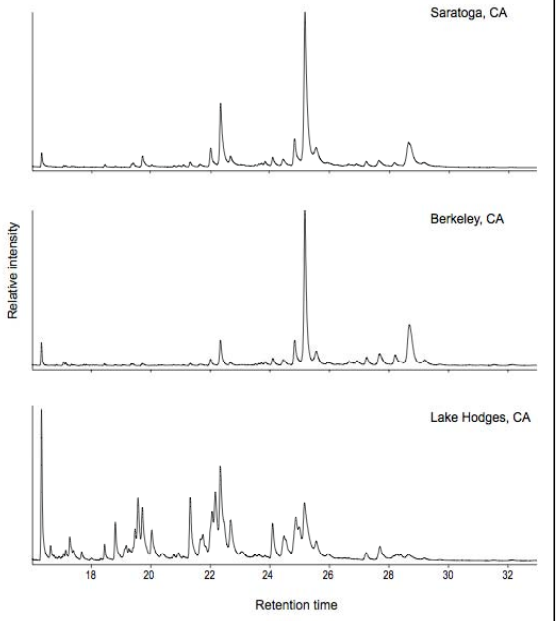

impact mass spectra were obtained with an ionization voltage of 70 eV and a source temperature of 250 °C.

Combined, these data indicate the Saratoga population is part of the large Californian supercolony.

RNA library preparation and EST sequencing

EST sequencing was performed on material from a combination of different castes and life stages: adult workers, queens and males, larvae of mixed age and caste, queen pupae, worker pupae, and RNA from worker heads and antennae (to enrich for behavioral and chemoreception genes)(Table S1). Most of this material was collected from sites belonging to the large California supercolony, but we also generated and sequenced cDNA from workers collected in the native range (Argentina). We extracted and purified the polyA+ RNA using an Ambion MicroPurist RNA kit, reverse transcribed and generated cDNA using the Joint Genome Institute protocol, quantified each extraction separately for each type of source material, then mixed them together prior to sequencing. The cDNA was nebulized and used to generate a 400-800bp library, which was then sequenced using a Roche 454 Genome Sequencer LR70 FLX. This run yielded about 128Mb of DNA sequence. These reads assembled into 20,070 contigs.

Preparation of a 3kb and 8kb paired-end genomic libraries, emulsion-based clonal amplification and sequencing on the 454 Genome Sequencer FLX-Titanium system were performed according to the manufacturer's instructions (454 Life Sciences, Branford, CT). Each library was sequenced on one GS-Titanium 70x75 picotiter plate. Signal processing and base calling were performed using the bundled 454 Data Analysis Software version 2.0.00. The sequencing of the 3kb and 8kb paired-end genomic libraries

produced a total of 1,206,954 and 1,400,165 reads with average read-lengths of 382bp and 386bp, respectively.

Illumina Sequencing

Shotgun Library construction and sequencing:

A shotgun genomic library was constructed from 5ug of genomic DNA using the Genomic DNA Sample Prep kit from Illumina (San Diego, CA). The library was loaded at 12pM on two lanes of a flowcell and sequenced on a Genome Analyzer II for 76 cycles from one end of the fragments according to the manufacturer's instructions (Illumina, San Diego, CA). The yield from both lanes was 33.7 million reads with a read-length of 75bp and an estimated error rate of 0.49% (based on the alignment of PhiX control DNA run on one lane to the PHiX reference genome).

3kb and 8kb mate-pairs library construction

These libraries were constructed according to the Illumina mate-pair sample preparation kit (Illumina, San Diego, CA) with one modification: the ends of the 3kb or 8kb fragments were ligated with a biotinylated linker so that, upon circularization, the ends of the 3kb or 8kb fragments are separated by this adaptor (5' TCGTATAACTTCGTATAATGTATGCTATACGAAGTTATTACG 3'). The libraries were loaded at a concentration of 12pM on one lane each and sequenced on a Genome Analyzer IIx for 76cycles on each end according to the manufacturer's protocol. The total numbers of reads were 19 million and 15 million for the 3kb and 8kb libraries, respectively. The error rate of the control DNA was 0.35% for each end.

Assembly

We used the Roche gsAssembler Version 2.3 to generate the initial assembly of the genome using both 454 and Illumina data. Briefly, Illumina reads were trimmed to 70bp and a FASTA file was used as input to gsAssembler requiring a minimal contig length of 100bp and coverage of 5 reads. The assembly was run in 'heterozygous' mode since we were assembling a diploid genome.

We used CABOG assembler (7) to create the assembly employing the optional MER overlapper and BOG unitigger modules. The data was first pre-processed to detect the linker in the 454 paired end reads and convert them into regular mate pairs. Since Illumina sequencing 3kb and 8kb paired end reads were prepared using a 454 Titanium linker, they had to be screened for linker as well. We also trimmed off the low quality sequence. For the 454 data we relied on the clear ranges (coordinates of the start and end of the high-quality sequence on the reads) given in the SFF files. We trimmed Illumina data based on the quality scores supplied by the sequencer.

After eliminating the low quality sequences and linkers, the 454 data contained nearly 6M (million) unmated reads, with 376bp average trimmed length, and 1.6M mate pairs in 3kb and 8Kb mate pairs with ~200bp average trimmed read length. Given the 250.8Mb estimated genome size this data set has 9x coverage by the unmated reads, 2.5x sequence and 36x clone coverage by the 3kb and 8kb mate pairs. The Illumina data contained 40M unmated 72bp reads, and 55M mate pairs in 3kb and 8Kb mate pairs. Both Illumina mate pair libraries have 72 bases sequenced on each end of the clone. This data set had 12x coverage by the unmated reads.

We note that this data set had significant redundancy problems in the paired end 8kb libraries produced by both sequencing technologies. Redundancy means that when

the library was generated, multiple identical copies of each pair of mated reads were created. It was ultimately necessary to discard 66% of the 454 8kb mate pairs and 32% of the Illumina 8kb mate pairs due to redundancy. To filter out redundant mate pairs we first created a partial preliminary assembly. We did not run the scaffolding step for this assembly. We then examined mated read positions in contigs to detect the mate pairs whose inserts appeared to start and end within +-1 base. We then eliminated all but one copy of each such redundant mate pair. Then we re-assembled the data to create the final assembly. Redundancy appears to be a problem in other projects and highlights the need for genome projects to test mate-paired libraries for redundancy using methods similar to those above or specialized tools such as 454 Replicate Filter) http://microbiomes.msu.edu/replicates/) prior to assembly since these oversampled clones can skew the assembly process.

Annotation

We used the automatic annotation pipeline MAKER (8) to annotate the genome of *L. humile*. MAKER generates high-quality annotations by taking into account evidence from multiple sources. MAKER first runs RepeatMasker (www.repeatmasker.org) over the genome to find simple repeats, satellites and interspersed repeats. These sequences are masked prior to protein and EST sequence database searching and gene prediction. To annotate the *L. humile* genome, we used a database that combined RepeatMasker's insect library with novel *P. barbatus* and *L. humile* repeats identified in this study by Repeat Modeler (www.repeatmasker.org/RepeatModeler.html) and PILER (Table 1) (9).

MAKER was configured to use WU-BLAST (10) to align EST and protein evidence to the genome; the resulting alignments were then clustered and filtered to

remove redundant hits. BLAST hits with high sequence identity were realigned to the non-RepeatMasked genome with the splice-site aware algorithm Exonerate (11) to ensure that splice-sites were correct. Misaligned ESTs and genomic contaminants were removed by checking each alignment for valid splice donors and acceptors. Only validly spliced ESTs were used to inform the gene predictors; this greatly cuts down on false positives. EST data from related organisms was aligned using TBLASTX (10) and subjected to the same filtering procedures. The ESTs used for annotation were derived from Newbler assemblies of *L. humile* RNA-seq reads generated by the 454 platform. MAKER also used TBLASTX to align a combined set of Genbank (12) hymenoptera ESTs and *P. barbatus* ESTs. MAKER's protein evidence came from a protein database comprised of UniProtKB (13), the *D. melanogaster* proteome (Release 5.25) from FlyBase (www.flybase.org), the *Apis* and *Nasonia* proteomes from Genbank (12) and insect chemosensory proteins from Genbank.

Three *ab-initio* predictors were trained for use with MAKER: SNAP (14), Augustus (15), and GeneMark (16). GeneMark was trained using a 30Mb genomic scaffold from the *L. humile* assembly. Augustus (15) was trained using its self-training pipeline autoAug.pl together with the MAKER aligned EST evidence. We then ran MAKER with the evidence described above, using GeneMark and Augustus as predictors. From the resulting MAKER predictions, we chose 3,352 genes with the best annotation quality scores (17) and used them as a training set for SNAP. We then added the trained SNAP to the MAKER configuration and re-ran MAKER. MAKER revises gene predictions *post-facto*, adding UTRs and alternatively spliced transcripts as suggested by the EST evidence. It then measures their congruency with the protein and

EST evidence, based upon their Annotation Edit Distances (AED) (17), choosing the best gene model for each gene. These comprise a high confidence gene-set for downstream analyses (8). Predictions without support or less congruent with the evidence are retained as predictions.

After producing MAKER based genome annotations, we used the program InterProScan (18) to identify putative protein domains in *ab initio* gene predictions not overlapping MAKER annotations. *Ab initio* predictions that contained a recognizable InterPro protein domain were then added as gene models to an updated gene annotation set. We later filtered this updated annotation set for representation of likely repetitive elements using RepeatMasker (http://repeatmasker.org). RepeatMasker was run with the RepBase (19) repeat libraries in conjunction with a species specific repeat library prepared for *L. humile*, and the results were filtered to remove repetitive elements labeled "low complexity", "simple repeat", or having a RepeatMasker score of at less than 200. Finally, transcripts for which at least 50% of their length was identified as being repetitive were removed from the final annotation dataset.

Annotating the *L. humile* genome took roughly 8000 CPU hours using the distributed computer clusters at CHPC, University of Utah (http://www.chpc.utah.edu). In total we found 15,345 genes and generated another 29,206 gene-predictions that did not overlap EST or protein sequence alignments. In total, 855 new gene annotations were added to the final annotation set based on the presence of InterPro protein domains, and 23 of the original MAKER annotations were removed because of repeat filtering. The final dataset contained a total of 16,123 protein coding genes and 16,177 transcripts.

All gene annotations and supporting evidence alignments produced by MAKER

as well as protein domain information derived from InterProScan were loaded into a Chado (20) (http://gmod.org/wiki/Chado) database to facilitate community access to genome annotations and supporting evidence. The annotation curation tool Apollo (21) was then deployed to allow researchers to view and manually edit the genome annotations contained within the database (Table S2). Apollo allows users to connect to a Chado database remotely thereby providing researchers the ability to curate the genome annotations from distant locations. Apollo was configured as a Java Web Start Application for distribution to the community, which kept configuration of the program under the control of a central server and ensured a degree of consistency in the way data could be viewed and accessed.

For manual annotation, users selected reference genes from a well-curated species (i.e. *D. melanogaster*, *A. mellifera*, *N. vitripennis*) and identified the best matching MAKER gene model using BLASTP. Exon-by-exon alignment was used to refine intron-exon boundaries in Apollo to create a gene model that had splice sites consistent with all EST data and comparative BLAST evidence. Effort was made to annotate a protein matching the full length of the reference gene, when possible, and irregular features such as missing start codons, stop codons, gaps, and other anomalies were noted in the comment form of Apollo. Final gene models were confirmed by BLAST back to the reference gene set to confirm reciprocal best hits, and relevant synonyms of orthologs were recorded into the Chado database. Prediction sets and the OGS1.1 can be obtained through http://HymenopteraGenome.org/linepithema/genome_consortium/datasets.html.

Table S2. Manually annotated genes. The following represents a list of manually curated genes as of the time of publication. The pathway, process, or predicted function of each gene is indicates as well as the *D. melanogaster* or other reference gene used to annotate the model. The MAKER identifiers are provided as the proposed name for each gene. Gustatory receptors (Grs) and Olfactory receptors (Ors) are listed separately in Tables S10 and S11, respectively.

Process/Function	**Drosophila Gene Name**	**Lhum MAKER Gene ID**
Aggression (inter-male)	ade5	lhum_ade5-like
Aggression (inter-male)	eca	lhum_eclair
Aggression (inter-male)	ed	lhum_echinoid-like
Aggression (inter-male)	noc	lhum_no ocelli-like
Aggression (inter-male)	sgl	lhum_sgl
behavior	homer	lhum_homer
Biogenic amine receptor / GPCR	DmDAMB/DopR2	lhum_DopR2
Biogenic amine receptor / GPCR	DmDOP1	lhum_DopR
Caste Implicated - larval storage	Hex110	Lhum_Hex110
Caste Implicated - larval storage	Hex70a	Lhum_Hex70a
Caste Implicated - larval storage	Hex70b	Lhum_Hex70b
Caste Implicated - larval storage	Hex70c	Lhum_Hex70c
Caste Implicated - Nutrition Sensing	AKT	Lhum_AKT
Caste Implicated - Nutrition Sensing	atg1	Lhum_atg1
Caste Implicated - Nutrition Sensing	4EBP	Lhum_4EBP
Caste Implicated - Nutrition Sensing	EIF-4B	Lhum_E1F4B
Caste Implicated - Nutrition Sensing	lkb1	Lhum_lkb1
Caste Implicated - Nutrition Sensing	Ilp	Lhumr_Ilp1
Caste Implicated - Nutrition Sensing	Ilp	Lhum_Ilp2
Caste Implicated - Nutrition Sensing	InR	Lhum_InR1
Caste Implicated - Nutrition Sensing	InR	Lhum_InR2
Caste Implicated - Nutrition Sensing	Mo25	Lhum_Mo25
Caste Implicated - Nutrition Sensing	PDK1	Lhum_PDK1
Caste Implicated - Nutrition Sensing	Pi3k21B	Lhum_ Pi3K21B
Caste Implicated - Nutrition Sensing	PI3K59F	Lhum_PI3K59F
Caste Implicated - Nutrition Sensing	Pi3K68D	Lhum_Pi3K68D
Caste Implicated - Nutrition Sensing	Pi3K92E	Lhum_Pi3K92E
Caste Implicated - Nutrition Sensing	Raptor	Lhum_Raptor
Caste Implicated - Nutrition Sensing	Rheb	Lhum_Rheb
Caste Implicated - Nutrition Sensing	Rector	Lhum_rictor
Caste Implicated - Nutrition Sensing	TOR	Lhum_Tor
Caste Implicated -	SNF1A	Lhum_SNF1A

Nutrition Sensing		
Caste Implicated - Nutrition Sensing	TSC1	Lhum_Tsc1
Caste Implicated - Nutrition Sensing	TSC2	Lhum_Tsc2
Caste Implicated Gene - yolk protein	Vg	Lhum_Yp1
Cell Cycle Control	CDC42	Lhum_CDC42
Cell Cycle Control	CycB	Lhum_CycB
Chitinase	CG5613	Lhum_CG5613
Chitinase	CG7565	Lhum_CG7565
Chitinase	Chit	Not Found
Chitinase	Cht2	Lhum_Cht2
Chitinase	Cht3	Lhum_Cht3
Chitinase	Cht4	Not Found
Chitinase	Cht5	Lhum_Cht5
Chitinase	Cht6	Lhum_Cht6
Chitinase	Cht7	Lhum_Cht7
Chitinase	Cht8	Lhum_Cht8
Chitinase	Cht9	Not Found
Chitinase	Cht11	Lhum_Cht11
Chitinase	Cht12	Not Found
Chitinase	K06A9.1b	Lhum_K06A9.1b
Chitinase - Cation Binding	CG8460	Lhum_CG8460
Circadian	clock	lhum_clock
Circadian	cryptochrome 2	lhum_cryptochrome2
Circadian	cycle	lhum_cycle
Circadian	timeless	lhum_timeless
Cytoskeleton dynamics/morphology	Rac1	Lhum_Rac1
Cytoskeleton dynamics/morphology	Rho1	Lhum_Rho1
Desaturase (delta-9)	CG9747	Lhum_CG9747_a
Desaturase (delta-9)	CG9747	Lhum_CG9747_b
Desaturase (delta-9)	CG9747	Lhum_CG9747_c
Desaturase (delta-9)	CG9747	Lhum_CG9747_d
Desaturase (delta-9)	CG9747	Lhum_CG9747_e
Desaturase (delta-9)	CG9747	Lhum_CG9747_f
Desaturase (delta-9)	CG9747	Lhum_CG9747_g
Desaturase (delta-9)	CG9747	Lhum_CG9747_h
Desaturase (delta-9)	CG9747	Lhum_CG9747_i
Desaturase (delta-9)	CG9747	Lhum_CG9747_j
Desaturase (delta-9)	CG9747	Lhum_CG9747_k
Desaturase (delta-9)	CG9747	Lhum_CG9747_l
Desaturase (delta-9)	CG9747	Lhum_CG9747_m
Desaturase (delta-9)	CG9747	Lhum_CG9747_n
Desaturase (delta-9)	CG9747	Lhum_CG9747_o
Desaturase (delta-9)	CG9747	Lhum_CG9747_p
Desaturase (delta-9)	CG9747	Lhum_desat_frag1
Desaturase (delta-9)	CG9747	Lhum_desat_frag7
Desaturase (delta-9)	CG9747	Lhum_desat_frag8
Desaturase (delta-9)	CG9747	Lhum_desat_frag9
Desaturase (delta-9)	CG8630	Lhum_CG8630_a
Desaturase (delta-9)	CG8630	Lhum_CG8630_b
Desaturase (delta-9)	CG8630	Lhum_CG8630_c
Desaturase (delta-9)	CG8630	Lhum_CG8630_d
Desaturase (delta-9)	CG9743	Lhum_CG9743
Desaturase (delta-9)	CG15531	Lhum_CG15531
Desaturase (delta-9)	desat1	Lhum_desat_frag2
Desaturase (delta-9)	desat1	Lhum_desat_frag3
Desaturase (delta-9)	desat1	Lhum_desat_frag4
Desaturase (delta-9)	desat1	Lhum_desat_frag5
Desaturase (delta-9)	desat1	Lhum_desat_frag6
Desaturase (delta-9) - CHC alkene synthesis	desat1	Lhum_desat1_a

Desaturase (delta-9) - CHC alkene synthesis	desat1	Lhum_desat1_b
DNA methylation	Dnmt1	Lhum_Dnmt1
DNA methylation	Dnmt2	Lhum_Dnmt2
DNA methylation	Dnmt3	Lhum_Dnmt3
EGF signaling	26- argos	lhum_argos
EGF signaling	27- star S	not found
EGF signaling	28-keren krn	lhum_keren
embryonic dev.	ecd	Lhum_ecd
Embryonic Development - HOX	Abdominal A	Lhum-Abd-A-like
Embryonic Development - HOX	Abdominal B	Lhum-Abd-B-like
Embryonic Development - HOX	Antennapedia	Lhum-Antp-like
Embryonic Development - HOX	Deformed	Lhum-Dfd-like
Embryonic Development - HOX	Fushi Tarazu	Lhum-ftz-like
Embryonic Development - HOX	Hox3-A	Lhum-Hox3-A-like
Embryonic Development - HOX	Labial	Lhum-lab-like
Embryonic Development - HOX	Proboscipedia	Lhum-pb-like
Embryonic Development - HOX	Sex Combs Reduced	Lhum-Scr-like
Embryonic Development - HOX	Ultrabithorax	Lhum-Ubx-like
Endocytosis	Aux	Lhum_Aux
Endocytosis	Chc	Lhum_Chc
Endocytosis	Rab5	Lhum_Rab5
Endocytosis	Rab7	Lhum_Rab7
Endocytosis	Rab8	Lhum_Rab8
Endocytosis	Syt1	Lhum_Syt1
errata	CG16979	lhum_CG16979
errata	CG34424	lhum_CG34424
Fertility	Eggless	lhum_egg
Fertility	Ovarian tumor	lhum_otu
Fertility	Sans fille	lhum_snf
Fertility	Sex combs extra	lhum_sce
Fertility	Sex lethal	lhum_sxl
Foraging	for	lhum_for_upstream/downstream*
glycolysis	Ald	Lhum_Ald
glycolysis	Gapdh1	Lhum_Gapdh1
glycolysis	Hex-C	Lhum_Hex-C
glycolysis	Pfk	Lhum_Pfk
glycolysis	Pgi	Lhum_Pgi
Heat shock response	Hsp 70Aa	Lhum_Hsp70
Heme binding	c-cup	Lhum_c-cup
Imaginal Disc Development	Idgf1	Not Found
Imaginal Disc Development	Idgf2	Not Found
Imaginal Disc Development	Idgf3	Not Found
Imaginal Disc Development	Idgf4	Lhum_Idgf4
Imaginal Disc Development	Idgf5	Not Found
Immune Genes	18w	lhum_18w
Immune Genes	Atg12	lhum_Atg12
Immune Genes	Atg5	lhum_Atg5
Immune Genes	Atg7	lhum_Atg7
Immune Genes	aub	lhum_aub
Immune Genes	bsk	lhum_bsk
Immune Genes	cact1	lhum_cact1a

Immune Genes	cact1	lhum_cact1b
Immune Genes	cactin	lhum_cactin
Immune Genes	casp	lhum_casp
Immune Genes	CG11372	lhum_galectin
Immune Genes	CG32226	lhum_galectin2
Immune Genes	Dcr-2	lhum_Dcr-2
Immune Genes	Def	lhum_def
Immune Genes	dl	lhum_dl
Immune Genes	dome	lhum_dome
Immune Genes	Duox	lhum_Duox
Immune Genes	egr	lhum_egr
Immune Genes	FADD	lhum_FADD
Immune Genes	galectin 1	lhum_galectin1
Immune Genes	GNBP1	lhum_GNBP1-1
Immune Genes	GNBP1	lhum_GNBP1-2
Immune Genes	GNBP1	lhum_GNBP1-2_like1
Immune Genes	GNBP1	lhum_GNBP1-2_like2
Immune Genes	hop	lhum_hop
Immune Genes	hymenoptaecin	lhum_hymenoptaecin
Immune Genes	Iap2	lhum_Iap2
Immune Genes	IKKg	lhum_IKKg
Immune Genes	imd	lhum_imd
Immune Genes	Jra	lhum_Jra
Immune Genes	kay	lhum_kay
Immune Genes	Lys-2	hum_Lys-2
Immune Genes	Lys-3	hum_Lys-3
Immune Genes	Myd88	lhum_MyD88
Immune Genes	NA	lhum_Naickin-1
Immune Genes	NA	lhum_Naickin-2a
Immune Genes	NA	lhum_Hisnavicin-3
Immune Genes	NA	lhum_Naickin-2b
Immune Genes	NimA	lhum_NimA
Immune Genes	NimC1	lhum_NimC
Immune Genes	NOS	lhum_NOS
Immune Genes	PGRP-LC	lhum_PGRP-LC
Immune Genes	PGRP-LC	lhum_PGRP-LC_like
Immune Genes	PGRP-S1	lhum_PGRP-S1
Immune Genes	PGRP-S2	lhum_PGRP-S2a
Immune Genes	PGRP-S2	lhum_PGRP-S2b
Immune Genes	PGRP-SA	lhum_PGRP-SA
Immune Genes	Pli	lhum_Pli
Immune Genes	pll	lhum_pll
Immune Genes	PPO	lhum_PPO
Immune Genes	Rel	lhum_Rel
Immune Genes	Rpn3	lhum_Rpn3
Immune Genes	SCR-B10	lhum_SCR-B10
Immune Genes	SCR-B2	lhum_SCR-B2
Immune Genes	SCR-B5	lhum_SCR-B5
Immune Genes	SCR-B9	lhum_SCR-B9
Immune Genes	SCR-C	lhum_SCR-C
Immune Genes	serpin-1	lhum_Serpin-1
Immune Genes	Serpin-3	lhum_Serpin-3
Immune Genes	Serpin-4	lhum_Serpin-4
Immune Genes	serpin-5	lhum_Serpin-5
Immune Genes	SP1	lhum_SP1a
Immune Genes	SP1	lhum_SP1b
Immune Genes	SP14	lhum_SP14
Immune Genes	SP2	lhum_SP2
Immune Genes	SP30	lhum_SP30
Immune Genes	SP46	lhum_SP46
Immune Genes	SP49	lhum_SP49
Immune Genes	spz1	lhum_spz1
Immune Genes	spz2	lhum_spz2
Immune Genes	spz4	lhum_spz4
Immune Genes	spz5	lhum_spz5
Immune Genes	spz6	lhum_spz6

Immune Genes	Stat92E	lhum_Stat92E
Immune Genes	Tab2	lhum_Tab2
Immune Genes	Tak1	lhum_Tak1
Immune Genes	TEP7	lhum_TEP7
Immune Genes	TEPA	lhum_TEPA
Immune Genes	TepIII	lhum_TepIII
Immune Genes	Toll-1	lhum_Toll-1a
Immune Genes	Toll-1	lhum_Toll-1b
Immune Genes	Toll-10	lhum_Toll-10
Immune Genes	Toll-6	lhum_Toll-6
Immune Genes	Toll-8	lhum_Toll-8
Immune Genes	Traf1	lhum_Traf1
Immune Genes	Traf6	lhum_Traf6
Immune Genes	tub	lhum_tub
juvenile hormone	jhamt	Lhum_jhamt
juvenile hormone	jhe	Lhum_jhe
Larval cuticle formation	GMCOX2	Lhum_GMCOX2
larval development	amon	Lhum_amon
learning and mem	14-3-3zeta	lhum_14-3-3zeta
Learning or memory	S6kII	lhum_S6KII-like
Memory	14-3-3epsilon	lhum_14-3-3epsilon
Memory	aPKC	lhum_aPKC
Memory	As	lhum_ubiquitin protein ligase E3A
Memory	CaMKII	lhum_CaMKII
Memory	cer	no ortholog
Memory	CrebB-17A	lhum_creb
Memory	Ddc	lhum_Ddc
Memory	dgs	lhum_dgs
Memory	dnc	lhum_dnc
Memory	drk	lhum_drk
Memory	eag	lhum_eag
Memory	eas	lhum_eas-like
Memory	exba	lhum_exba
Memory	Gld2	lhum_Gld2-like
Memory	per	lhum_per
Memory	Phm	lhum_cytochrome P450-like
Memory	pum	lhum_pumilio-like
Memory	sbr	lhum_small bristles-like
Memory	stau	lhum_stau-like
Memory	Tbh	lhum_tbh
Memory	Tequila	lhum_tequila-like
Memory	w	lhum_white
Memory	yu	lhum_yu-like
methyl binding protein	mbd2	lhum_mbd2
miRNA	67 distinct orthologs	
mushr. body dev	mbt	lhum_mbt
nervous sys dev.	shd	Lhum_shd
nuclear transport	Ran	Lhum_Ran
Olfactory Learning	14-3-3zeta	lhum_14-3-3zeta
Olfactory Learning	cher / cheerio	lhum_cher
Olfactory Learning	dikar	lhum_dikar-like
Olfactory Learning	Fas2 / Fasciclin 2	lhum_Fas2
Olfactory Learning	Fas3 / Fasciclin 3	lhum_Fas3-like
Olfactory Learning	futsch	lhum_futsch-like
Olfactory Learning	gclm / Glutamate-cysteine ligase modifier subunit	lhum_gclm
Olfactory Learning	gp210	lhum_gp210
Olfactory Learning	gry / gryzun	lhum_gry
Olfactory Learning	klingon	lhum_klingon-like
Olfactory Learning	lat / latheo	lhum_lat
Olfactory Learning	ltd / lightoid	lhum_ltd-like
Olfactory Learning	mnb / minibrain	lhum_mnb-like
Olfactory Learning	mob2	lhum_mob2-like

Olfactory Learning	mol / moladietz	lhum_mol
Olfactory Learning	mura / murashka	lhum_mura-like
Olfactory Learning	nf1 / Neurofibromin 1	lhum_Nf1
Olfactory Learning	NMDA receptor 1	lhum_NMDA Receptor 1
Olfactory Learning	nord	lhum_nord-like
Olfactory Learning	pigeon	pbar_pigeon
Olfactory Learning	pka-C1	lhum_cAMP-dependent protein kinase
Olfactory Learning	pka-R1 / cAMP-dependent protein kinase R1	lhum_Pka_R1
Olfactory Learning	Pp1-87B	pbar_Pp1
Olfactory Learning	pst / pastrel	lhum_pastrel-like
Olfactory Learning	rad / radish	lhum_radish-like
Olfactory Learning	rho / rhomboid	lhum_rhomboid-like
Olfactory Learning	rogdi	lhum_rogdi
Olfactory Learning	sarah	lhum_sra
Olfactory Learning	scb / scab	lhum_scab-like
Olfactory Learning	sgg / shaggy	lhum_sgg-like
Olfactory Learning	shi / shibire	lhum_shibire
Olfactory Learning	shn / schnurri	lhum_shn-like
Olfactory Learning	supernumerary limbs	lhum_slmb
Olfactory Learning	trp / transient receptor potential	lhum_trp-like
Olfactory Learning	tun / tungus	lhum_tungus
OXPHOS	ACPM	Lhum_Ndufab1_like
OXPHOS	AT91	Lhum_Atp5g2_like
OXPHOS	ATP5E	Lhum_Atp5e_like
OXPHOS	ATPA	Lhum_Atp5a1
OXPHOS	ATPB	Lhum_Atp5b_like
OXPHOS	ATPD	Lhum_Atp5d_like
OXPHOS	ATPF	Lhum_Atp5f1_like
OXPHOS	ATPG	Lhum_Atp5c1_like
OXPHOS	ATPJ	Lhum_Atp5i_like
OXPHOS	ATPK	Lhum_Atp5j2_like
OXPHOS	ATPN	Lhum_Atp5l_like
OXPHOS	ATPO	Lhum_Atp5o_like
OXPHOS	ATPQ	Lhum_Atp5h_like
OXPHOS	ATPR	Lhum_Atp5j_like
OXPHOS	C560	Lhum_SdhC_like
OXPHOS	CG8728	Lhum_Pmpca_like
OXPHOS	COX4	Lhum_Cox4i1_like
OXPHOS	COX5A	Lhum_Cox5a_like
OXPHOS	COX5B	Lhum_Cox5b_like
OXPHOS	COX6A	Lhum_Cox6a1_like_A
OXPHOS	COX6A	Lhum_Cox6a1_like_B
OXPHOS	COX6B	Lhum_Cox6b1_like_A
OXPHOS	COX6B	Lhum_Cox6b1_like_B
OXPHOS	COX6C	Lhum_Cox6c_like
OXPHOS	COX7C	Lhum_Cox7c_like
OXPHOS	CY1	Lhum_Cyc1_like_a
OXPHOS	CY1	Lhum_Cyc1_like_b
OXPHOS	DHSA	Lhum_Sdha_A
OXPHOS	DHSA	Lhum_Sdha_like_B
OXPHOS	DHSB	Lhum_SdhB_like_A
OXPHOS	DHSB	Lhum_SdhB_like_B
OXPHOS	DHSD	Lhum_SdhD_like
OXPHOS	N4AM	Lhum_Ndufa7_like
OXPHOS	N4BM	Lhum_Ndufc2_like
OXPHOS	N5BM	Lhum_Ndufa11_like
OXPHOS	N7BM	Lhum_Ndufa12_like
OXPHOS	N7BM	Lhum_Ndufa12_pseudo
OXPHOS	NB2M	Lhum_Ndufb3_like
OXPHOS	NB4M	Lhum_Ndufa6_like

OXPHOS	NB5M	Lhum_Ndufb4_like
OXPHOS	NB6M	Lhum_Ndufa13_like
OXPHOS	NB7M	Lhum_Ndufb6_like
OXPHOS	NB8M	Lhum_Ndufb7_like
OXPHOS	NI2M	Lhum_Ndufb9_like
OXPHOS	NI8M	Lhum_Ndufa2_like
OXPHOS	NIAM	Lhum_Ndufb8_like
OXPHOS	NIDM	Lhum_Ndufb10_like
OXPHOS	NIGM	Lhum_Ndufb2_like
OXPHOS	NIMM	Lhum_Ndufa1_like
OXPHOS	NINM	Lhum_Ndufb1_like
OXPHOS	NIPM	Lhum_Ndufs5_like
OXPHOS	NISM	Lhum_Ndufb5_like
OXPHOS	NUAM	Lhum_Ndufs1
OXPHOS	NUBM	Lhum_Ndufv1_like_a
OXPHOS	NUCM	Lhum_Ndufs2_like
OXPHOS	NUDM	Lhum_Ndufa10_like
OXPHOS	NUEM	Lhum_Ndufa9_like
OXPHOS	NUFM	Lhum_Ndufa5_like
OXPHOS	NUGM	Lhum_Ndufs3_like
OXPHOS	NUHM	Lhum_Ndufv2_like
OXPHOS	NUIM	Lhum_Ndufs8_like
OXPHOS	NUKM	Lhum_Ndufs7_like
OXPHOS	NUML	Lhum_Ndufa4_like
OXPHOS	NUMM	Lhum_Ndufs6_like
OXPHOS	NUPM	Lhum_Ndufa8_like
OXPHOS	NUYM	Lhum_Ndufs4_like
OXPHOS	UCR1	Lhum_Pmpcb_like
OXPHOS	UCR2	Lhum_Uqcrc2_like
OXPHOS	UCR6	Lhum_Uqcrb_like
OXPHOS	UCRH	Lhum_Uqcrh_like
OXPHOS	UCRI	Lhum_Uqcrfs1_like_A
OXPHOS	UCRI	Lhum_Uqcrfs1_like_B
OXPHOS	UCRQ	Lhum_Uqcrc2_like_a
OXPHOS	UCRQ	Lhum_Uqcrq_like
OXPHOS	UCRX	Lhum_Uqcr10_like_a
OXPHOS	UCRX	Lhum_Uqcr10_like_b
OXPHOS	UCRY	Lhum_Uqcr11_like
OXPHOS	Vha55	Lhum_Atp12a
OXPHOS	Vha68	Lhum_Atp6v1a
pigmentation	Pink	Lhum_Pink
Protein coding	cappuccino	lhum_capu
protein coding	maleless	lhm_mle
protein coding	nemy	lhum_nemy
protein coding	Pdk	Lhum_Pdk
protein coding	Rap	Lhum_Rap
protein coding/cholinergic receptor	nAChRa1	Lhum_nAChRa1
protein coding/GPCR	mGlutR1	Lhum_mGlutR1
protein coding/GPCR	Rab 6	Lhum_rab6
protein coding/RTK	EphR	Lhum_Eph
protein folding	Cnx99a	Lhum_Cnx99a-1
protein folding	Gp 93	Lhum_GP93
protein folding	PDI	Lhum_PDI-1
Protein kinase	Asator	Lhum_Asator
protein kinase	Fak56D	Lhum_Fak56D
ras protein signal transduction	f-cup	Lhum_f-cup
Regulation of Ca +2 dependent processes	Cam/ Calmodulin	lhum_cam
REPRODUCTION DNA Damage/TE	Armi, Armitage	lhum_armi
REPRODUCTION DNA Damage/TE	ATM, Ataxia-telangiectasia gene	lhum_ATM
REPRODUCTION	ATR, Ataxia	lhum_ATR

DNA Damage/TE	telangiectasia and Rad3-related gene	
REPRODUCTION DNA Damage/TE	Chk2, Checkpoint kinase 2 or Loki	lhum_loki
REPRODUCTION DNA Damage/TE	CK2beta; casein kinase II beta	lhum_CK2beta
REPRODUCTION DNA Damage/TE	Csul, Capsuleen	lhum_csul
REPRODUCTION DNA Damage/TE	Cuff, Cutoff or Dom3Z	lhum_Dom3Z
REPRODUCTION DNA Damage/TE	eIF5b, eukaryotic translation initiation factor 5b	lhum_EIF5b
REPRODUCTION DNA Damage/TE	Gbb; glass bottom boat/ protein 60A	lhum_gbb
REPRODUCTION DNA Damage/TE	Hen1, Hua enhancer 1 or pimet;	lhum_pimet
REPRODUCTION DNA Damage/TE	HP1, heterochromatin protein 1	lhum_HP1-like
REPRODUCTION DNA Damage/TE	Hsp90/ Dmel Hsp83	lhum_hsp90A lhum_hsp90B
REPRODUCTION DNA Damage/TE	PIWI, P-element-induced wimpy testis	Lhum_Piwi-like
REPRODUCTION DNA Damage/TE	Spn-E, Spindle-E	lhum_SpnE
REPRODUCTION DNA Damage/TE	Stam; Signal transducing adaptor molecule	lhum_stam
REPRODUCTION DNA Damage/TE	Tf, Traffic Jam	lhum_trafficjam
REPRODUCTION DNA Damage/TE	Tud, Tudor protein;	lhum_tud
REPRODUCTION DNA Damage/TE	Zuc, Zucchini	lhum_zuc
REPRODUCTION Maternal Determ	6-Vasa	Lhum_Vasa-like-RB
Ribosomal Protein	RACK1	lhum_Rack1
Ribosomal Protein	RpL10	lhum_RpL10
Ribosomal Protein	RpL10Ab	lhum_RpL10A
Ribosomal Protein	RpL11	lhum_RpL11
Ribosomal Protein	RpL12	lhum_RpL12
Ribosomal Protein	RpL13	lhum_RpL13
Ribosomal Protein	RpL13A	lhum_RpL13A
Ribosomal Protein	RpL14	lhum_RpL14
Ribosomal Protein	RpL15	lhum_RpL15
Ribosomal Protein	RpL17	lhum_RpL17
Ribosomal Protein	RpL18	lhum_RpL18
Ribosomal Protein	RpL18A	lhum_RpL18A
Ribosomal Protein	RpL19	lhum_RpL19
Ribosomal Protein	RpL21	lhum_RpL21
Ribosomal Protein	RpL22	lhum_RpL22
Ribosomal Protein	RpL23	lhum_RpL23
Ribosomal Protein	RpL23A	lhum_RpL23A
Ribosomal Protein	RpL24	lhum_RpL24
Ribosomal Protein	RpL24-like	lhum_RpL24-like
Ribosomal Protein	RpL26	lhum_RpL26
Ribosomal Protein	RpL27	lhum_RpL27
Ribosomal Protein	RpL27A	lhum_RpL27A
Ribosomal Protein	RpL28	lhum_RpL28
Ribosomal Protein	RpL29	lhum_RpL29
Ribosomal Protein	RpL3	lhum_RpL3
Ribosomal Protein	RpL30	lhum_RpL30
Ribosomal Protein	RpL31	lhum_RpL31
Ribosomal Protein	RpL32	lhum_RpL32

Ribosomal Protein	RpL34a	lhum_RpL34
Ribosomal Protein	RpL35	lhum_RpL35
Ribosomal Protein	RpL35A	lhum_RpL35A
Ribosomal Protein	RpL36	lhum_RpL36
Ribosomal Protein	RpL36A	lhum_RpL36A
Ribosomal Protein	RpL37a	lhum_RpL37
Ribosomal Protein	RpL37A	lhum_RpL37A
Ribosomal Protein	RpL38	lhum_RpL38
Ribosomal Protein	RpL39	lhum_RpL39
Ribosomal Protein	RpL4	lhum_RpL4
Ribosomal Protein	RpL40	lhum_RpL40
Ribosomal Protein	RpL41	lhum_RpL41
Ribosomal Protein	RpL5	lhum_RpL5
Ribosomal Protein	RpL6	lhum_RpL6
Ribosomal Protein	RpL7	lhum_RpL7
Ribosomal Protein	RpL7A	lhum_RpL7A
Ribosomal Protein	RpL8	lhum_RpL8
Ribosomal Protein	RpL9	lhum_RpL9
Ribosomal Protein	RpLP0	lhum_RpLP0
Ribosomal Protein	RpLP0-like	lhum_RpLP0-like
Ribosomal Protein	RpLP1	lhum_RpLP1
Ribosomal Protein	RpLP2	lhum_RpLP2
Ribosomal Protein	RpS10b	lhum_RpS10
Ribosomal Protein	RpS11	lhum_RpS11
Ribosomal Protein	RpS12	lhum_RpS12
Ribosomal Protein	RpS13	lhum_RpS13
Ribosomal Protein	RpS14a	lhum_RpS14
Ribosomal Protein	RpS15	lhum_RpS15
Ribosomal Protein	RpS15Aa	lhum_RpS15A
Ribosomal Protein	RpS16	lhum_RpS16a
Ribosomal Protein	RpS16	lhum_RpS16b
Ribosomal Protein	RpS17	lhum_RpS17
Ribosomal Protein	RpS18	lhum_RpS18
Ribosomal Protein	RpS19a	lhum_RpS19
Ribosomal Protein	RpS2	lhum_RpS2
Ribosomal Protein	RpS20	lhum_RpS20
Ribosomal Protein	RpS21	lhum_RpS21
Ribosomal Protein	RpS23	lhum_RpS23a
Ribosomal Protein	RpS23	lhum_RpS23b
Ribosomal Protein	RpS24	lhum_RpS24
Ribosomal Protein	RpS25	lhum_RpS25
Ribosomal Protein	RpS26	lhum_RpS26
Ribosomal Protein	RpS27	lhum_RpS27
Ribosomal Protein	RpS27A	lhum_RpS27A
Ribosomal Protein	RpS28b	lhum_RpS28a
Ribosomal Protein	RpS28b	lhum_RpS28b
Ribosomal Protein	RpS29	lhum_RpS29
Ribosomal Protein	RpS3	lhum_RpS3
Ribosomal Protein	RpS30	lhum_RpS30a
Ribosomal Protein	RpS30	lhum_RpS30b
Ribosomal Protein	RpS3A	lhum_RpS3A
Ribosomal Protein	RpS4	lhum_RpS4
Ribosomal Protein	RpS5a	lhum_RpS5
Ribosomal Protein	RpS6	lhum_RpS6
Ribosomal Protein	RpS7	lhum_RpS7
Ribosomal Protein	RpS8	lhum_RpS8
Ribosomal Protein	RpS9	lhum_RpS9
Ribosomal Protein	RpSA	lhum_RpSA
RNAi Pathway	AGO1	lhum_AGO1
RNAi Pathway	AGO2	lhum_AGO2
RNAi Pathway	AGO3	lhum_AGO3
RNAi Pathway	dcr1	lhum_dcr1
RNAi Pathway	drosha	lhum_drosha
RNAi Pathway	loqs	lhum_loqs
RNAi Pathway	pasha	lhum_pasha
RNAi Pathway	Belle	Lhum_Belle-like

RNAi Pathway	Elp1	Lhum_Elp1-like
RNAi Pathway	Embargoed	Lhum_Crm1-like
RNAi Pathway	Exportin 5	Lhum_Xpo5-like
RNAi Pathway	Fmr1	Lhum_Fmr1-like
RNAi Pathway	Loqs2	Lhum_Loqs2-like
RNAi Pathway	Pros45	Lhum_Pros45-like
RNAi Pathway	R2D2	Lhum_similar-to-R2D2
RNAi Pathway	Sid1	Lhum_Sid1-like
RNAi Pathway	Translin	Lhum_Trsn-like
RNAi Pathway	Trax	Lhum_Trax-like
RNAi Pathway	VIG	Lhum_VIG-like
Serotonic Transporter	dmel_SerT	lhum_SerT
signaling pathways	L(2)TID	Lhum_l(2)tid
unfolded protein response	ATF6	Lhum_ATF6-1
unfolded protein response	IRE1	Lhum_IRE-1-1
unfolded protein response	XBP-1	Lhum_XBP-1-1
Vesicular Transport	Arf2	Lhum_Arf2
Vision	blue opsin	lhum_blueopsin
Vision	long wavelength opsin 1	lhum_LWopsin1
Vision	long wavelength opsin 2	lhum_LWopsin2
Vision	pteropsin-like	lhum_pteropsin-like
Vision	UV opsin	lhum_UVopsin
WBSCR gene	hsap_EIF4H	lhum_EIF4H_like
WBSCR gene	hsap_LAT2	lhum_LAT2_like
WBSCR gene	hsap_LIMK1	lhum_LIMK1_like
WBSCR gene	hsap_STX1A	lhum_STX1A_like
WBSCR gene	hsap_TBL2	lhum_TBL2_like
WBSCR gene	hsap_WBSCR16	lhum_WBSCR16_like
WBSCR gene	hsap_WBSCR22	lhum_WBSCR22_like
WBSCR genes	hsap_ABHD11	lhum_ABHD11_like
WBSCR genes	hsap_BAZ1B	lhum_BAZ1B_like
WBSCR genes	hsap_BCL7B	lhum_BCL7B_like
WBSCR genes	hsap_CLIP2	lhum_CLIP2_like
WBSCR genes	hsap_FKBP6	lhum_FKBP6_like
WBSCR genes	hsap_HIP1	lhum_HIP1_like
WBSCR genes	hsap_PMS2	lhum_PMS2_like
WBSCR genes	hsap_RFC2	lhum_RFC2_like
WBSCR genes	hsap_STAG3	lhum_STAG3_like
WING-A/P pattern	10-decapentaplengic	lhum_dpp
WING-A/P pattern	11-hedgehog	lhum_hedgehog
WING-A/P pattern	12-thinkveins	lhum_thickveins
WING-A/P pattern	13-daughters against dpp	lhum_dad
WING-A/P pattern	14-mothers against dpp	lhum_mad
WING-A/P pattern	15-smoothened	lhum_smoothened
WING-A/P pattern	16-knirps	lhum_knirps
WING-A/P pattern	17-baboon	lhum_baboon
WING-A/P pattern	19-punt	lhum_punt
WING-A/P pattern	1-brinker	lhum_brinker
WING-A/P pattern	20-saxophone	lhum_saxophone
WING-A/P pattern	2-engrailed	lhum_engrailed
WING-A/P pattern	3-escargot	lhum_escargot
WING-A/P pattern	4- medea	lhum_medea
WING-A/P pattern	5-optomotorblind	lhum_omb
WING-A/P pattern	6-patched	lhum_patched
WING-A/P pattern	7-cubitus interruptus	lhum_cubitusinterruptus
WING-A/P pattern	8-smad on x	lhum_smox
WING-A/P pattern	9a-spalt-related	lhum_spalt-related

WING-A/P pattern	9-spalt	lhum_spalt
WING-Apoptosis	11-p53	lhum_p53
WING-Apoptosis	12-JNK basket bsk	lhum_JNK
WING-Apoptosis	13-Eiger egr	lhum_eiger
WING-Apoptosis	14-wengen wgn	lhum_wengen
WING-Apoptosis	15-Buffy	lhum_bcl-like
WING-Apoptosis	16- Ras1 Ras85D	lhum_ras1
WING-Apoptosis	19- Dredd	lhum_dredd
WING-Apoptosis	1-dronc Nc	lhum_dronc
WING-Apoptosis	20- caspase-like	lhum_caspase-like
WING-Apoptosis	21- caspase-likeB	lhum_caspase-likeB
WING-Apoptosis	22- caspase-likeC	lhum_caspase-likeC
WING-Apoptosis	2-drice ICE	lhum_drICE
WING-Apoptosis	3-diap-1/thread th	lhum_diap1
WING-Apoptosis	8-dcp-1	lhum_dcp-1
WING-D/V pattern	10-serrate	Lhum_serrate
WING-D/V pattern	11-mindbomb	Lhum_mindbomb
WING-D/V pattern	12-dsrf(blistered)	Lhum_blistered
WING-D/V pattern	13-notum/wingful	Lhum_notum
WING-D/V pattern	14-Hipk	Lhum_hipk
WING-D/V pattern	15-tartan/capricious	Lhum_tartan-capricious-likeA
WING-D/V pattern	16-tartan/capricious	Lhum_tartan-capricious-likeB
WING-D/V pattern	17-arrow	Lhum_arrow
WING-D/V pattern	18-dally	Lhum_dally
WING-D/V pattern	19-nemo	Lhum_nemo
WING-D/V pattern	1-wingless	Lhum_wingless
WING-D/V pattern	20-armadillo	Lhum_armadillo
WING-D/V pattern	21-suppressor of hairless(Su(H))	Lhum_suppressorofhairless
WING-D/V pattern	22-Nipped-A	Lhum_nipped-a
WING-D/V pattern	23-mastermind	Lhum_mastermind
WING-D/V pattern	2-apterous	Lhum_apterous
WING-D/V pattern	3-distaless	Lhum_distal-less
WING-D/V pattern	4-cut	Lhum_cut
WING-D/V pattern	5-scalloped	Lhum_scalloped
WING-D/V pattern	6-vestigial	Lhum_vestigial
WING-D/V pattern	7-delta	Lhum_delta
WING-D/V pattern	8-fringe	Lhum_fringe
WING-D/V pattern	9-notch	Lhum_notch
WING-muscle dev	23 -mef2	lhum_mef2
WING-muscle dev	24 -spl1	lhum_spl1
WING-muscle identity	18-twist	lhum_twist

Figure S4. Neighbor joining tree of DNA methyltransferases using the BLOSUM 62 matrix (made using Jalview, 22). The tree includes Dnmts from two mammal species, *Homo s*apiens and *Mus musculus*, for reference (only *Dnmt3b* shown for reference).

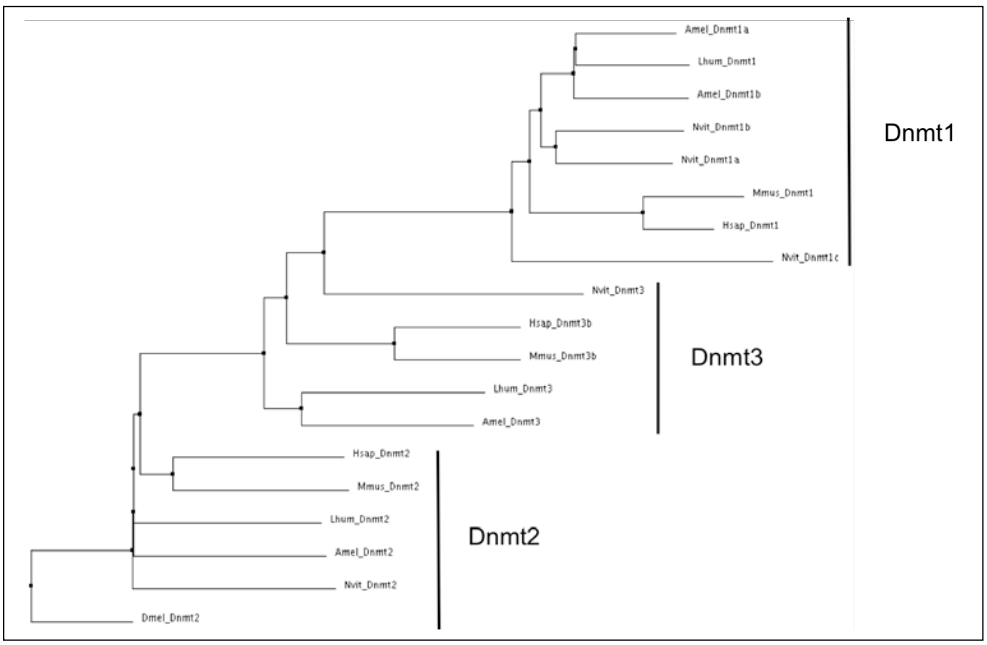

Cytoplasmic ribosomal protein genes

Up to 10% of a cell's protein inventory is estimated to be an integral part of its ribosomes, the macromolecular complexes that catalyze protein synthesis in all organisms (24). While ribosomal RNA lies both structurally and functionally at the heart of each ribosome, a suite of peripherally arranged ribosomal proteins fulfills many critical roles pertaining to the assembly and stability of the complex. Riboproteins are, however, far more than 'RNA glue' – many serve as a binding platform for other factors in the translational process, and mediate the manifold molecular interactions of the ribosome (25). In one particular example, RACK1 (now recognized as an integral ribosomal component, 26) links several signal transduction pathways to the ribosome and can thus regulate translation in response to cell stimuli. It may also be involved in the regulation of specific mRNA translation, and the recruitment of ribosomes to sites that

require a localized boost of protein synthesis (27). In addition, various extra-ribosomal functions have been described for some ribosomal proteins, lending credibility to the hypothesis that they were co-opted from a set of pre-existing proteins during the evolution of the ribosome from a RNA-only complex to a ribonucleoprotein particle (28). In concurrence with their indispensable role, ribosomal proteins are highly conserved within eukaryotes, both in terms of number and sequence. Cytoplasmic ribosomes contain about 80 proteins (CRPs) that are encoded by a variable number of genes (mitochondrial ribosomes, being of prokaryotic origin, possess a slightly different protein makeup). However, it is widely believed that in animals, only one gene copy acts as the principal template for each riboprotein (29, 30). Conservedness and wide genomic distribution – as found in *D. melanogaster* and humans (29, 31) – make riboprotein genes ideally suited to evaluate the coverage and fidelity of both genome assemblies and automatically annotated gene sets.

Gene models coding for the cytoplasmic ribosomal proteome of *L. humile* were identified by performing a BLAST search against the OGS1.1. Ribosomal protein sequences of *D. melanogaster* from FlyBase (http://flybase.org) served as query sequences. These models were inspected and edited if necessary, using Apollo (21). Care was taken to ensure that the predicted gene structures matched corresponding transcriptomic data. Models were also aligned to homologous protein sequences from *D. melanogaster* and *A. mellifera* (the latter obtained from the Ribosomal Protein Gene Database, http://ribosome.med.miyazaki-u.ac.jp) using the default parameters in MAFFT v6 (32) to monitor the integrity of the reading frame and the extent of the predicted coding domains. Gene homology relations were inferred by querying the annotated *D.*

melanogaster proteins deposited at FlyBase with the translated gene models. Best reciprocal BLAST hits were interpreted as orthologs (33). Non-functional gene copies were identified by searching the *L. humile* genome assembly using the TBLASTN program and the *D. melanogaster* CRP sequences as queries, with the low complexity filter disabled and the e-value cut-off set to 10^{-4}. The same strategy was employed to assess the number of CRP genes in *N. vitripennis*.

A total of 83 genes were found in the *L. humile* genome, encoding the full set of 79 cytoplasmic ribosomal proteins recognized in insect and mammalian genomes (29, 31). Four proteins are represented by two genes (RpS16, RpS23, RpS28 and RpS30); these duplicates seem to have arisen in evolutionary recent time, as is indicated by identical gene structures and an average sequence identity of 97% between the pairs.

In addition, we identified the *receptor of activated c kinase* (RACK1), which is now known to be a constituent ribosomal protein even though it is not counted among the 'traditional' CRPs. Two CRP-like genes (*RpL24-like* and *RpLP0-like*) that are presumably of ancient origin and present in all eukaryotic genomes (29) were also found, although their functions remain unknown. As in other animals, three genes, *RpL40*, *RpS27A* and *RpS30*, code for fusion proteins that consist of ubiquitin or ubiquitin-like sequences at the N-terminus and the respective CRPs at the C-terminal end. All of the above-mentioned genes are represented by EST data and thus transcriptionally active, although it can be hypothesized that only one copy of each duplicate pair acts as the primary gene, while the other one is generally expressed at considerably lower levels (29, 30).

Evidence for non-functional gene copies was scarce. Lack of EST support, a

truncated open reading frame and comparably low similarity to its mother gene *RpL18*, indicate the presence of a single pseudogene. In contrast to the *D. melanogaster* genome, and particularly the human genome with its thousands of processed CRPs pseudogenes (30), no pseudogenes derived from retrotransposition events were discovered.

Overall, the CRP gene repertoire of the Argentine ant shows high similarity to that of other insects. The number of genes and recent duplicates is within the same range as in *D. melanogaster* (88 genes), *A. mellifera* (80 genes) and *N. vitripennis* (79 genes), and the average sequence identity compared to the *D. melanogaster* orthologs is 77% (range: 52–100%). The high sequence similarity to the reference genes made it possible to reliably identify sequencing errors that resulted in reading frame shifts or premature stop codons. Relative to the total number of nucleotide positions coding for CRP genes (including RACK1), the five cases of presumable sequencing error that were discovered indicate one erroneous position in every 8300 nucleotides. The fidelity of the assembly sequence thus amounts to an excellent 99.988 % in coding regions of the genome, comparable to the accuracy achievable with Sanger technology. The completeness of the gene set also suggests that the *L. humile* genome assembly thoroughly covers the gene space of the genome. Further evidence for the quality of the assembly is given by the fact that no instances of scaffold misassembly could be identified during the annotation of the CRP genes.

Oxidative phosphorylation

The oxidative phosphorylation (OXPHOS) pathway produces ATP, the major source of cellular energy, by utilizing a proton gradient across the inner mitochondrial membrane. This pathway is unique in its composition; incorporating 67 nuclear-encoded genes as

well as all 13 mitochondrial protein-coding genes (34). These mitochondrial genes tend to accumulate substitutions more quickly than nuclear genes, potentially leading to incompatibility with the nuclear genes with which they normally interact. This may lead to selective pressure on the nuclear genes to compensate for the mitochondrial change (35). This potentially very rapid evolution within a highly functionally constrained pathway may implicate this pathway in hybrid incompatibility between recently diverged populations.

We found evidence for 79 nuclear encoded OXPHOS genes in the genome sequence of *L. humile*, compared to the 81 reported in *D. melanogaster* (36). Of the *D. melanogaster* genes, 14 are duplicated from the other 67 "core" nuclear encoded OXPHOS genes). One of these core genes (*cox7a*) is missing from the *L. humile* genome assembly. This gene is also not found in *A. mellifera* but is found in other holometabolous insects, including *N. vitripennis*, which may indicate that this is a deletion specific to aculeate hymenopterans. One of the 79 *L. humile* genes may be a processed pseudogene, since it is the result of a duplication and contains the full transcript in a single exon. There appear to be eight *L. humile*-specific duplications (not including the aforementioned pseudogene) that are not found in other taxa. All of the conserved copies of these duplications (that is, the copy that is most similar to the *D. melanogaster* reference gene) have EST support, consistent with the relatively high expression level of the nuclear encoded OXPHOS genes. However, all but one of the divergent copies had no EST support, indicating that these genes may have been co-opted for a different purpose.

Single nucleotide polymorphisms (SNPs)

Since the genomic reads used for the *L. humile* assembly were derived from multiple diploid females (1 queen pupa and ~100 workers) (Table S1), it was possible to identify single nucleotide polymorphisms (SNPs) from the natural genetic diversity captured in the raw reads. Such SNP-rich regions might indicate genes or regulatory regions under selection and since our genomic sequences were from the introduced range, these SNPs could be excluded from other polymorphisms that differ in the native range.

We used the Roche gsMapper tool and custom Perl scripts to identify SNPs in the V0.4 Celera assembly of the *L. humile* genome. Briefly, individual unpaired 454 and Illumina reads were mapped back to the reference assembly using the Roche gsMapper tool. We intentionally only evaluated cases in which a single nucleotide in one read had another single base transition or transversion mutation and omitted cases of insertions and deletions. Custom Perl scripts were used to extract SNPs that were present in 10% or more of the reads and to identify C->T and T->C SNPs followed by a G. All SNP data were converted to GFF3, then loaded into the Chado database to determine intersections with InterProScan and other results. Overall, we discovered a total of 381,232 SNPs with two supporting reads and 231,248 with three or more overlapping reads where the SNP is present in at least 10% of the read data. Overall, single base transition mutations accounted for 78.84% of SNPs, while transversions accounted for 21.15%. In the main text we report results for all single base SNPs occurring in at least three reads and in more than 10% of mapped reads. The top 100 ranked genes with SNPs can be found in Table S3.

Table S3. Top 100 genes containing the most SNPs. The total number of SNPs present in at least hree reads and 10% of mapped reads were tabulated over the exons for OGS1.1 and manually annotated genes. The genes with the highest number of SNPs per kilobase (kb) are listed in ranked order along with the predicted function based on InterProScan and GO analyses. Genes that also rank in the top 100 genes with a CG<->TG SNP are listed with an asterisk.

L. humile Gene ID	# SNPs	Sum Exon Length (bp)	# SNP/kb	Interproscan/GO Function
LH10736	66	763	87	Unknown
LH15115	48	610	79	Unknown
LH10737*	140	1992	70	Unknown
LH14822	23	337	68	Unknown
LH10484	39	574	68	Unknown
LH10768	19	281	68	Male sterility, NAD-binding
LH10490	17	253	67	ATP synthesis coupled proton transport
LH11476*	30	447	67	Unknown
LH15774	54	807	67	Zinc finger, C2CH-type
LH10566	28	421	67	Unknown
LH10738	107	1702	63	Unknown
LH24234	26	425	61	MoeA, N-terminal, domain I and II
LH19459*	114	1922	59	Glucose-methanol-choline oxidoreductase
LH13364	47	800	59	Unknown
LH23737	17	293	58	Unknown
LH11566	17	301	56	Male sterility, NAD-binding
LH10423	34	602	56	Maternal tudor protein
LH10777	20	355	56	Unknown
LH13452	21	397	53	Cellular retinaldehyde-binding/triple function
LH10522	18	347	52	Cytochrome b/b6
LH19086	18	356	51	Cytochrome P450
LH10523	12	238	50	Respiratory-chain NADH dehydrogenase
LH10151	21	421	50	Unknown
LH14397	29	587	49	Retrotransposon
LH10668	13	267	49	Alanyl tRNA synthetase
LH14471	30	641	47	Male sterility, NAD-binding
LH11410	17	369	46	S-adenosyl-L-methionine-dependent methyltransferases
LH10428	35	763	46	Unknown
LH18354	34	752	45	Protein tyrosine phosphatase activity
LH10554	83	1861	45	Zinc finger, CCHC-type
LH23198	26	589	44	Unknown
LH10564	15	340	44	Unknown
LH14669	13	296	44	Unknown
LH15116*	60	1397	43	Unknown
LH10361	11	258	43	Cytochrome P450
LH20971	11	269	41	Unknown
LH10002	21	517	41	Unknown
LH15114	63	1552	41	Male sterility, NAD-binding

LH12438	28	690	41	Retroviral Protease-related
LH14791	23	580	40	Unknown
LH23196	17	436	39	Unknown
LH13453	11	286	38	Cellular retinaldehyde-binding/triple function
LH10295	17	442	38	Cytochrome P450
LH20452	11	289	38	Male sterility, NAD-binding
LH12750	23	614	37	Unknown
LH22547	65	1814	36	Beta-ketoacyl synthase
LH14710	28	789	35	Unknown
LH10691	9	255	35	Unknown
LH10371	17	484	35	Zinc finger, CCHC-type
LH10368	8	229	35	EGF-like
LH12706	36	1043	35	Unknown
LH10485	16	466	34	Unknown
LH10031	30	877	34	Unknown
LH10275	21	615	34	Unknown
LH10294	14	410	34	Cytochrome P450
LH10175	18	528	34	Unknown
LH15775	11	324	34	Unknown
LH10223	26	767	34	Beta-ketoacyl synthase
LH10240	13	386	34	Unknown
LH10172	8	239	33	Cytochrome P450
LH24208	58	1744	33	M,I,L,Y,V Aminoacyl-tRNA synthetase, class I
LH10528	7	212	33	Unknown
LH23634	16	499	32	Unknown
LH20022	9	284	32	Unknown
LH19133	20	639	31	Unknown
LH10562	11	352	31	Unknown
LH13944	28	904	31	Unknown
LH10118	8	260	31	Beta-ketoacyl synthase
LH11789	38	1237	31	Male sterility, NAD-binding
LH11587	37	1207	31	Unknown
LH23651	26	850	31	Zinc finger, C2CH-type
LH10713	4	131	31	Unknown
LH10769	23	766	30	Cellular retinaldehyde-binding/triple function
LH10557	9	300	30	Unknown
LH23236	13	434	30	Unknown
LH10539	6	202	30	Unknown
LH10845	17	586	29	Cellular retinaldehyde-binding/triple function
LH10221	34	1174	29	Unknown
LH23116	37	1279	29	Unknown
LH14821	10	346	29	Unknown
LH10861	21	730	29	Unknown
LH19443	33	1150	29	Nose resistant to fluoxetine-4
LH15067	28	978	29	Unknown
LH18214	18	629	29	Copper ion homeostasis
LH18957	38	1340	28	Unknown
LH10061	12	425	28	Collagen alpha
LH15199	16	567	28	FAD-dependent pyridine nucleotide-disulphide oxidoreductase

LH15106	21	745	28	Unknown
LH10510	8	284	28	Cytochrome P450
LH14782	22	786	28	Unknown
LH10194	10	358	28	Unknown
LH10072	41	1486	28	EGF-like
LH11848	21	769	27	Unknown
LH13469	6	221	27	Histone Acetyl Transferase Dimerization
LH13456	13	487	27	Unknown
LH11735	30	1133	26	General trancription factor 2-related
LH15598	14	529	26	Zinc finger, CCHC-type
LH22726	9	345	26	Unknown
LH10292	23	884	26	Unknown

L. humile Gene ID	# SNPs	Sum Exon Length (bp)	# SNP/kb	**Interproscan/GO Function**

Table S8. Top 100 genes containing the most CG <-> TG SNPs. The total number of CG->TG and TG->CG SNPs present in at least 10% of mapped reads were tabulated over the introns and exons for OGS1.1 and manually annotated genes. The genes with the highest number of SNPs are listed in ranked order along with the predicted function based on InterProScan and GO analyses. Genes that also rank in the top 100 genes with any SNP are listed with an asterisk.

***L. humile* Gene ID**	**# CG <->TG SNPs**	**Interproscan/GO Function**
LH22547*	26	Beta-ketoacyl synthase
LH10223*	13	ABC transporter
LH19567	12	ABC transporter
LH15114*	12	Male sterility, NAD-binding
LH13099	12	Unknown
LH21678	11	Major facilitator superfamily general substrate transporter
LH19774	11	Zinc finger, C6HC-type
LH12438*	11	Retroviral Protease-related
LH10072*	11	EGF-like
LH14263	11	Immunoglobulin-like fold
LH10281*	11	Male sterility, NAD-binding
LH10324	10	Helicase-related
LH11824	10	Beta-ketoacyl synthase
LH10984	10	Syntaxin/epimorphin, conserved site
LH23430	10	Maternal tudor protein
LH12427	10	Unknown
LH17005	10	Unknown
LH15975	10	Protein kinase C, phorbol ester/diacylglycerol binding
LH10554*	9	Zinc finger, CCHC-type
LH23822	8	Acetylcholine Receptor Protein Alpha 1, 2, 3, 4
LH10737	8	Unknown
LH19108*	8	Carboxylesterase, type B
LH16800	8	Unknown
LH24790	8	Guanine nucleotide exchange factor for Ras-like GTPases, N-terminal

LH19987	8	Unknown
LH25151	8	Serine/threonine protein kinase
LH11485	8	Tetratricopeptide region
LH14375	8	TonB box
LH12706*	8	Unknown
LH14824	8	Rab GTPase activator activity
LH21310	8	Peptidase M2, peptidyl-dipeptidase A
LH19459	8	Glucose-methanol-choline oxidoreductase
LH21309	8	EGF-like
LH14856	7	Glycoside hydrolase, family 47
LH15643	7	EGF-like
LH15694	7	Cytochrome P450
LH16977	7	Low density lipoprotein-receptor, class A / serine-type endopeptidase
LH16271	7	Peptidase S8 and S53, subtilisin, kexin, sedolisin
LH10850	7	Cytochrome P450
LH24147	7	Guanine nucleotide exchange factor for Ras-like GTPases
LH11563	7	Restriction endonuclease, type II-like
LH15429	7	Helix-turn-helix, Psq
LH22089	7	Pyridoxal phosphate-dependent decarboxylase
LH17329	7	Unknown
LH18215	7	Zinc finger, LIM-type
LH16950	7	Cholesterol transporter
LH14700*	7	Unknown
LH17535	6	Plectin/Plakin repeat
LH23698	6	Tyrosyl-DNA phosphodiesterase
LH11284	6	Peptidase S54, rhomboid
LH19447	6	Formate C-acetyltransferase
LH10442*	6	Ribonuclease H-like
LH15166	6	Zinc finger, SWIM-type
LH22562	6	Multidrug resistance ABC transporter MsbA
LH17034	6	Fibronectin, type III-like
LH12749*	6	Unknown
LH14073	6	Fibronectin, type III-like
LH16922	6	Armadillo-like helical
LH12090	6	Calcium-binding EF-hand
LH17201	6	Dynein heavy chain
LH14988	6	Transmembrane 4 Superfamil, Invertebrate
LH20348	6	Pyridoxal phosphate-dependent transferase
LH22813	6	Family A G protein-coupled receptor-like
LH13835	6	Peptidase M14, carboxypeptidase A
LH15363	6	Zinc finger, C2H2-type
LH16103	6	Vestigial/tondu
LH18363	6	Acyltransferase ChoActase/COT/CPT
LH19470	6	Unconventional myosin/plant kinesin-like protein/non-motor protein conserved region MyTH4
LH20070	6	Eukaryotic translation initiation factor 3 subunit 8
LH22201	6	Adenylosuccinate synthetase
LH19132	6	Beta-ketoacyl synthase
LH11476	6	Unknown
LH23873	6	Exonuclease, RNase T and DNA polymerase III

LH23224	6	Pleckstrin homology-type
LH22559	6	Toll-Interleukin receptor
LH21367	6	HLH, helix-loop-helix DNA-binding domain
LH15624	6	Unknown
LH17494	6	Zinc finger, SWIM-type
LH13503	6	Eukaryotic type KH-RNA binding domain
LH15116	6	Unknown
LH22554	6	Fatty Acid Desaturase
LH12365	6	Unknown
LH20017	5	Nose resistant to fluoxetine-4
LH24965	5	Peptidase S8 and S53, subtilisin, kexin, sedolisin
LH22590	5	Unknown
LH10979	5	Spermadhesin, CUB domain
LH20799	5	Troponin
LH12319	5	Huntington Associated Protein
LH13791	5	WD40/YVTN repeat-like
LH22256	5	Peptidase M1, membrane alanine aminopeptidase
LH13741	5	Serine/threonine protein kinase
LH14883	5	Sterile alpha motif homology
LH18967	5	Formin binding protein-related, Arthropod
LH17974	5	Unknown
LH16209	5	Unknown
LH13522	5	Lissencephaly-1 protein
LH16463	5	Spermadhesin, CUB domain
LH24778	5	SCY1-related Serine/Thereonine Kinase-like
LH22593	5	Armadillo-like
LH20546	5	Protein serine/threonine phosphatase 2C

Repetitive DNA

We analyzed the repeat content of the *L. humile* genome using RepeatMasker (37) and the RepeatRunner (19) subroutine that is integrated into the MAKER annotation pipeline (Table 2)(8). One difficulty in the analysis of metazoan genomes is that repeat libraries from even closely related species often fail to identify potential repetitive regions, making it necessary to create *de novo* repeat libraries. In addition to 30 known microsatellites for *L. humile*, we generated *de novo* repeat libraries using RepeatModeler (v1.03) and PILER-DF. RepeatModeler integrates RECON (38), TRF (39), and RepeatScout (40) data and classifies repeats with the RepBase Repeatmasker library. We also used PILER-DF (9) to identify regions from whole genome self-alignments that were present three or more times. We then screened for false positives using BLASTX against

known *D. melanogaster* genes (Release 5.25).

Initial runs of PILER-DF and RepeatModeler against the *L. humile* genome assembly returned 554 total raw repeat predictions of which RECON, RepeatScout, and PILER-DF generated 362, 135, and 57, respectively (Table 2). We then removed 16 redundant sequences that were greater than 80% identical over 80% of their length and identified 15 sequences to be false positives via a BLASTX analysis against known genes. Alignments displaying sequence identities greater than a threshold value while scoring higher than 30 bits were manually checked for homology to repetitive gene clusters such as histones and *Stellate* elements, well-conserved functional sites, or genes with repetitive exon structures such as *mucin* or *dumpy*. The sequence identity threshold was iteratively relaxed until diminishing returns converged to zero at 50% sequence identity. At each iteration, sequences identified as false positives were culled from the repeat library. In addition, we found additional LTRs and DNA transposons using a custom script to identify long terminal repeats (LTR) and terminal inverted repeats (TIR) at the terminal ends of unclassified repeat predictions.

Published data for the honeybee (*A. mellifera*, 41) and jewel wasp (*N. vitripennis*, 42) genomes illustrate two extremes of genomic repeat composition for Hymenoptera: the honeybee is AT-rich (67%) but devoid of all except a few mariner (43) and rDNA-specific R2 (44) transposable elements, while *Nasonia* has an AT content (58%) similar to other *D. melanogaster* (56%) and numerous retroid elements. The *L. humile* genome assembly has a 62% AT composition, intermediate to *Nasonia* and *Apis*, but also contains 23.6Mb (11%) of interspersed TEs. A total of 7,828 retroid and 8,720 DNA transposon fragments were identified, however, the majority of interspersed elements (67,928,

17.1Mb, 6.8% of genome) were identified with *de novo* predications and could not be classified to a specific TE family. We discovered most known families of transposable elements with the exception of L1 and CRE/SLAC LINE-like elements. Gypsy/DIR1 and R1/LOA/Jockey elements were the most abundant retroid elements and Tc1 repeats were the most abundant DNA TEs.

Viruses and viroids

Viruses specifically infecting hymenopterans have been reported for the red imported fire (*Solenopsis invicta*, 45, 46) and *A. mellifera* (47), and may play a significant role in colony survival and fitness. We screened the *L. humile* genome for the presence of 1778 sequenced virus and viroid genomes and report TBLASTX hits that had bit scores greater than 100 or had more than 50% of the virus aligned in the genome with 50% or greater sequence identity. This analysis yielded ~300 significantly aligning regions spanning over 400 kilobases (Table S4). Previous studies in *N. vitripennis* identified poxvirus-associated PRANC domains in the genome that appeared to be laterally transferred from *Wolbachia* endosymbionts. We downloaded *Nasonia*-defined PRANC domains from www.treebase.org (Study #S10521) and used them to train a custom hidden Markov model using HHMER 3.0 (48). We then scanned the *L. humile* genome using this HMM, but could not identify statistically significant PRANC domains.

Table S4. Viral and viroid DNA. Viruses and viroids found in the *L. humile* genome, ranked by total number of bases aligned by TBLASTX. Viruses & viroids restricted to insect (orange), plant or algae (green), microbes (purple), vertebrates (grey), or unknown (white) are indicated. *, Iridoviridae also infect fish, amphibians, and reptiles.

Virus Family	Bases Aligned
Baculoviridae	144,777
Polydnaviridae	112,214
Caulimoviridae	59,001
Poxviridae	45,497
Phycodnaviridae	26,643
Unclassified dsDNA viruses	8,762
Mimiviridae	8,564
Herpesvirales	7,395
Iridoviridae*	6,526
Ascoviridae	5,031
Caudovirales	3,981
Apscaviroid	1,923
Pospiviroid	1,629
Nimaviridae	1,542
Cocaviroid	1,503
Coleviroid	924
Hostuviroid	486
Avsunviroid	459
Unclassified phage	282
Asfarviridae	222
Unclassified viroids	186
TOTAL	**437,781 bp**

KEGG, InterProScan, and Gene Ontology Analysis

We used InterProScan (49) and KEGG (50) (Fig. S2, Table S5) to identify putative functional domains and looked for enriched Gene Ontology (GO) gene functions both in the species-specific genes identified from the *L. humile* OGS1.1 and for all Argentine ant genes relative to *D. melanogaster*, *A. mellifera*, and *N. vitripennis* (Tables S6 and S7). We analyzed the complete set of *L. humile* MAKER predictions (15,345) and *ab initio* gene predictions (29,206) with InterProScan and KEGG to identify gene regions with similarity to known functional domains. Raw InterProScan results were parsed using custom Perl scripts to generate a Gene Ontology GAF2.0 file that was used as an input to identify enriched Gene Ontology terms using Go-Term-Finder v0.86 (51)

(http://search.cpan.org/dist/GO-TermFinder/). For comparative purposes we performed a similar GO enrichment analysis on the *D. melanogaster* GO annotations (geneontology.org, 52). Since we were unaware of an existing GO annotation for the *A. mellifera* and *N. vitripennis* genomes, we generated one using InterProScan analysis of the 'preOGS2 honeybee peptides' and OGS1.2 *Nasonia* peptides (www.beebase.org). Enrichments were tested for statistical significance using a Fisher exact test with Bonferroni correction and a 0.05 false discovery rate.

In total, 23,575 GO terms were reported for *L. humile*. This is a similar proportion of the genes as in other Hymenoptera, but distinct from *D. melanogaster* (Tables S6 and S7). This difference may, however, be partially due to ascertainment bias, as all three Hymenoptera had automated annotations, whereas *D. melanogaster* genomes are human-curated with biological verification.

Figure S2. Overview of annotated KEGG pathways. Brightly shaded lines indicate pathways with *L. humile* genes that have been annotated in OGS1.1. Specific KEGG maps can be downloaded from http://HymenopteraGenome.org/linepithema/genome_consortium/datasets.html

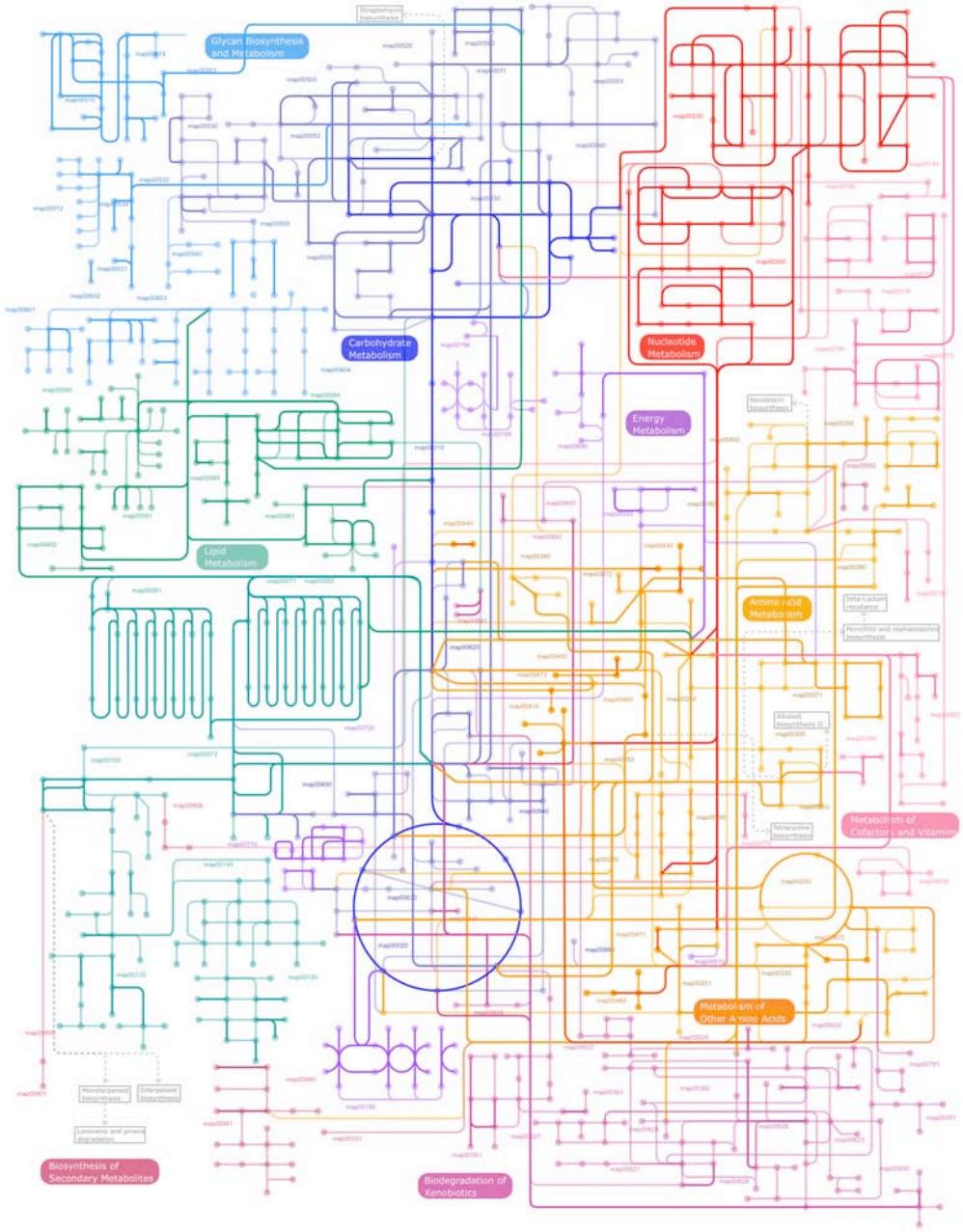

Figure S3. GO enrichment figures. GO terms for *L. humile*-specific genes were compared to the genome-wide statistics and evaluated for enrichment using Go-Term-Finder. The number of genes annotated with each GO terms are shown along with the percentage indicidence for *L. humile*-specific genes (blue) and all *L. humile* genes (red). P-value for enrichements are indicated to the right. Yellow highlighting indicates example GO terms that describe genes seen to have expansions in *L. humile* from other data in this study. GO cellular location terms are highlighted in green.

A)

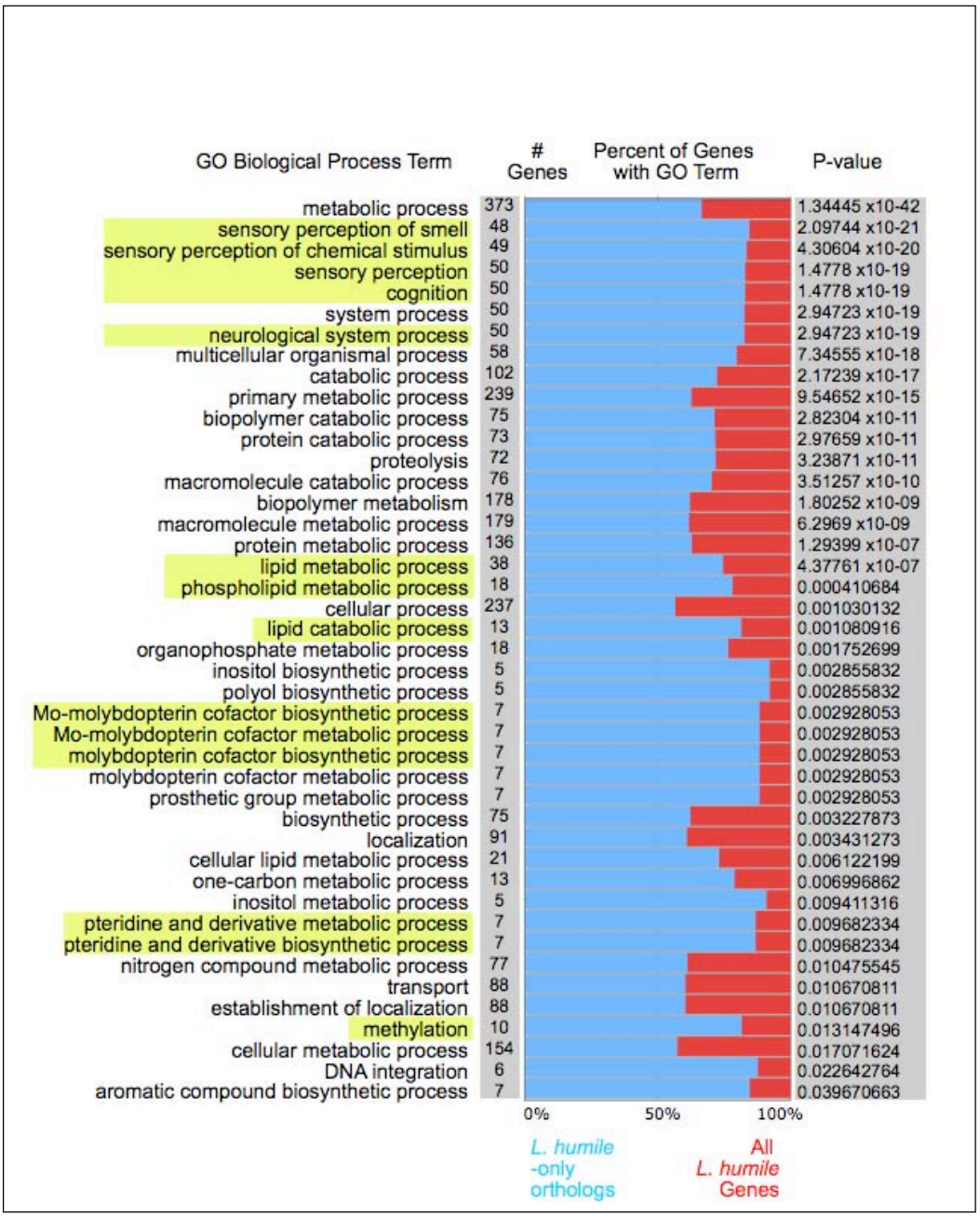

B)

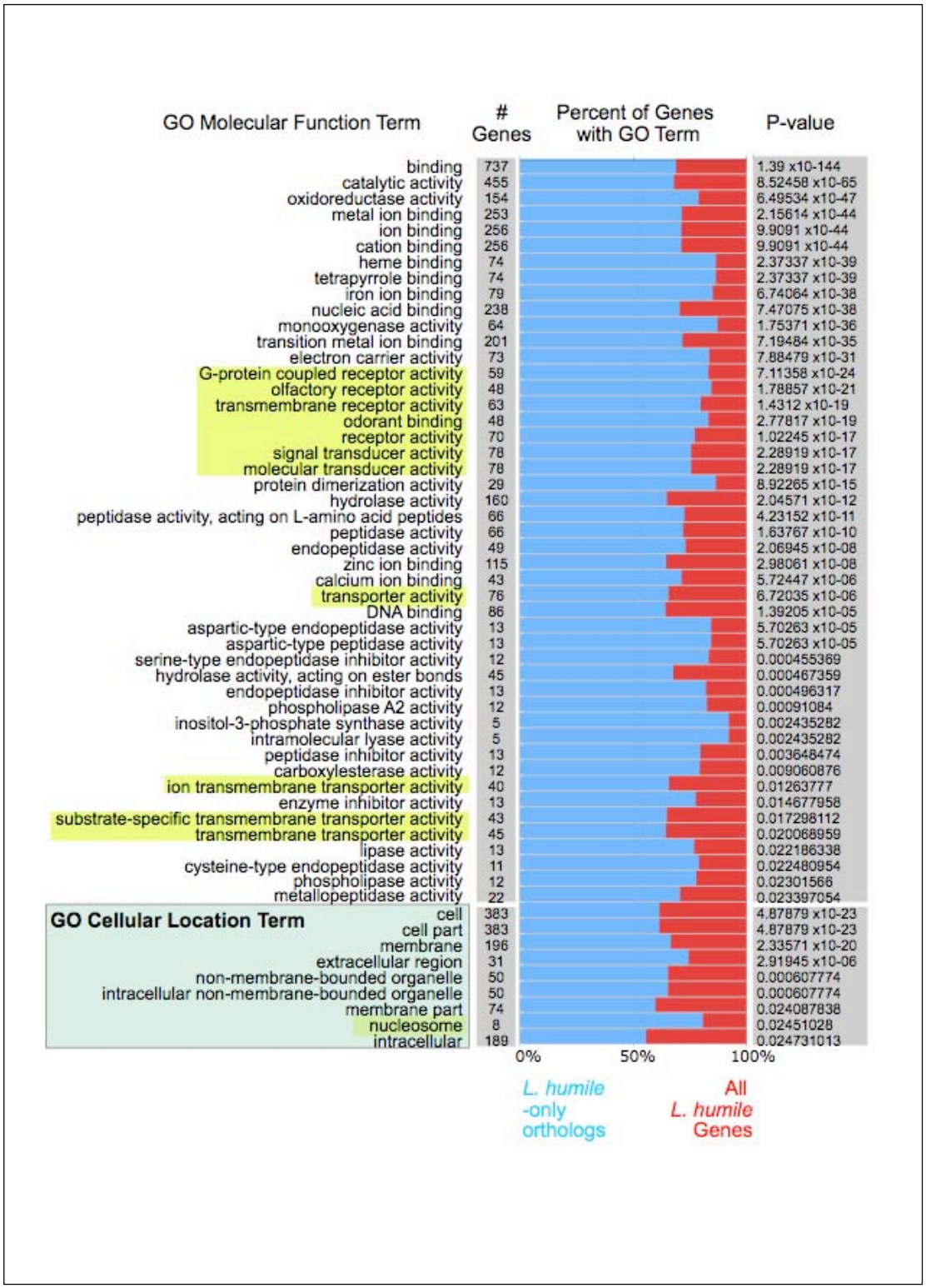
GO Molecular Function Term
Genes
Percent of Genes with GO Term
P-value
binding 737 1.39 x10-144
catalytic activity 455 8.52458 x10-65
oxidoreductase activity 154 6.49534 x10-47
metal ion binding 253 2.15614 x10-44
ion binding 256 9.9091 x10-44
cation binding 256 9.9091 x10-44
heme binding 74 2.37337 x10-39
tetrapyrrole binding 74 2.37337 x10-39
iron ion binding 79 6.74064 x10-38
nucleic acid binding 238 7.47075 x10-38
monooxygenase activity 64 1.75371 x10-36
transition metal ion binding 201 7.19484 x10-35
electron carrier activity 73 7.88479 x10-31
G-protein coupled receptor activity 59 7.11358 x10-24
olfactory receptor activity 48 1.78857 x10-21
transmembrane receptor activity 63 1.4312 x10-19
odorant binding 48 2.77817 x10-19
receptor activity 70 1.02245 x10-17
signal transducer activity 78 2.28919 x10-17
molecular transducer activity 78 2.28919 x10-17
protein dimerization activity 29 8.92265 x10-15
hydrolase activity 160 2.04571 x10-12
peptidase activity, acting on L-amino acid peptides 66 4.23152 x10-11
peptidase activity 66 1.63767 x10-10
endopeptidase activity 49 2.06945 x10-08
zinc ion binding 115 2.98061 x10-08
calcium ion binding 43 5.72447 x10-06
transporter activity 76 6.72035 x10-06
DNA binding 86 1.39205 x10-05
aspartic-type endopeptidase activity 13 5.70263 x10-05
aspartic-type peptidase activity 13 5.70263 x10-05
serine-type endopeptidase inhibitor activity 12 0.000455369
hydrolase activity, acting on ester bonds 45 0.000467359
endopeptidase inhibitor activity 13 0.000496317
phospholipase A2 activity 12 0.00091084
inositol-3-phosphate synthase activity 5 0.002435282
intramolecular lyase activity 5 0.002435282
peptidase inhibitor activity 13 0.003648474
carboxylesterase activity 12 0.009060876
ion transmembrane transporter activity 40 0.01263777
enzyme inhibitor activity 13 0.014677958
substrate-specific transmembrane transporter activity 43 0.017298112
transmembrane transporter activity 45 0.020068959
lipase activity 13 0.022186338
cysteine-type endopeptidase activity 11 0.022480954
phospholipase activity 12 0.02301566
metallopeptidase activity 22 0.023397054
GO Cellular Location Term
cell 383 4.87879 x10-23
cell part 383 4.87879 x10-23
membrane 196 2.33571 x10-20
extracellular region 31 2.91945 x10-06
non-membrane-bounded organelle 50 0.000607774
intracellular non-membrane-bounded organelle 50 0.000607774
membrane part 74 0.024087838
nucleosome 8 0.02451028
intracellular 189 0.024731013
0%
50%
100%
L. humile -only orthologs
All L. humile Genes

Table S6. Summary of GO Slim Terms for *L. humile*, *N. vitripennis*, *A. mellifera*, and *D. melanogaster*. GO terms were 'slimmed' using the Amigo online tool. Percent of genes mapped to each GO term is shown for each species. Blue cells indicate terms that are represented fewer times than *D. melanogaster*, while yellow stippled cells are found a higher percent of the time than in fruitfly. Frequencies comparable to *Drosophila* are shaded grey.

BIOLOGICAL PROCESS	*L. humile*	*N. vitripennis*	*A. mellifera*	*D. melanogaster*
biological_process	11.62	11.52	11.52	16.36
transport	1.52	1.61	1.5	1.57
cell communication	0.7	0.69	0.71	1.3
signal transduction	0.61	0.58	0.6	0.93
ion transport	0.39	0.49	0.4	0.21
response to stress	0.36	0.35	0.35	0.64
transcription	0.34	0.35	0.33	0.33
generation of precursor metabolites and energy	0.32	0.37	0.29	0.11
protein transport	0.25	0.32	0.22	0.24
cell cycle	0.18	0.14	0.18	0.89
cell death	0.11	0.12	0.11	0.3
death	0.11	0.12	0.11	0.32
response to external stimulus	0.09	0.06	0.09	0.38
growth	0.07	0.06	0.07	0.22
regulation of gene expression, epigenetic	0.07	0.06	0.07	0.16
reproduction	0.05	0.06	0.07	**1.09**
cell-cell signaling	0.05	0.06	0.07	0.3
cell differentiation	0.05	0.03	0.04	**1.72**
response to abiotic stimulus	0.05		0.04	0.33
cell proliferation	0.02	0.03	0.02	0.14
response to biotic stimulus	0.02	0.03	0.02	0.2
cell growth	0.02		0.02	0.05
MOLECULAR FUNCTIONS				
molecular_function	16.31	15.99	16.52	11.08
catalytic activity	10.85	10.2	11.1	6.45
transferase activity	3.49	2.94	3.65	2.38
hydrolase activity	3	3.23	3.05	1.82
binding	2.86	3.17	2.81	2.4
transporter activity	1.45	1.41	1.48	1.28
kinase activity	1.07	0.89	1.02	0.69
protein binding	0.91	0.98	0.91	1.05
enzyme regulator activity	0.68	0.72	0.69	0.41
signal transducer activity	0.57	0.49	0.69	0.81
nucleic acid binding	0.52	0.58	0.46	0.42
peptidase activity	0.48	0.52	0.46	0.17
receptor activity	0.45	0.37	0.57	0.65
nuclease activity	0.41	0.52	0.42	0.23
protein kinase activity	0.34	0.23	0.31	0.36

ion channel activity	0.32	0.35	0.33	0.27
transcription regulator activity	0.29	0.37	0.31	0.17
DNA binding	0.27	0.29	0.22	0.16
receptor binding	0.25	0.23	0.22	0.27
lipid binding	0.23	0.26	0.22	0.12
nucleotide binding	0.18	0.2	0.2	0.07
cytoskeletal protein binding	0.14	0.17	0.13	0.15
RNA binding	0.14	0.14	0.13	0.2
structural molecule activity	0.14	0.14	0.15	0.11
carbohydrate binding	0.11	0.12	0.11	0.06
phosphoprotein phosphatase activity	0.09	0.12	0.09	0.09
translation factor activity, nucleic acid binding	0.09	0.12	0.09	0.04
antioxidant activity	0.09	0.12	0.09	0.05
translation regulator activity	0.09	0.12	0.09	0.06
chromatin binding	0.05	0.06	0.04	0.03
motor activity	0.05	0.06	0.04	0.03
actin binding	0.05	0.06	0.04	0.02
transcription factor activity	0.02	0.03	0.02	0.01
neurotransmitter transporter activity	0.02	0.03	0.02	0.04
calcium ion binding	0.02	0.03	0.02	0.01
oxygen binding	0.02		0.02	0.01

CELLULAR LOCATION

cellular_component	3.83	4.06	3.69	3.54
cell	3.59	3.77	3.47	3.36
intracellular	3.02	3.17	2.87	2.66
cytoplasm	1.52	1.67	1.41	1.2
nucleus	0.61	0.52	0.57	0.74
mitochondrion	0.29	0.37	0.31	0.24
cytoskeleton	0.27	0.32	0.29	0.39
nucleoplasm	0.27	0.23	0.27	0.31
plasma membrane	0.25	0.26	0.24	0.35
chromosome	0.2	0.26	0.2	0.34
endoplasmic reticulum	0.2	0.26	0.18	0.11
Golgi apparatus	0.18	0.23	0.18	0.12
extracellular region	0.14	0.14	0.13	0.12
cytosol	0.09	0.12	0.09	0.09
ribosome	0.09	0.06	0.09	0.04
nuclear chromosome	0.07	0.09	0.07	0.12
vacuole	0.07	0.09	0.07	0.04
peroxisome	0.07	0.09	0.07	0.02
external encapsulating structure	0.02	0.06	0.04	0.02
cell envelope	0.02	0.06	0.04	0.01
extracellular space	0.02	0.03	0.02	0.03
nucleolus	0.02	0.03	0.02	0.03
lysosome	0.02	0.03	0.02	0.02
microtubule organizing center	0.02	0.03	0.02	0.08

Table S7. GO terms from *L. humile*-specific genes that are enriched relative to *D. melanogaster*, *A. mellifera*, and *N. vitripennis*.

GO ID	GO Term	p-value	Ontology Aspect	# Genes
GO:0005623	cell	5.72E-13	Cell Loc	3396
GO:0044464	cell part	5.72E-13	Cell Loc	3396
GO:0005622	intracellular	2.44E-05	Cell Loc	2134
GO:0044456	synapse part	1.96E-04	Cell Loc	43
GO:0045202	synapse	1.96E-04	Cell Loc	43
GO:0045211	postsynaptic membrane	4.47E-04	Cell Loc	41
GO:0043167	ion binding	1.63E-20	Molc Fxn	1463
GO:0043169	cation binding	1.63E-20	Molc Fxn	1463
GO:0046872	metal ion binding	1.14E-19	Molc Fxn	1424
GO:0005509	calcium ion binding	8.41E-16	Molc Fxn	245
GO:0008270	zinc ion binding	2.96E-09	Molc Fxn	892
GO:0046914	transition metal ion binding	1.87E-08	Molc Fxn	1119
GO:0004674	protein serine/threonine kinase activity	1.68E-07	Molc Fxn	201
GO:0004803	transposase activity	6.51E-05	Molc Fxn	29
GO:0004623	phospholipase A2 activity	8.76E-05	Molc Fxn	36
GO:0005488	binding	1.98E-04	Molc Fxn	4713
GO:0004190	aspartic-type endopeptidase activity	4.06E-04	Molc Fxn	34
GO:0070001	aspartic-type peptidase activity	4.06E-04	Molc Fxn	34
GO:0004091	carboxylesterase activity	2.04E-03	Molc Fxn	44
GO:0004620	phospholipase activity	2.37E-03	Molc Fxn	48
GO:0016298	lipase activity	8.88E-03	Molc Fxn	55
GO:0016042	lipid catabolic process	1.59E-05	Biol Proc	42
GO:0006313	transposition, DNA-mediated	8.45E-05	Biol Proc	29
GO:0032196	transposition	8.45E-05	Biol Proc	29
GO:0007165	signal transduction	1.36E-04	Biol Proc	502
GO:0007154	cell communication	1.95E-04	Biol Proc	534
GO:0007264	small GTPase mediated signal transduction	7.17E-04	Biol Proc	92
GO:0032501	multicellular organismal process	9.12E-03	Biol Proc	208
GO:0050794	regulation of cellular process	2.71E-02	Biol Proc	1075
GO:0065007	biological regulation	3.11E-02	Biol Proc	1075
GO:0006644	phospholipid metabolic process	3.77E-02	Biol Proc	71
GO:0019637	organophosphate metabolic process	4.88E-02	Biol Proc	78
GO:0007242	intracellular signaling cascade	2.13E-02	Biol Proc	195

Table S5. KEGG automated annotation server (KAAS) annotation results. The total number of nodes in KEGG pathways were manually tallied and used to calculate percent coverage for each pathway. Individual KEGG pathway maps are available from http://genomes.arc.georgetown.edu/drupal/linepithema/?q=genome_consortium_datasets

KEGG Map #	Pathway Name	Total # of KEGG nodes	# *L. humile* OGS1.1 Genes Mapped to Map	% Pathway Coverage
10	Glycolysis / Gluconeogenesis	52	24	44.2
20	Citrate cycle (TCA cycle)	27	22	85.2
30	Pentose phosphate pathway	42	15	35.7
40	Pentose and glucuronate interconversions	61	9	14.8
51	Fructose and mannose metabolism	70	16	21.4
52	Galactose metabolism	50	11	22.0
53	Ascorbate and aldarate metabolism	53	4	7.5
61	Fatty acid biosynthesis	178	5	2.8
62	Fatty acid elongation in mitochondria	34	6	17.6
71	Fatty acid metabolism	83	18	21.7
72	Synthesis and degradation of ketone bodies	6	5	83.3
100	Steroid biosynthesis	72	4	4.2
120	Primary bile acid biosynthesis	46	3	6.5
130	Ubiquinone and other terpenoid-quinone biosynthesis	27	8	25.9
140	Steroid hormone biosynthesis	134	4	2.2
190	Oxidative phosphorylation	189	79	42.3
195	Photosynthesis	65	0	0.0
230	Purine metabolism	167	80	50.3
232	Caffeine metabolism	28	1	7.1
240	Pyrimidine metabolism	106	62	60.4
250	Alanine, aspartate and glutamate metabolism	45	21	46.7
260	Glycine, serine and threonine metabolism	71	19	25.4
270	Cysteine and methionine metabolism	82	16	19.5
280	Valine, leucine and isoleucine degradation	56	26	46.4
281	Geraniol degradation	17	0	0.0
290	Valine, leucine and isoleucine biosynthesis	33	7	21.2
300	Lysine biosynthesis	37	5	16.2
310	Lysine degradation	61	21	34.4

330	Arginine and proline metabolism	59	23	39.0
340	Histidine metabolism	42	5	9.5
350	Tyrosine metabolism	111	15	12.6
351	1,1,1-Trichloro-2,2-bis(4-chlorophenyl)ethane (DDT) degradation	12	1	8.3
360	Phenylalanine metabolism	52	9	13.5
361	gamma-Hexachlorocyclohexane degradation	40	6	15.0
362	Benzoate degradation via hydroxylation	58	3	6.9
363	Bisphenol A degradation	16	2	6.3
380	Tryptophan metabolism	78	13	16.7
400	Phenylalanine, tyrosine and tryptophan biosynthesis	45	3	6.7
401	Novobiocin biosynthesis	35	2	5.7
410	beta-Alanine metabolism	36	13	36.1
430	Taurine and hypotaurine metabolism	20	4	20.0
440	Phosphonate and phosphinate metabolism	15	3	26.7
450	Selenoamino acid metabolism	22	9	40.9
460	Cyanoamino acid metabolism	21	3	9.5
471	D-Glutamine and D-glutamate metabolism	13	2	15.4
480	Glutathione metabolism	61	18	31.1
500	Starch and sucrose metabolism	90	17	17.8
510	N-Glycan biosynthesis	38	32	84.2
511	Other glycan degradation	9	9	100.0
512	O-Glycan biosynthesis	14	2	14.3
513	High-mannose type N-glycan biosynthesis	15	1	6.7
514	O-Mannosyl glycan biosynthesis	13	1	7.7
520	Amino sugar and nucleotide sugar metabolism	40	25	62.5
521	Streptomycin biosynthesis	16	6	37.5
523	Polyketide sugar unit biosynthesis	32	1	3.1
524	Butirosin and neomycin biosynthesis	25	1	4.0
531	Glycosaminoglycan degradation	21	11	52.4
532	Chondroitin sulfate biosynthesis	18	7	38.9
533	Keratan sulfate biosynthesis	19	2	10.5
534	Heparan sulfate biosynthesis	30	10	36.7
561	Glycerolipid metabolism	42	18	38.1
562	Inositol phosphate metabolism	38	23	57.9
563	Glycosylphosphatidylinositol (GPI)-anchor biosynthesis	23	15	69.6

564	Glycerophospholipid metabolism	70	33	44.3
565	Ether lipid metabolism	31	7	22.6
590	Arachidonic acid metabolism	55	5	12.7
591	Linoleic acid metabolism	15	3	20.0
592	alpha-Linolenic acid metabolism	25	2	8.0
600	Sphingolipid metabolism	46	16	34.8
601	Glycosphingolipid biosynthesis - lacto and neolacto series	16	3	12.5
603	Glycosphingolipid biosynthesis - globo series	19	3	15.8
604	Glycosphingolipid biosynthesis - ganglio series	38	2	5.3
620	Pyruvate metabolism	73	22	30.1
623	2,4-Dichlorobenzoate degradation	33	1	0.0
624	1- and 2-Methylnaphthalene degradation	37	4	10.8
625	Tetrachloroethene degradation	11	1	0.0
626	Naphthalene and anthracene degradation	47	3	6.4
628	Fluorene degradation	28	1	3.6
630	Glyoxylate and dicarboxylate metabolism	63	10	19.0
631	1,2-Dichloroethane degradation	5	1	20.0
632	Benzoate degradation via CoA ligation	54	8	16.7
633	Trinitrotoluene degradation	15	0	6.7
640	Propanoate metabolism	53	15	28.3
641	3-Chloroacrylic acid degradation	9	3	33.3
642	Ethylbenzene degradation	19	1	5.3
643	Styrene degradation	26	4	11.5
650	Butanoate metabolism	53	16	30.2
660	C5-Branched dibasic acid metabolism	19	1	5.3
670	One carbon pool by folate	28	12	42.9
680	Methane metabolism	34	6	20.6
710	Carbon fixation in photosynthetic organisms	35	13	37.1
720	Reductive carboxylate cycle CO2	14	7	50.0
730	Thiamine metabolism	25	3	12.0
740	Riboflavin metabolism	16	4	25.0
750	Vitamin B6	35	4	8.6
760	Nicotinate and nicotinamide metabolism	58	6	12.1
770	Pantothenate and CoA biosynthesis	29	7	27.6
780	Biotin metabolism	17	2	11.8
785	Lipoic acid metabolism	8	3	37.5

790	Folate biosynthesis	35	8	22.9
830	Retinol metabolism	41	6	12.2
860	Porphyrin and chlorophyll metabolism	86	17	19.8
900	Terpenoid backbone biosynthesis	22	11	45.5
901	Indole alkaloid biosynthesis	28	1	3.6
903	Limonene and pinene degradation	39	6	20.5
908	Zeatin biosynthesis	16	1	6.3
910	Nitrogen metabolism	69	9	13.0
920	Sulfur metabolism	29	4	13.8
930	Caprolactam degradation	23	3	13.0
940	Phenylpropanoid biosynthesis	70	2	1.4
944	Flavone and flavonol biosynthesis	32	1	3.1
945	Stilbenoid, diarylheptanoid and gingerol biosynthesis	25	1	4.0
950	Isoquinoline alkaloid biosynthesis	48	4	8.3
960	Tropane, piperidine and pyridine alkaloid biosynthesis	19	5	21.1
965	Betalain biosynthesis	15	1	6.7
970	Aminoacyl-tRNA biosynthesis	21	25	119.0
980	Metabolism of xenobiotics by cytochrome P450	36	6	13.9
981	Insect hormone biosynthesis	21	5	28.6
982	Drug metabolism - cytochrome P450	60	6	8.3
983	Drug metabolism - other enzymes	32	16	50.0
1040	Biosynthesis of unsaturated fatty acids	28	6	28.6
1051	Biosynthesis of ansamycins	39	1	2.6
1055	Biosynthesis of vancomycin group antibiotics	34	1	2.9
2010	ABC transporters	304	10	3.6
2020	Two-component system	249	4	1.6
3010	Ribosome	143	83	60.1
3018	RNA degradation	71	47	64.8
3020	RNA polymerase	46	24	52.2
3022	Basal transcription factors	26	23	88.5
3030	DNA replication	46	31	65.2
3040	Spliceosome	77	101	131.2
3050	Proteasome	52	35	65.4
3060	Protein export	23	21	82.6
3070	Bacterial secretion system	21	2	9.5
3320	PPAR signaling pathway	53	14	26.4
3410	Base excision repair	60	21	35.0

3420	Nucleotide excision repair	51	34	66.7
3430	Mismatch repair	30	17	53.3
3440	Homologous recombination	55	18	34.5
3450	Non-homologous end-joining	20	7	30.0
4010	MAPK signaling pathway	125	60	47.2
4011	MAPK signaling pathway - yeast	57	8	15.8
4012	ErbB signaling pathway	60	26	41.7
4013	MAPK signaling pathway - fly	30	15	43.3
4020	Calcium signaling pathway	48	28	60.4
4060	Cytokine-cytokine receptor interaction	299	7	2.0
4062	Chemokine signaling pathway	50	35	70.0
4070	Phosphatidylinositol signaling system	43	23	51.2
4080	Neuroactive ligand-receptor interaction	90	26	28.9
4110	Cell cycle	81	68	82.7
4111	Cell cycle - yeast	118	55	44.9
4112	Cell cycle - Caulobacter	31	2	6.5
4114	Oocyte meiosis	72	43	59.7
4115	p53 signaling pathway	60	19	30.0
4120	Ubiquitin mediated proteolysis	109	78	70.6
4130	SNARE interactions in vesicular transport	35	20	54.3
4140	Regulation of autophagy	23	11	39.1
4142	Lysosome	67	51	76.1
4144	Endocytosis	97	67	67.0
4146	Peroxisome	64	44	68.8
4150	mTOR signaling pathway	30	21	70.0
4210	Apoptosis	60	16	23.3
4260	Cardiac muscle contraction	23	19	87.0
4270	Vascular smooth muscle contraction	46	24	56.5
4310	Wnt signaling pathway	71	54	73.2
4320	Dorso-ventral axis formation	27	17	63.0
4330	Notch signaling pathway	24	19	83.3
4340	Hedgehog signaling pathway	19	19	89.5
4350	TGF-beta signaling pathway	55	27	47.3
4360	Axon guidance	79	29	38.0
4370	VEGF signaling pathway	28	17	64.3
4510	Focal adhesion	60	46	78.3
4512	ECM-receptor interaction	116	12	10.3
4514	Cell adhesion molecules (CAMs)	21	4	23.8
4520	Adherens junction	74	25	33.8
4530	Tight junction	56	31	55.4
4540	Gap junction	43	21	51.2
4610	Complement and coagulation cascades	49	2	4.1

4612	Antigen processing and presentation	42	12	26.2
4614	Renin-angiotensin system	21	3	14.3
4620	Toll-like receptor signaling pathway	78	19	21.8
4621	NOD-like receptor signaling pathway	56	13	21.4
4622	RIG-I-like receptor signaling pathway	52	12	19.2
4623	Cytosolic DNA-sensing pathway	33	9	27.3
4626	Plant-pathogen interaction	74	7	9.5
4630	Jak-STAT signaling pathway	27	16	55.6
4640	Hematopoietic cell lineage	140	2	1.4
4650	Natural killer cell mediated cytotoxicity	82	16	20.7
4660	T cell receptor signaling pathway	59	25	39.0
4662	B cell receptor signaling pathway	38	17	39.5
4664	Fc epsilon RI signaling pathway	40	16	40.0
4666	Fc gamma R-mediated phagocytosis	47	26	57.4
4670	Leukocyte transendothelial migration	79	22	29.1
4672	Intestinal immune network for IgA production	55	0	1.8
4710	Circadian rhythm - mammal	14	5	28.6
4711	Circadian rhythm - fly	17	7	41.2
4712	Circadian rhythm - plant	35	2	5.7
4720	Long-term potentiation	25	17	68.0
4722	Neurotrophin signaling pathway	77	38	44.2
4730	Long-term depression	34	17	52.9
4740	Olfactory transduction	15	6	33.3
4742	Taste transduction	28	3	14.3
4810	Regulation of actin cytoskeleton	71	45	67.6
4910	Insulin signaling pathway	63	46	71.4
4912	GnRH signaling pathway	40	25	62.5
4914	Progesterone-mediated oocyte maturation	39	34	84.6
4916	Melanogenesis	38	28	73.7
4920	Adipocytokine signaling pathway	37	15	37.8
4930	Type II diabetes mellitus	25	11	40.0
4940	Type I diabetes mellitus	23	3	13.0
4950	Maturity onset diabetes of the young	42	6	11.9
4960	Aldosterone-regulated sodium reabsorption	19	11	57.9
4962	Vasopressin-regulated water reabsorption	23	22	100.0

4964	Proximal tubule bicarbonate reclamation	13	7	53.8
5010	Alzheimer's disease	26	80	303.8
5012	Parkinson's disease	38	68	178.9
5014	Amyotrophic lateral sclerosis (ALS)	40	17	42.5
5016	Huntington's disease	64	100	156.3
5020	Prion diseases	57	8	14.0
5110	Vibrio cholerae infection	39	26	66.7
5120	Epithelial cell signaling in Helicobacter pylori infection	50	27	52.0
5130	Pathogenic Escherichia coli infection	47	16	34.0
5140	Leishmania infection	50	9	18.0
5200	Pathways in cancer	210	92	43.8
5210	Colorectal cancer	51	22	43.1
5211	Renal cell carcinoma	50	25	48.0
5212	Pancreatic cancer	44	17	38.6
5213	Endometrial cancer	33	19	60.6
5214	Glioma	58	17	31.0
5215	Prostate cancer	43	23	53.5
5216	Thyroid cancer	20	12	45.0
5217	Basal cell carcinoma	20	18	85.0
5218	Melanoma	26	11	42.3
5219	Bladder cancer	28	8	32.1
5220	Chronic myeloid leukemia	45	21	46.7
5221	Acute myeloid leukemia	35	13	37.1
5222	Small cell lung cancer	37	22	56.8
5223	Non-small cell lung cancer	39	16	41.0
5322	Systemic lupus erythematosus	50	11	22.0
5340	Primary immunodeficiency	46	2	2.2
5410	Hypertrophic cardiomyopathy (HCM)	39	10	23.1
5412	Arrhythmogenic right ventricular cardiomyopathy (ARVC)	59	9	15.3
5414	Dilated cardiomyopathy (DCM)	38	12	31.6
5416	Viral myocarditis	37	8	24.3
	TOTALS	**244**	**245**	

OrthoMCL

We used OrthoMCL v2.0 (53) to identify ortholog groups between between the three Hymenoptera species, *A. mellifera* (preOGS2 41), *N. vitripennis* (OGS1.2, 42), and *L. humile* (OGS1.1, this study) as well as *D. melanogaster* (Release 5.27, 54) OrthoMCL

also identified species-specific gene expansion families (inparalogs) based on BLASTP protein sequence similarity. To avoid complicating orthology-paralogy results, we first reduced each protein dataset using custom Perl scripts to contain only the single longest isoform when multiple isoforms were present. Next, the results from an all-by-all BLAST were parsed determine best reciprocal hits and MCL v09-308 Markov Clustering algorithm was used to define final ortholog, inparalog, and co-ortholog groupings. We used the suggested parameter values and options for OrthoMCL for all steps in the pipeline.

Mitochondrial genome

Animal mitochondrial genomes are approximately 16Kb in length and typically contain 37 genes (55). The mitochondrial sequence of *L. humile* did not fully assemble in the v4.0 genome assembly; the longest scaffold of mitochondrial DNA was 5Kb long and contained >8 genes (partial genes on either end). Using an iterative process of searching

Figure S1. The Argentine ant mitochondrial genome. The general arrangement of the *L. humile* mitochondrial genome based on that of *A. mellifera*. Red dashed lines represent the approximate location of the ends of scaffolds

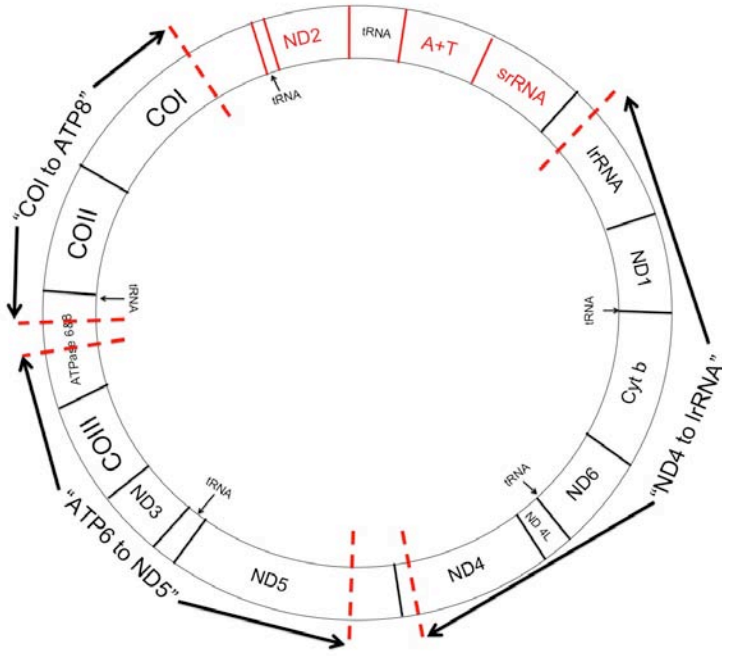

the *L. humile* v4.0 scaffolds, contigs, transcriptome, raw sequencing reads, and *L. humile* mitochondrial sequences deposited at NCBI, we were able to assemble three large scaffolds covering an estimated 77% (12,516bp) of the mitochondrial genome (Fig. S1) (calculated using the *Apis mellifera ligustica* mitochondrial genome as a reference) (56). The program Sequencher v4.5 (Gene Codes Corp. 2005) was used to align and assemble fragments; all merged fragments had at least 20bp of overlap. This assembly at least partially covers 24 genes and there is EST support for 20. This includes 12 of the 13 protein coding genes, 11 of 22 tRNAs and one of the two ribosomal RNAs. The EST support and multiple genes covered by scaffolds is good evidence that none of the scaffolds included in this assembly are of nuclear origin (NuMts). We estimate that the three major scaffolds are separated by two short gaps and one large gap that includes the origin of replication (a highly repetitive AT-rich region) (Fig. S1). There is complete synteny within each scaffold with the *A. mellifera* mitochondrial genome, but without bridging gaps between scaffolds we are not able to judge larger scale synteny. Additionally, the *L. humile* mitochondrial genome appears more similar to *A. mellifera* than *N. vitripennis*, which contained an inversion that resulted in the juxtaposition of COI (+tRNA-L) and ND5 (57). In *L. humile* ND5 and ND3 were recovered within a single scaffold, confirming their proximity and the absence of the inversion seen in *N. vitripennis*.

GC Compositional Domain Analysis

The DNA contains segments that have a characteristic GC-content that differ significantly from the GC-content of adjacent segments. These are referred to as compositional domains. Compositional domains that are compositionally more

homogeneous than the chromosome on which they reside are termed "compositionally homogeneous domains," while a subset of long (≥ 300kb) compositionally homogeneous domains retains the traditional name "isochores." The isochore theory depicts the genome as a mosaic of long homogeneous domains (58); however, this description has been repeatedly refuted (59-61), and a new model has been proposed to describe the complex nature of the genome. The compositional-domain model portrays the genome as a mixture of short and long domains that may be homogeneous or nonhomogeneous in respect to the chromosome on which they reside. Indeed, in all animals studied so far, the distribution of compositional-domain lengths showed an abundance of short domains and a paucity of long ones. The genome of the *L. humile* is no exception in this respect (Table S9). The composition and organization of compositional domains was shaped by different evolutionary processes involving either fusion or fission of domains. By identifying compositional domains over multiple genomes, it is possible to track the evolutionary processes affecting compositional-domain architecture.

Table S9. Distribution of compositional domain lengths.

Order	Species	Number of compositional domains in length group				Total number	Assembly size (Mb)
		1 kb - 10 kb (%)	10 kb - 100 kb (%)	100 kb - 1 Mb (%)	1 Mb - 10 Mb (%)		
Hymenoptera	*L. humile*	31,978 (89)	3,755 (10.5)	188 (0.5)	0 (0)	35,921	250.8
	A. mellifera	42,006 (91.1)	3,944 (8.6)	150 (0.3)	0 (0)	46,100	230
	N. vitripennis	51,064 (92.8)	3,870 (7.0)	72 (0.1)	0 (0)	55,006	240
Coleoptera	*T. castaneum*	15,432 (90.0)	1,535 (8.9)	183 (1.1)	3 (0.02)	17,153	131
Diptera	*A. gambiae*	36,941 (91.5)	3,185 (7.9)	231 (0.6)	0 (0)	40,357	223
	D. melanogaster	12,297 (85.3)	1,973 (13.7)	154 (1.1)	0 (0)	14,424	120

*Number of non-ambiguous nucleotides in the assembly

Recursive segmentation procedures that partition genomic sequences into compositional domains have been shown to be the most accurate segmentation methods (60, 62). Here, we partitioned the genomic sequences into compositional domains using *IsoPlotter*, a segmentation algorithm that employs a dynamic halting criterion (60). IsoPlotter recursively segments the chromosomes by maximizing the difference in GC content between adjacent subsequences. The process of segmentation was terminated when the difference in GC content between two neighboring segments was no longer statistically significant.

We carried out four analyses to study genome architecture in insects. In the first analysis, we calculated the distribution of compositional-domain lengths. For convenience, compositional domains were divided by the order of magnitude of their lengths into short (10^3-10^4 bp), medium (10^4-10^5 bp), and long (10^5-10^7 bp). We, next, tested whether the lengths of compositional domains follow a power-law distribution. The minimum domain length and the power-law exponent were estimated using the method of Clauset, Shalizi, and Newman (63). To test the power-law hypothesis, the observed data were compared to data generated from a power-law distribution and the similarity between the two distributions was calculated using the Kolmogorov-Smirnov statistic (64). Based on the observed goodness-of-fit, we calculated a *p*-value that quantifies the probability that the data were drawn from the hypothesized distribution. We used the Matlab scripts provided by Clauset, Shalizi, and Newman (63) at http://www.santafe.edu/~aaronc/powerlaws/. In the third analysis, we compared the distributions of GC contents of compositional domains. Finally, we compared the compositional-domain GC contents versus their lengths in a log scale.

We computed the genomic distribution of the ratio of observed to expected CpG dinucleotides (CpG(O/E)) by computing CpG(O/E) for each compositional domain and then determining the total number of nucleotides for compositional domains with equivalent CpG(O/E). CpG(O/E) is defined as CpG(O/E) = PCpG/(PC*PG), where PCpG, Pc and PG are the frequencies of CpG dinucleotides, C nucleotides, and G nucleotides, respectively. We also computed the distribution of CpG(O/E) for coding exons and introns, after concatenating coding exons or introns, respectively, for each gene.

We also completed a CpG(O/E) analysis of the genome using a 1kb sliding window over the genome sequence similar to Elango et al (Figure S5). Overall this method produced a distibution comparable to the CpG(O/E) analysis performed on compositional domains.

Figure S5. Dinucleotide NpN Observed/Expected (OE) analysis using 1kb sliding window across genomic scaffolds.

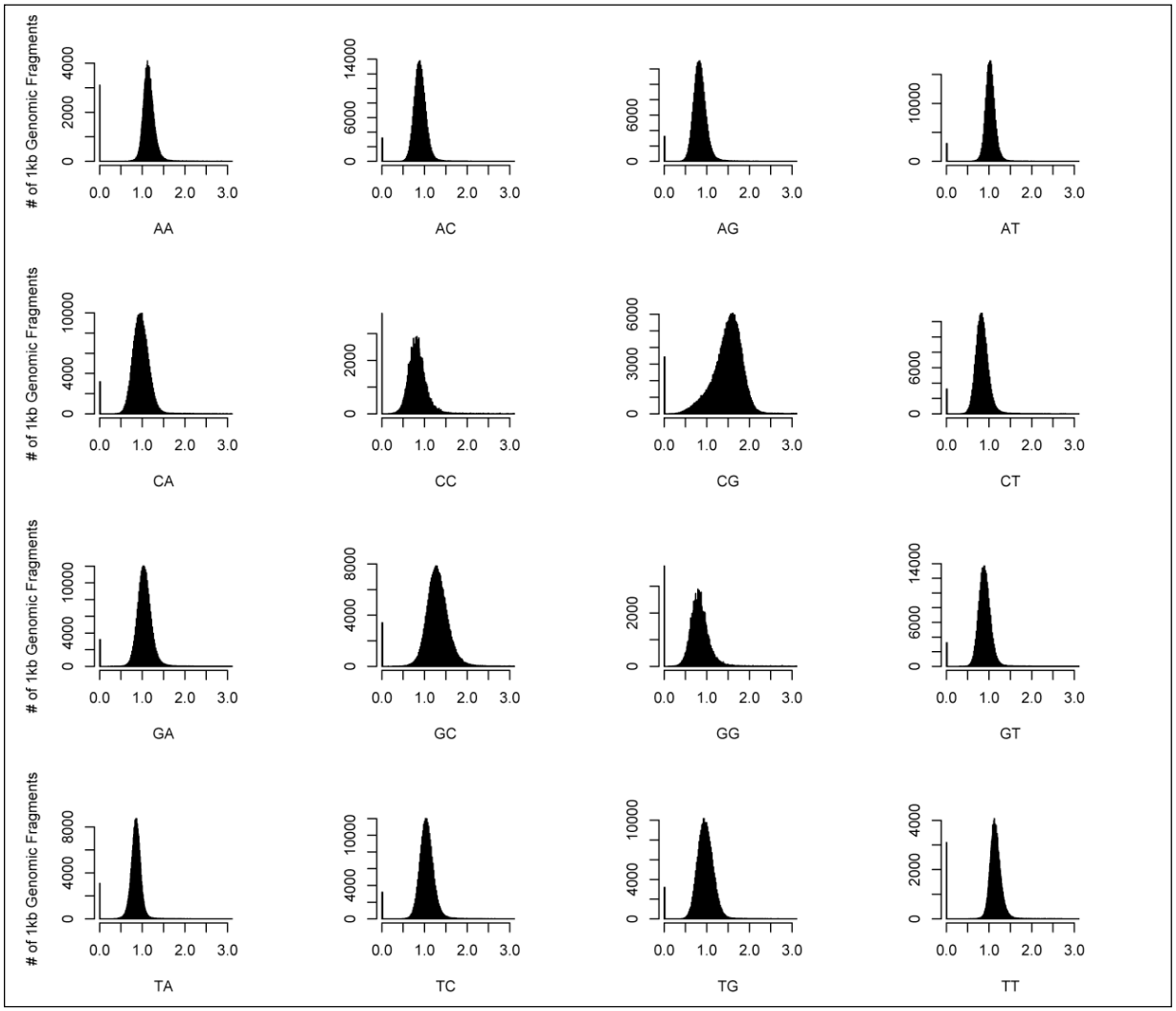

Figure S6. Dinucleotide NpN Observed/Expected (OE) analysis for OGS1.1 genes.

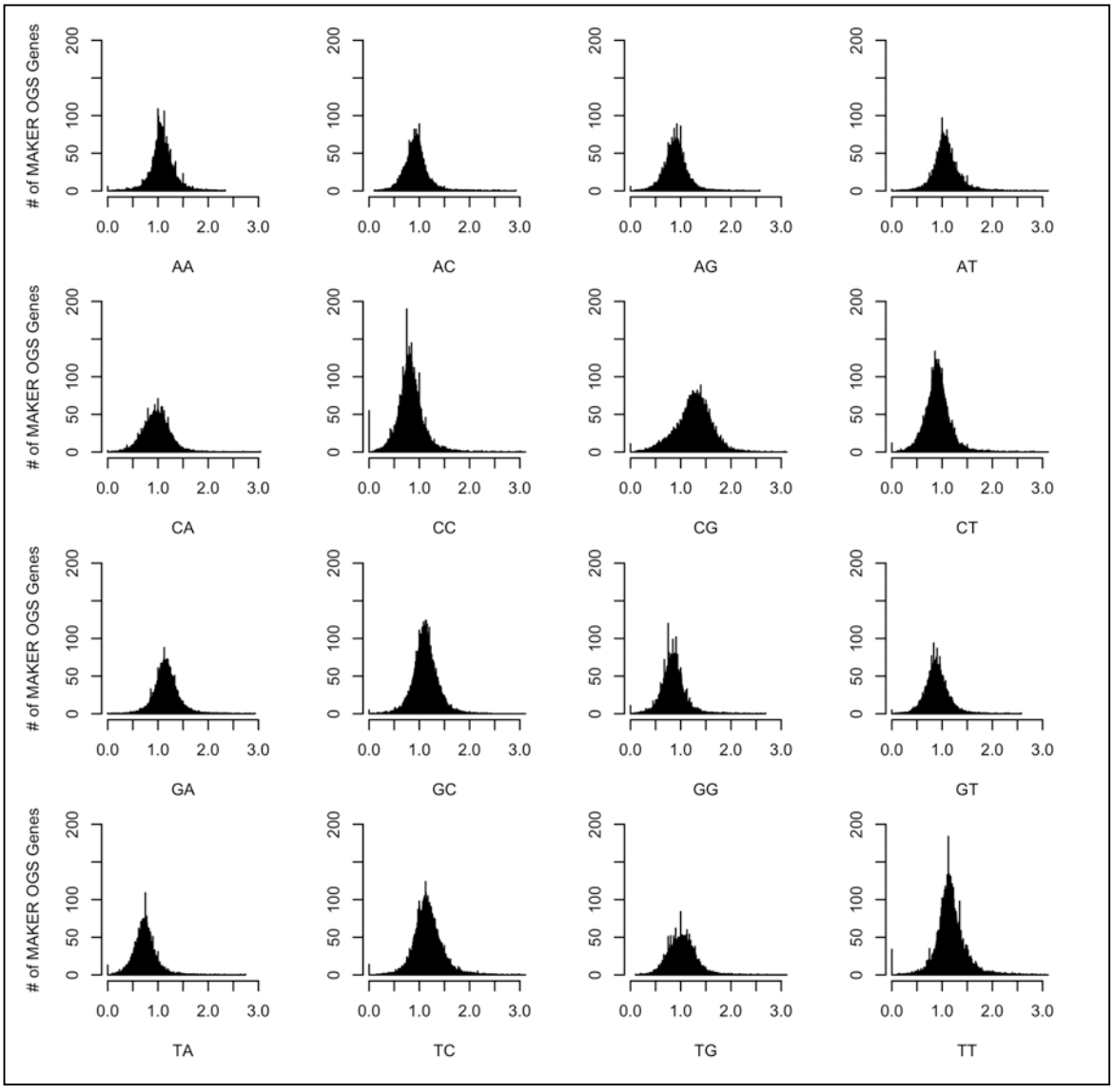

Figure S7. Compositional domain GC content versus compositional domain lengths on a log scale. The middle horizontal line (solid red) represents the mean genome GC content within margins of ± 5% (dashed black).

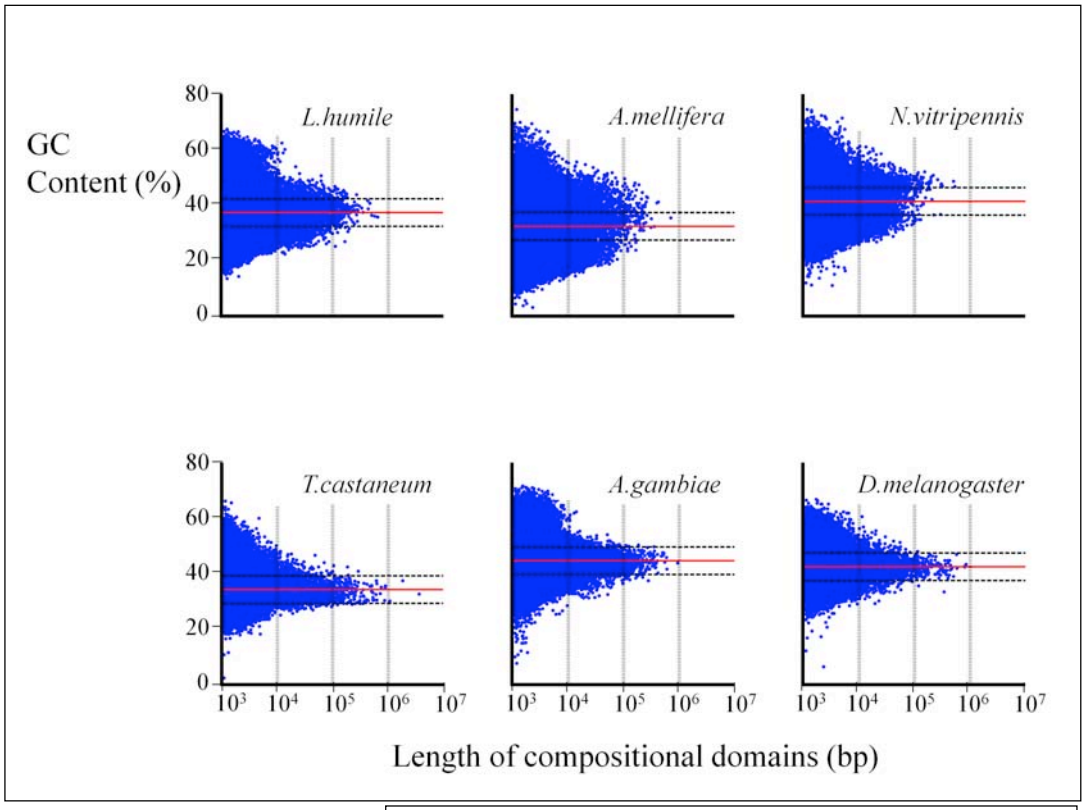

Figure S8. Comparison of GC content of compositional domains in the *L. humile*, *A. mellifera*, *N. vitripennis* and *D. melanogaster*. Cumulative distributions show the fraction of nucleotides in compositional domains containing genes (thick lines) or all genomic compositional domains (thin lines) (< x GC%). Similar to the other hymenopterans, *L. humile* genes tend to occur in the AT-rich parts of the genome.

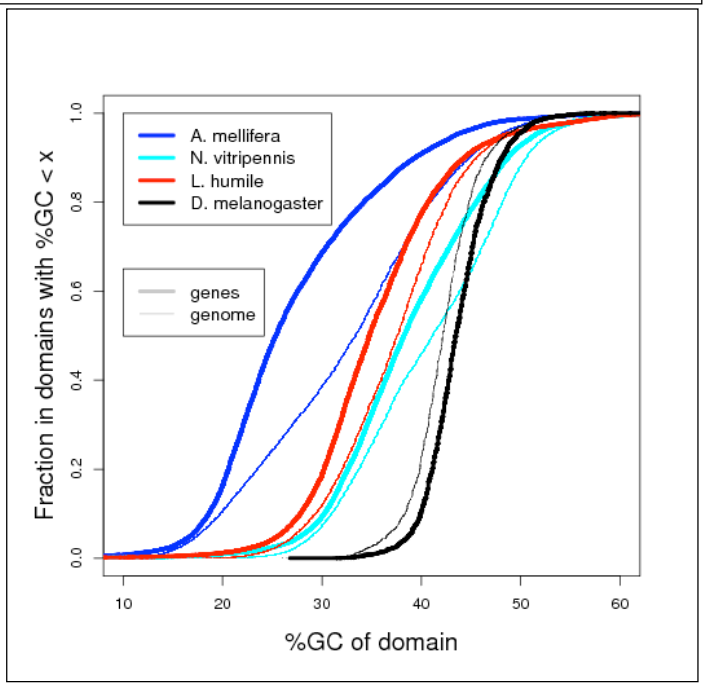

Figure S9. Distribution of GC content in compositional domains, introns and coding exons of *A. mellifera, L. humile* and *N. vitripennis*.

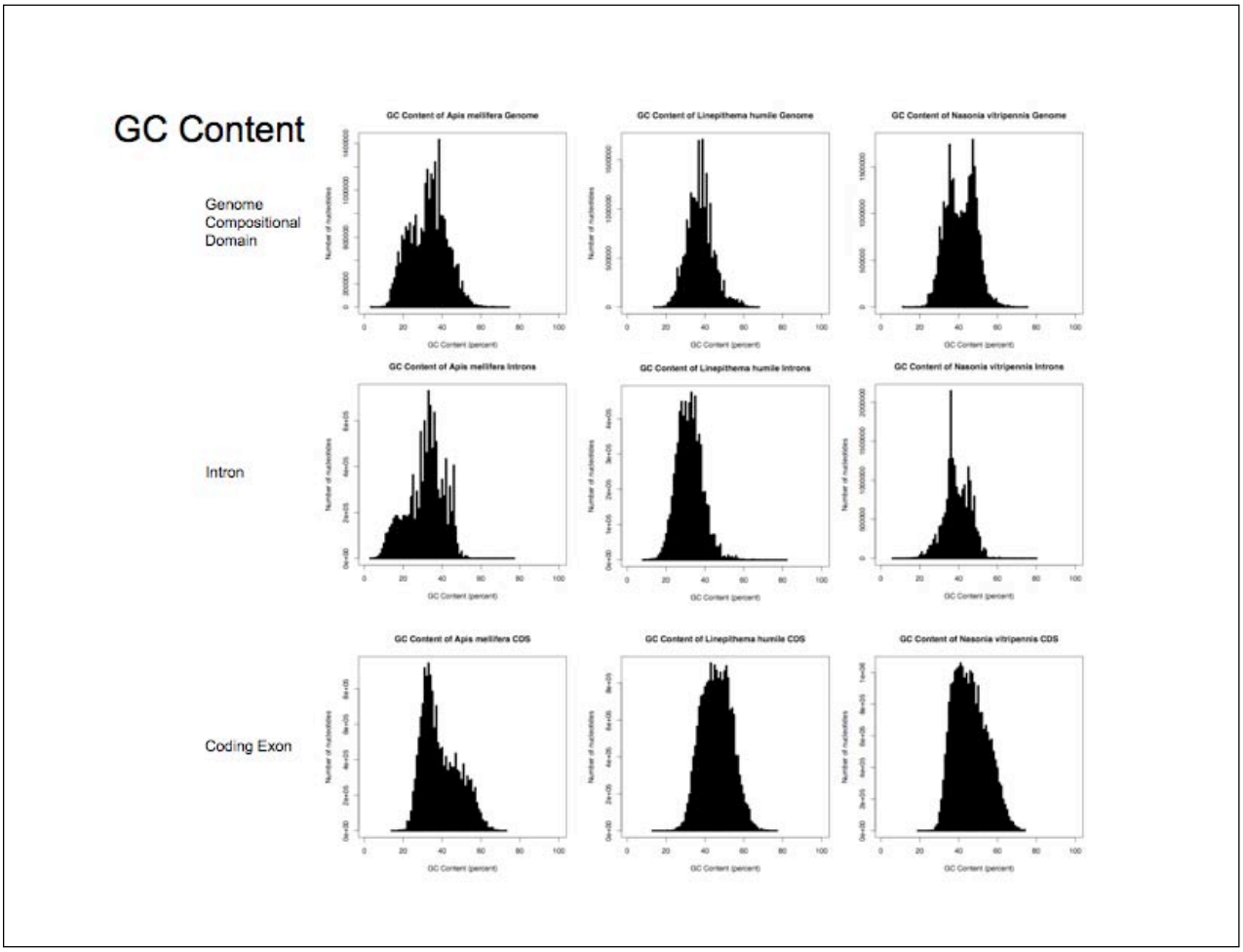

Figure S10. Distribution of CpG(O/E) in compositional domains, introns and coding exons of *A. mellifera*, *L. humile* and *N. vitripennis*.

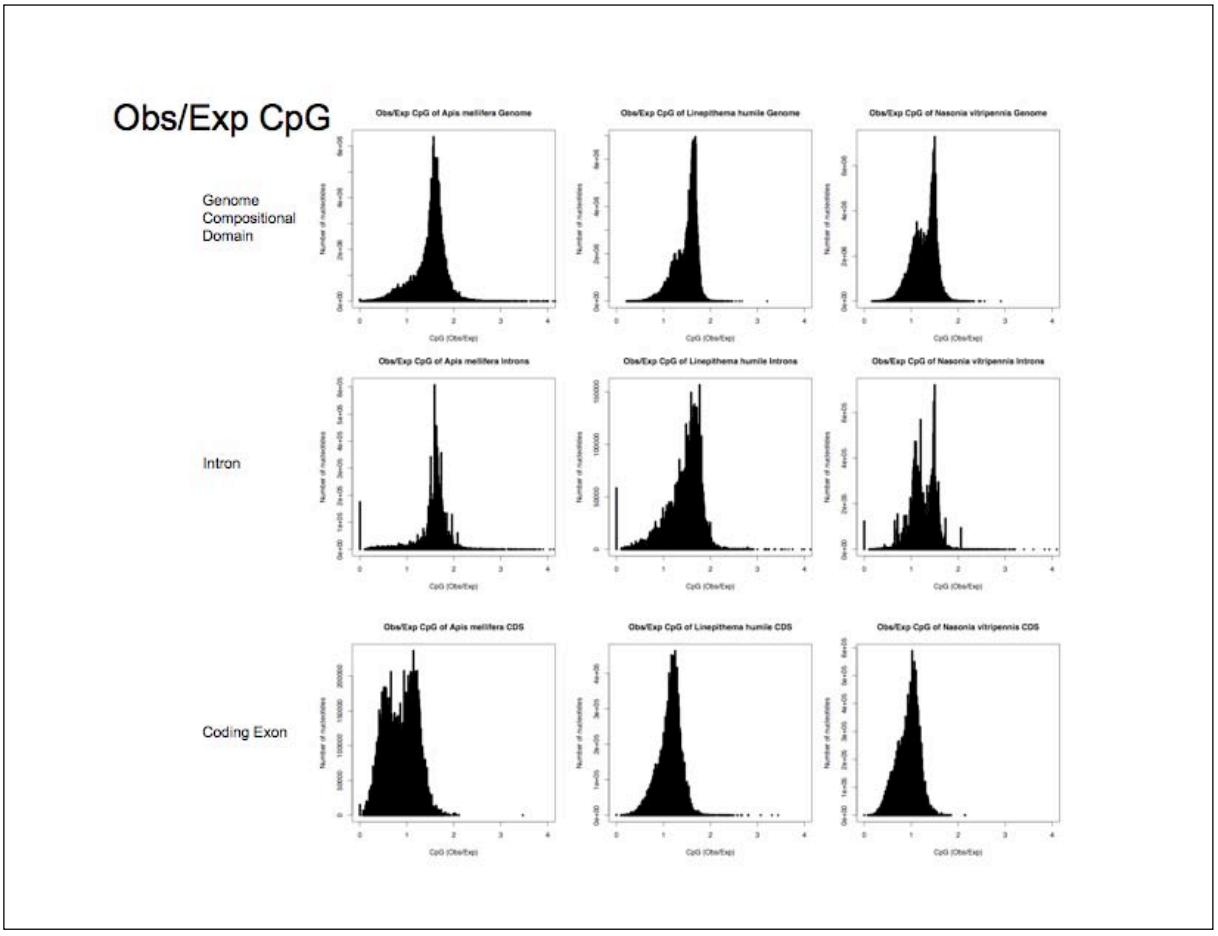

MicroRNAs

To identify miRNAs within the genome of *L. humile* we employed two strategies. The first strategy used previously identified miRNAs to identify conserved homologs in the ant. To do this, we queried the *L. humile* genome with known miRNAs from miRBase release 14.0 (65-67) using BLASTN with a word size of 7 and and e-value threshold $\leq$ 0.001. This query yielded 81 sequences with some degree of sequence similarity to conserved miRNAs from other species. *L. humile* sequence was extracted and included approximately 15 nucleotides of flanking sequence. To assess homology, PRSS (68) was used with 1000 shuffles. This step eliminated several sequences with similarity to murine and plant miRNAs. This is not surprising as these miRNAs are composed of simple sequences. Nucleotide sequence alignments were performed using ClustalW (69), aligning the putative miRNA sequence with known miRNAs from the genome sequences of *A. mellifera*, *N. vitripennis*, and *D. melanogaster*. The putative *L. humile* miRNAs were trimmed to retain the most likely pre-miRNA sequence. RNAfold (70) was finally used to score the folding energy (minimum 20 Kcal/mol) and assess the structure of the pre-miRNA candidates. Our analysis resulted in the identification of 71 conserved *L. humile* miRNAs.

The second strategy for miRNA identification uses three-way genome comparison between *L. humile*, *A. mellifera*, and *N. vitripennis*, for the identification of micro-conserved sequence elements (MCEs). MCEs are typically 20–29 nt in length and have previously been exploited to identify miRNAs (71, 72). The identification of three-way genome intersections results in hundreds of thousands of MCEs across a rather large evolutionary distance (approximately 190 million years). MCEs representing simple sequence repeats were excluded and the remaining sequences were clustered to reduce

redundancy before being mapped back to the genome. Approximately 75 nucleotides of sequence flanking the MCEs were extracted. We mapped the extended *L. humile* sequences to the *N. vitripennis* and *A. mellifera* genomes and retained only those sequences with identifiable homology. With approximately 10,000 sequences remaining in our study, we expect to identify additional miRNA candidates by scoring, and folding the extended sequences, similar to the methods described above.

RNAi

RNA interference (RNAi) is a double-stranded RNA (dsRNA)-mediated gene silencing mechanism through target mRNA cleavage and/or translational repression (41). We annotated 30 genes in the *L. humile* genome that are associated with the RNAi pathway, including all the genes potentially involved in biogenesis and biological function of miRNAs, siRNAs and piRNAs (Table S2, Fig. S16). Interestingly, all of these genes appear as single copies except *loquacious* (*loqs*), which is duplicated in the *L. humile* genome. Domain analysis by InterProScan shows that *L. humile* Loquacious 1 and 2 have three and two double stranded RNA binding domains (RBD), respectively. The dsRBD3 of *L. humile* Loquacious is noncanonical (Fig. S16*B*), consistent with its homolog in *D. melanogaster* (42, 43).

A)

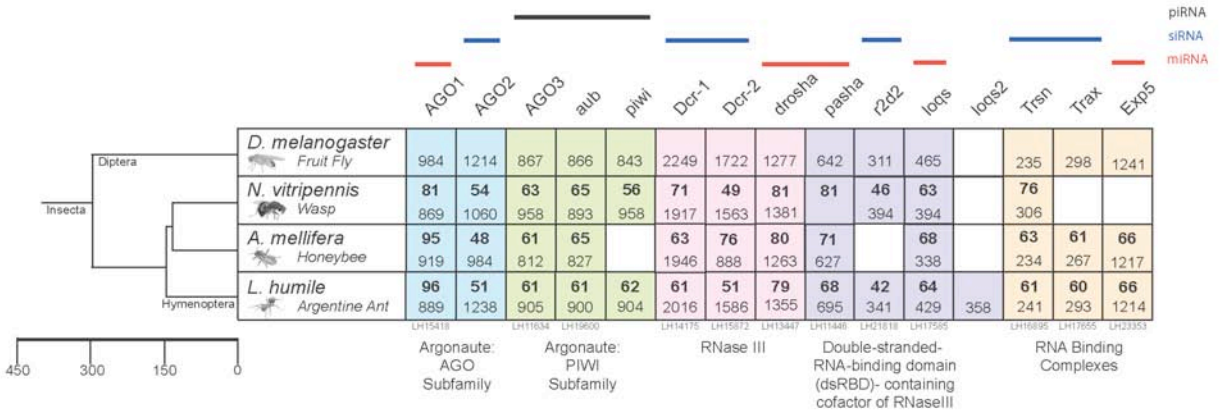

B)

```
Xlrbpa-2          NPVGSLQELAVQKGWRL--PEYTVAQESGPPHK-REFTITCRVE-------TFVETGSGTSKQVAKRVAAEKLLTKFKT
Lhum_Loq1_RBD1    TPVSVLQELLSRRGTI---PKYELVQIEGAIHE-PTFRYRVTVADVVEADPIVSAMGTGRSKKEAKHAAAKAVLDKLIG
Lhum_Loq1_RBD2    NPIGALQEMCMSRHWPP--PKYTMEGEEGLPHE-RQFTIVCTIL-------KYREIGQGKSKKVAKRHAAHKMWQALHD
Lhum_Loq1_RBD3    NLVQFLQEIASEQQFE---VTYVDIEEKSISGKFQCLVQLSTL-------PVAVCYGCGVTSKDAQASAAQNALEYLKI
Lhum_Loq2_RBD1    -PISFLQEFAIKQGYV---PMY-DFKIMNPN-----------G-------NNLSTDGTGNSKKEAKQKAAENMLLLLGQ
Lhum_Loq2_RBD2    NYIGVLQELCVRQKLSPRDISYKVIGESGPSHM-RCFIIEVSVK-------SLRAHGTAQSKKIAKQEAAKNLLHDLGL
```

Figure S16. RNAi genes. **A)** Reference *D. melanogaster* genes for RNA interference pathways were used to manually annotate *L. humile* genes. The percent protein similarity (bold numbers) and length of annotated orthologs (unbolded numbers) are shown for each gene. Genes are classified according to the functional subfamily which they shared similarity to and whether they function primarily in piRNA (black lines), siRNA (blue lines), and miRNA (red lines) pathways. Empty boxes indicate instances where no clear ortholog was found. **B)** Comparison between *L. humile loquacious* double stranded RNA binding domain (RBD) and the second RBD of *Xlrbpa* (*Xlrbpa-2*). Three regions important for binding dsRNA (23) are highlighted. Regions 1 (red) and 2 (blue) are associated with the interaction between the secondary structures of protein and the dsRNA minor groove, and Region 3 (pink) is involved in the interaction of the C-terminal secondary structure and the dsRNA major groove (23). The invariable histidine (H), which is specifically responsible for recognizing the minor groove, is missing in Region 2 of *Lhum_Loq1_RBD3* and *Lhum_Loq2_RBD1* suggesting that these two RBDs are noncanonical.

Wing and reproductive system development

Wing polyphenism and reproductive division of labor between queens and workers are two major and universal features of eusociality in ants (73). Both of these features evolved approximately 150 million years ago (74, 75), and have been key to their amazing evolutionary success – wing polyphenism was key for allowing ants to colonize the ground, while reproductive division of labor was key for their organization into eusocial colonies (73). The gene networks that underlie wing polyphenism and reproductive system development are generally conserved between ants and *D. melanogaster* (76, 77). In ants, however, these networks have evolved to be differentially expressed between winged reproductive castes and wingless sterile worker castes in response to either environmental or genetic factors (76, 77). In response to these factors, these networks must simultaneously produce fully functional wings and reproductive organs in the queen and male castes, but interrupt the expression of specific genes in the network to halt the development of wings and constrain reproduction in worker castes. While some candidate genes that are differentially expressed between queens and workers have been cloned and identified (76, 77), our ability to understand the evolutionary and developmental dynamics of these genes both within and between species has been limited by the absence of an ant genome.

The unicolonial colony structure of introduced *L. humile* populations may have been facilitated by changes in wing polyphenism and reproductive division of labor. The multiple queens of *L. humile* colonies still produce wings, but these queens do not fly, and existing colonies grow primarily through colony budding (78). Workers, which still possess reproductive organs, are functionally sterile (79).

We followed the method of Elango et al. (80) to assess whether or not the genes we annotated show signatures of putative methylation relative to the rest of the *L. humile* genome. For each annotated gene, we calculated the frequency of the observed number of CG dinucleotides for the coding region (exons and introns), as well as promoter regions (approximately 5kb upstream of the start codon) using a custom Perl script. For both regions of each gene, we calculated the mean CpG(O/E) values for three sets of genes: genes underlying wing polyphenism, genes involved in reproductive system development, and genes known to control apoptosis. We included genes that control apoptosis in our analysis because they are intimately linked to the networks that control wing development (81, 82) and oogenesis (83).

Figure S11. CpG(OE) for wing development, reproduction, and apoptosis genes in A) *L. humile* and B) *D. melanogaster*. The observed mean for genes in the networks underlying wing polyphenism (red line), reproductive division of labour (green line), and apoptosis (blue line) are plotted relative to the distribution of CpG(O/E) values for all genes in the genome.

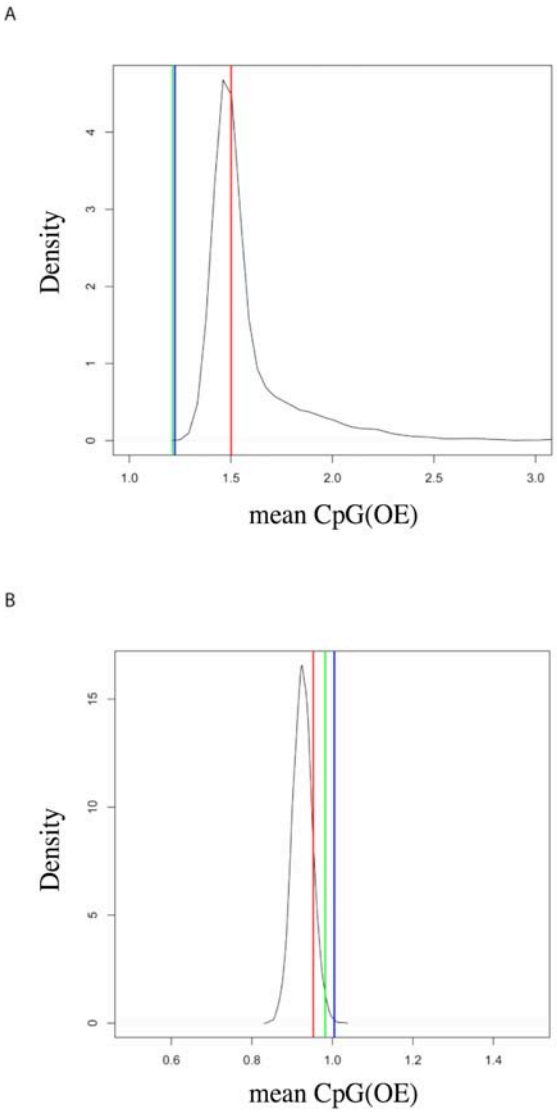

To compare the mean CpG(O/E) values for these three sets of genes (coding and promoter regions) to a genome-wide mean CpG(O/E), we segmented the scaffolds from the draft assembly of the *L. humile* genome into 1kb, non-overlapping, fragments using custom Perl scripts. We measured the frequency of CG dinucleotides and calculated the CpG(O/E) values for each 1kb fragment using custom Perl scripts based on the same equation as above. We then calculated a genome-wide mean CpG(O/E) by taking the mean CpG(O/E) of all 1kb fragments. Although there are alternative methods for generating a genome-wide mean CpG(O/E), we used this specific method because it was the only way we could perform the equivalent analyses in and compare them to *Drosophila*, an insect species which lacks a CpG methylation system.

To test whether or not there are any significant differences in the mean CpG(O/E) values between the three sets of genes that we annotated and the genome-wide mean CpG(O/E), we performed a statistical randomization procedure as follows: first, we generated a random distribution of CpG(O/E) values by randomly selecting 50 CpG(O/E) values from the genome-wide distribution. We selected 50 because this is approximately the same number of genes as that contained within each of the three sets of genes we manually annotated. We then calculated the mean CpG(O/E) for this random distribution. Second, we repeated this first step 10,000 times, and then ploted all 10,000 randomly generated mean CpG(O/E) values (x-axis representing the mean CpG(O/E) values and y-axis representing the frequency). Third, we determined where the observed mean CpG(O/E) for each of the three sets of genes we annotated fell with respect the randomly generated mean CpG (O/E) values. If it fell within the top or bottom 5% of the distribution of randomly generated mean CpG(O/E) values, then the observed mean

CpG(O/E) values were significantly different than the genome-wide mean CpG(O/E). We performed the same statistical analyses in *Drosophila* using *Drosophila* orthologs of the genes we annotated in *L. humile* (Figs. 2, S11).

We discovered that the mean CpG(O/E) for genes (coding regions) in the network underlying reproductive division of labor (n=38; Mean = 1.21; $p < 0.00$) and apoptosis (n=18; Mean = 1.22; $p < 0.00$) are significantly less (Figure S11) than the genome-wide mean CpG(O/E) (Mean = 1.63). The genes (coding regions) in the network underlying wing polyphenism is not (Figure S11) significantly different than the genome-wide mean CpG(O/E) (n=37; Mean = 1.50; $p = 0.4865$). The mean CpG(O/E) of the Drosophila orthologs (coding regions) that underlie wing development (Mean = 0.95; $p = 0.86$), reproduction (Mean = 0.98; $p= 0.98$), and apoptosis (Mean = 1.00; $p= 0.99$) are not significantly different (Figure S11) than the genome-wide mean CpG(O/E). Together, these results indicate that developmental genes in the network underlying reproductive division of labor and apoptosis have a distinct methylation signature relative to the rest of the *L. humile* genome, while genes in the network underlying wing polyphenism in ants.

According to Elango et al. (80), genes that are methylated in the germline should exhibit a mean CpG(O/E) that is under 1.0. The fact that mean CpG(O/E) values of the three sets of developmental genes are greater than 1.0, but significantly less than the genome-wide mean CpG(O/E), may indicate that they are still methylated but have a different methylation signature than the rest of the genes in the genome. The high level of significance for genes underlying reproductive system development and apoptosis may be due to their markedly different regulation between the two castes. This differential regulation may be due to the fact that many of the genes underlying reproductive division

of labor are these genes are germline specific, and because apoptosis is a major mechanism to differentiate castes during development. The majority of genes in the network underlying wing polyphenism are not specific to wing development, and many of them are used so broadly, and in so many different structures, that they maybe require a different methylation signature. Although these intriguing results await empirical validation, they open many avenues for future research.

Chemoreception (Grs, OBPs, Ors, Irs)

Gustatory receptors (Grs). The ant chemosensory gene families were manually annotated (OBPs, Grs, and Ors), essentially as described earlier (84). One difficulty was that a few genes had single apparent frameshifts, but upon examination of the raw reads from both 454 and Illumina contributing to these regions, it was apparent that these might be persistent 454 homopolymer sequencing errors because not all reads contained the same number of homopolymer bases as the assembly, and they were accordingly fixed. Several more gene models had gaps in the assembly, and we also attempted to repair these using raw reads to extend into the gap. Missing parts of these genes were sometimes found amongst a small number of unassembled contigs, in which case the most appropriate contig was joined to the gene model to complete it. Supplementary Table S10 provides details of the GR family genes and encoded proteins, and the encoded proteins are provided in FASTA format as a supplementary file. Only three genes were already perfectly built, another 20 existing automated gene models correspond to some of these genes, but with many changes required, including fusions and splits of models. Twenty of the 116 LhGr models are pseudogenes (compared to 50-60 Gr pseudogenes in *Apis*, and 11 in *Nasonia*), and 14 required repair of the genome assembly, so these could not have

been automatically annotated perfectly anyway. The remainder are all new gene models. We attempted to name these genes in a concordant way with the existing AmGr and NvGr names, but this is difficult because of gene losses and duplications in different lineages. For example, the two candidate sugar receptors, Gr1 and 2, were apparently duplicated as a block, and then one duplicate in each block degenerated to a pseudogene. To preserve the gene numbering for the remainder of the "orthologous" Grs, we named these LhGr1.1, 1.2, and 2.1 and 2.2 (LhGr1.3 is yet another pseudogene duplicate). Similarly, LhGr9 was duplicated, yielding a new pseudogene, hence the names 9.1 and 9.2. Finally, no gene was given the LhGr5 name.

We constructed a corrected distance tree depicting the relationship among the hymenopteran Grs as in Robertson et al. (84). The two candidate sugar receptor lineages were defined as the outgroup to root the tree, based on the highly divergent sequence and gene structure of this gene subfamily (85, 86). The *Nasonia*, *Apis*, and *Linepithema* gene/protein names are highlighted in blue, amber, and green, respectively, as are the branches leading to them to emphasize gene lineages. Numbers above branches are percentage support from 10000 bootstrap replications of uncorrected distance analysis. Double thickness branches indicate inferred independent GR lineages. Comments on each gene lineage are on the right. Suffixes after the gene/protein names are: PSE – pseudogene; CTE – C-terminus missing; INT – internal sequence missing; FIX – sequence fixed with raw reads; JOIN – gene model joined across scaffolds (combined suffixes are abbreviated).

Odorant binding proteins (OBPs). We identified 12 genes in the *L. humile* genome encoding odorant binding proteins (OBPs), which are short secreted proteins typically containing 6 highly conserved cysteines that form three disufide bonds (although some have lost two of these cysteines, in this set only LhOBP2 and 3) (e.g. 87). The genes and their encoded proteins are summarized in Table S15. There were at least partial automated gene models for all 12 OBPs. Seven of these were perfect, with others requiring fixes of assembly gaps, correction of frameshifting homopolymers, or addition of missing exons. Only one gene could not be fully built, that for OBP9 is missing the expected N-terminal exon that typically encodes the signal sequence at the start of these secreted proteins, and unfortunately there are no ESTs for it. Like OBPs in other insects, most of these genes are highly expressed enough to have ESTs in whole body EST projects like that undertaken for this ant. These ranged from zero ESTs for two genes, to fewer than 10 for four more, and up to around 113 for OBP4.

There are simple apparent orthologs for a subset of the 21 OBPs known from the honey bee genome, some of which are conserved throughout endopterygote insects (87). These are AmOBPs 1, 5, 6/8, 9, 10, and 11. The apparently orthologous ant OBPs were given the same names. This ant also has a small expansion of OBPs distantly related to AmOBPs 7 and 12, given the numbers 2, 3, 4, 8, 12. There are no obvious ant relatives of the AmOBPs 2, 3, 4 and 7. Finally, this ant has a single OBP7 with a possible relationship to the bee OBP expansion of 13-21. Thus ants and bees share a core set of six conserved OBPs that are probably involved in multiple functions, some not even related to odorant binding, given their expression in other tissues (87). On the other hand, they have differentially expanded different lineages of species-specific OBPs, which are more

likely to be involved in olfaction. One of these is the fire ant *Solenopsis invicta* gp-9 protein, which is an OBP implicated in regulation of queen numbers in colonies (88), however there is no particularly closely related OBP in *L. humile*.

Odorant receptors (Ors). The odorant receptor (Or) family of seven-transmembrane proteins in insects mediates most of insect olfaction (e.g. 89, 90), with additional contributions from a subset of the distantly related gustatory receptor (Gr) family, for example, the carbon dioxide receptors in flies (91-93), and a subset of the recently described and unrelated Ionotropic Receptors (IRs) (94). The Or family ranges in size from a low of 10 genes in the human body louse (95), to 50-100 receptors in *Drosophila* (85, 96), mosquitoes (97, 98), the silk moth *Bombyx mori* (99, 100), and the pea aphid *Acyrthosiphon pisum* (e.g. 101), and from 100-300 in the beetle *Tribolium castaneum* (102), the honey bee (103), and *Nasonia* wasps (84). Although most genes in *Drosophila* are scattered around the genome, with only a few in small tandem arrays, tandem arrays are more typical of the other species, especially those with large repertoires, from which it is inferred that these larger repertoires may result, in part, from the retention of gene duplicates that are generated in these tandem arrays by unequal crossing over.

Ants are expected to have a large Or gene family. Their sensory ecology and social behavior are largely dependent on chemical information, and several species have been shown to have ~400 glomeruli in the antennal lobes of their brains (e.g. 104, 105). Assuming that ants are like flies in usually having one specific Or (plus the obligate heterodimer DmOr83b ortholog) per neuron type, with all neurons that express a particular Or converging on a single glomerulus in the antennal lobe, the so-called “one

receptor - one neuron - one glomerulus" hypothesis, we anticipated approximately 400 Ors. This assumes that an unknown subset of the 116 Grs and the 32 IRs in *L. humile* are also expressed in discrete olfactory sensory neurons that send axons to glomeruli in the antennal lobe.

The Or family was manually annotated using methods previously employed for the *Drosophila*, mosquito, moth, beetle, bee, wasp, aphid, and louse genomes. Briefly, TBLASTN searches were performed using bee, and sometimes wasp, Ors as queries, and gene models were manually assembled in the text editor of PAUP*v4.0b10 (106), using the gene structures of the bee and wasp relatives to inform the ant genes. Iterative searches were also conducted with each new ant protein as query until no new genes were identified in each major subfamily or lineage. Occasionally the gene structures of ant genes were useful in informing improved gene models for some bee genes, specifically the 9-exon subfamily which is highly expanded in ants and wasps. The bee relatives are scattered throughout the AmOr naming system, because their relationship was not properly understood when they were annotated. A short exon was missed from several of them, specifically AmOr122-139. In addition, recognition of the conserved 9-exon structure of these genes allowed refinement of the AmOr172-174 genes, which were only recognized in light of the NvOr genes, but could not be completely built at that time (84). In addition, AmOr175-177 were newly built in this large subfamily, and there are additional fragments of related genes in the poorly assembled AT-rich regions of the bee genome that might represent additional genes. All of the LhOr genes and encoded proteins are detailed in Table S11. LhOr and AmOr proteins are available as FASTA format text files.

The *L. humile* genome assembly suffers from an unusual minor problem of bases in the assembly that are not in any of the raw reads, causing frameshifts when they occur in exons. These are not obviously caused by homopolymer length errors in the 454 reads, and their origin is unclear. Therefore each instance of a simple single-base frameshift was checked in both the 454 and ILLUMINA raw reads. In these cases the assembled sequence was fixed and these problems are noted in Table S11. In addition, as is typical of draft genome assemblies, gaps between contigs often interrupt gene models, especially when very similar genes are found in tandem arrays. These were repaired as best possible using the raw reads and are similarly noted in Table S11. There were several gene fragments resulting from assembly gaps that encode less than half the typical length of an insect Or (200 amino acids), and these were not included in the analysis, although they likely represent intact genes. Pseudogenes were translated as best possible to provide an encoded protein that could be aligned with the intact proteins for phylogenetic analysis, and particular attention was paid to the precise number of pseudogenizing mutations in each pseudogene. Again a 200 amino acid minimum was enforced for including pseudogenes in the analysis. All ant, bee, and wasp Ors were aligned in CLUSTALX v2.0 (69) using default settings, and problematic gene models and pseudogenes were refined in light of these alignments.

For phylogenetic analysis, the poorly aligned and variable length N-terminal and C-terminal regions were excluded (specifically before the conserved GhWP motif in the N-terminus and after the conserved SYFT motif in the C-terminus), as were major internal regions of length differences, especially a long length difference region between the longer DmOr83b orthologs (PbOr1, AmOr2, and NvOr1) and most of the other Ors.

Other regions of potentially uncertain alignment between these highly divergent proteins were retained because, while potentially misleading for relationships of the subfamilies (which are poorly supported), they provide important information for relationships within subfamilies.

Phylogenetic analysis of this large set of 844 proteins is difficult, but was successfully carried out in the same fashion as for previous Or analyses (e.g. 84, 103). This involved a combination of model-based correction of distances between each pair of proteins, and distance-based phylogenetic tree building. Pairwise distances were corrected for multiple changes in the past using the BLOSUM62 amino acid exchange matrix in the maximum likelihood phylogenetic program TREEPUZZLE v5.2 (107). These corrected distances were fed into PAUP*v4.0b10 where a full heuristic distance search was conducted with tree-bisection-and-reconnection branch swapping to search for the shortest tree. Given the large number of proteins, this search was unlikely to end and was terminated after two days with ~12 million trees examined. The resultant tree is shown in Figure S12. Unfortunately this large number of proteins precludes distance-based bootstrap analysis to assess the confidence of major branches in the tree, but likely orthologs and obvious gene losses and subfamily expansions are noted on the right margin of the tree. Unlike previous large Or trees which were split into multiple page-sized images, it is presented as a single image.

The LhOr gene set herein consists of 367 models. Thirty of these (8.2%) are apparent pseudogenes, 19 frameshifts were corrected, and 20 gene models required repair of assembly gaps. The result is 337 apparently intact Or proteins, although six of these are still missing N-terminal, C-terminal, or internal regions, so their functionality remains

uncertain (excluding the sets of Or60-70 and Or171-203 which have short N-terminal exons that are difficult to recognize with confidence). Less obvious pseudogenes (for example with small in-frame deletions or insertions, crucial amino acids changes, or promoter defects) would not be recognized, so this total might be high. A few gene fragments remain so short and incomplete that they were not included, but some might represent intact genes.

The automated gene modeling process had access to all available AmOrs and NvOrs, as well as other insect Ors in GenBank, for comparative information, and succeeded in building at least partial gene models for 201 of these 367 genes. However, as has been true for most other insect genome projects, just five of these are precisely correct. Most others require multiple changes, while many instances of concatenated gene models were observed (Table S11), resulting in a total of 140 automated models representing these 367 Ors (the most extreme was LH22493, which includes parts of eight genes and spans 20 kb on scaffold 7180001005020). Unfortunately because these genes are typically expressed at very low levels in only a few cells, they are seldom represented by ESTs in the whole body 454-sequencing project, as was employed for this genome, indeed just seven genes had one or two useful ESTs representing them (Table S11), hence there is little experimental support for most gene models. Nevertheless, there is EST support for representatives of most NvOr subfamilies and many AmOr subfamilies (84) so these manually built gene models are of high confidence. This situation again reveals the importance of manual annotation for these rapidly evolving and highly divergent genes. Manual annotation was also obviously essential for detailed analysis of pseudogenes.

As expected, there is a single highly conserved ortholog of the DmOr83b protein, named LhOr1 in hopes of encouraging this convention for this gene and protein in other species. It shares 77% amino acid identity with AmOr2, 76% with NvOr1, and 61% with DmOr83b. Unfortunately this gene region has suffered an assembly problem in v4 (but is intact in v3), and is now split across two scaffolds, but not at the ends of these scaffolds (similar aberrant assembly problems occurred with Or211 and 233). Only two other possible examples of relatively simple orthology across these three hymenopteran genomes were observed, those of LhOr204PSE (which is a severely damaged pseudogene with 10 major problems) with AmOr161 and NvOr296 (and 297PSE), and LhOr2/3, which are clearly orthologous to AmOr1/3 and NvOr2 at the base of a large expansion in both bees and ants which include several complicated relationships as well as the only hymenopteran Or whose ligand is known, AmOr11 perceiving the major queen pheromone 9-ODA in bees (108).

There are many instances of differential gene lineage or subfamily expansions, as previously seen for the bee/wasp comparison (84), including differential expansions in the ant, for example an expansion of 33 ant genes related to AmOr121 (at the top of the Fig. S12). The largest ant gene subfamily expansions, however, have occurred in a subfamily of 9-exon genes in the middle of the tree. This subfamily consists of several discrete lineages in the bee totaling 43 genes, including AmOr98-105, 106-113, 122-139, 140, 159, 162, 172-174, and 175-177. This subfamily is expanded in *Nasonia*, where it consists of 90 genes (NvOr129-217 and 301). This distinctive subfamily consists of 136 genes in the Argentine ant, and is of particular interest as it may include candidates for the cuticular hydrocarbon receptors. The details have only been established for one ant,

Campanotus japonicus (105, 109), in which females have a distinctive set of sensilla that house 150-200 neurons, each of which is presumed to express a particular Or, sending their neurons to a distinctive set of 150-200 glomeruli in the antennal lobe. Cuticular hydrocarbons are long non-volatile chemicals of enormous variety (e.g 110) that regulate important behavioral interactions (such as colonymate recognition), and it has not been obvious which receptors are used to perceive them. In *Drosophila melanogaster* two related lineages of gustatory receptors or Grs have been implicated in the perception of female cuticular hydrocarbons by males, but the exact ligand-receptor identification has yet to be made, these are expressed in contact chemosensilla on the male foretarsi, and their neurons send axons to the sub-oesophageal ganglion instead of the antennal lobe (111, 112). As described above, *L. humile* has two expansions of Grs, but neither is large enough to encode such a repertoire of CHC receptors, and at least one is likely to encode receptors for bitter plant defensive chemicals. Therefore, this expansion of 9-exon Or genes appears to be the strongest candidate for contaning CHC receptors.

These species-specific expansions have typically occurred in large tandem arrays, some of which are evidently very old because they are shared with bee and even wasp, and commonly the genes within an array are so divergent they barely find each other in TBLASTN searches. For example, LhOr2-46 is a 45-gene tandem array that spans 164 kb on the reverse strand of the 5' end of 170kb scaffold 7180001005020 and continuing on the reverse strand of the 3' end of 254kb scaffold 7180001004633 (Table S11). This feature is related to a 60-gene tandem array in *A. mellifera*, which is described in detail in Robertson and Wanner (103), although the nine related genes in the wasp, *N. vitripennis*, (NvOr2-10) are split across three scaffolds (84). Indeed the first and/or second gene in

this array appears to be orthologous (noted above – LhOr2/3, AmOr1/3, and NvOr2), while the remainder form multiple species-specific gene lineage expansions (Figure S12). LhOr71-116 is another large tandem array of 46 genes spanning 157kb on 1.591Mb scaffold 7180001004912.

Finally, the Or family reveals many instances of apparent gene loss, with some lineages completely absent from one or more of these three hymenopterans. In the abscence of bootstrap analysis the numbers of these losses in each species cannot be confidently determined, and the uncertain orthology of several subfamily lineages also makes it difficult to determine the number of losses, but obvious examples are noted in Figure S12. Separate subfamily tree analysis confirms all of these, and adds several more, confirming the dynamic gene family evolution known already from comparisons of other species Or repertoires.

Figure S12 (separate file). Phylogenetic tree of the hymenopteran Ors. This is a corrected distance tree generated. The DmOr83b orthologs LhOr1, AmOr2, and NvOr1 were declared as the outgroup to root the tree, based on the basal position of this gene in the Or family in analysis of the entire chemoreceptor superfamily in *Drosophila melanogaster* (85). The *Nasonia*, *Apis*, and *Linepithema* gene/protein names are highlighted in blue, amber, and green, respectively, as are the branches leading to them to emphasize gene lineages. Double thickness branches indicate inferred independent Or lineages. Comments on each gene lineage are on the right. Suffixes after the gene/protein names are: PSE – pseudogene; NTE – N-terminus missing; CTE – C-terminus missing; INT – internal sequence missing; FIX – sequence fixed with raw reads; JOI – gene model joined across scaffolds; multiple suffixes are abbreviated to single letters.

Table S10. Details of LhGr family genes and proteins. Columns are: Gene – the gene and protein name we are assigning; OGS – the official gene number; Scaffold# – the V4 genome assembly scaffold ID (preceded by scf18000100 in full name); Coordinates – the nucleotide range from the first position of the start codon to the last position of the stop codon in the scaffold; Strand – + is forward and - is reverse; Introns – number of introns; AAs – number of encoded amino acids in the protein; ESTs – number of ESTs (amongst 532,809 454 reads, * indicates aberrantly spliced); Comments – comments on the OGS gene model, repairs to the genome assembly, and pseudogene status (numbers in

parentheses are the number of pseudogenizing mutations). Suffixes after the gene/protein names are: PSE – pseudogene; CTE – C-terminus missing; INT – internal sequence missing; FIX – sequence fixed with raw reads; JOIN – gene model joined across scaffolds (combined suffixes are abbreviated).

Gene	OGS	Scaffold#	Coordinates	Strand	Introns	AAs	ESTs	Comments
Gr1.1	LH14807	4828	74106-108737	-	10	459	-	Multiple changes
Gr1.2PI	LH13968	4748	51542-71539	+	9	354	-	Pseudogene (2); has gap
Gr1.3PJ	LH12478	4608	10048-26232	-	10	442	-	Pseudogene (1) joined
		3431	1239-1787	-				across two scaffolds
Gr2.1PSE	LH14798	4828	64675-67419	+	5	212	-	Pseudogene (1)
Gr2.2	LH14676/5	4807	6885-24895	-	8	473	1	Join gene models
Gr3	LH19341	4967	83594-86853	-	8	538	1*	Multiple changes
Gr4	LH11242	4450	22954-24621	+	3	457	-	Fine as is
Gr6	LH21487	5009	652146-656146	+	5	391	1	Fine as is
Gr7FIX	LH19885	4974	44323-48477	-	6	428	-	Fix frameshift
Gr8	LH13821	4715	6008073-6009590	-	4	371	1	Part of large gene model
Gr9.1	LH13821	4715	6005287-6006803	-	4	364	-	Part of large gene model
Gr9.2PSE	LH13821	4715	6001485-6002981	-	4	358	-	Part of model; Pseudogene (1)
Gr10	LH19939	4979	84660-97730	-	5	363	-	Fine as is
Gr11	LH21303	5005	2838498-2840486	-	2	430	1	Second half missing
Gr12	-	5013	2768-5020	-	4	377	-	New gene model
Gr13	-	5018	2245014-2246416	-	2	414	-	New gene model
Gr14	-	5018	755164-756641	+	2	415	-	New gene model
Gr15PSE	-	5018	761347-763072	+	2	420	-	Pseudogene (1)
Gr16	-	5018	764333-765842	+	2	422	-	New gene model
Gr17	-	5018	767066-768565	+	2	417	-	New gene model
Gr18	-	5018	769831-771330	+	2	422	-	New gene model
Gr19	LH19887	4974	50648-53593	-	6	406	-	Multiple changes
Gr20	LH10133	2461	100167-102910	+	6	408	-	Multiple changes
Gr21	-	2461	104060-106547	+	6	408	-	New gene model
Gr22PSE	-	2461	107105-108998	+	4	320	-	Pseudogene (6)
Gr23	-	2461	109340-111809	+	6	409	-	New gene model
Gr24PSE	-	2461	112327-114201	+	4	314	-	Pseudogene (13)
Gr25	-	2461	115110-117567	+	6	408	-	New gene model
Gr26	-	2461	118086-120716	+	6	407	-	New gene model
Gr27	LH10136	2461	121216-124072	+	6	411	-	First 1/2 of gene model
Gr28PSE	LH10136	2461	124705-126863	+	6	397	-	Second 1/2; Pseudogene (1)
Gr29FIX	-	2461	127508-128817	+	6	396	-	Fix assembly gap
Gr30	-	2461	129677-132618	+	6	384	-	New gene model
Gr31	-	2461	133514-135509	+	6	396	-	New gene model
Gr32FIX	-	2461	136377-138246	+	6	393	-	Fix assembly gap

Gr33	LH10134	2461	139146-141321	+	6	402	-	Multiple changes
Gr34	-	2461	142088-144495	+	6	393	-	New gene model
Gr35FIX	-	2461	146592-149078	+	6	396	-	Fix frameshift
Gr36	-	2461	150692-153515	+	6	392	-	New gene model
Gr37	-	2461	154369-156965	+	6	397	-	New gene model
Gr38	-	2461	157687-159966	+	6	386	-	New gene model
Gr39	-	2461	161247-163572	+	6	377	-	New gene model
Gr40PF	-	2461	164888->165553	+	6	411	-	Fix gap; pseudogene (1)
Gr41CTE	-	2461	168688->170350	+	6	325	-	C-terminus missing
Gr42	LH22029	5018	516-3147	+	6	382	-	Part of large gene model
Gr43	-	5018	4344-6901	+	6	392	-	New gene model
Gr44	LH22029	5018	7935-10872	+	6	395	-	Part of large gene model
Gr45	LH22029	5018	11233-13986	+	6	398	-	Part of large gene model
Gr46	LH22029	5018	14738-18673	+	6	397	-	Part of large gene model
Gr47	-	5018	19034-21774	+	6	397	-	New gene model
Gr48PSE	LH22028	5018	22532-24684	+	6	356	-	Pseudogene (7)
Gr49	-	5018	26012-28169	+	6	396	-	New gene model
Gr50	-	5018	28859-31033	+	6	396	-	New gene model
Gr51FIX	-	5018	32493-34590	+	6	396	-	Fix assembly gap
Gr52PSE	-	5018	35969-38870	+	6	383	-	Pseudogene (2)
Gr53	-	5018	39572-42186	+	6	389	-	New gene model
Gr54	-	5018	42654-44687	+	6	388	-	New gene model
Gr55	-	5018	45414-48282	+	6	391	-	New gene model
Gr56	-	5018	50233-52120	+	6	397	-	New gene model
Gr57	-	5018	52978-55148	+	6	397	-	New gene model
Gr58	-	5018	55788-57965	+	6	389	-	New gene model
Gr59PSE	-	5018	58989-61164	+	6	397	-	Pseudogene (2)
Gr60FP	-	5018	<61480-63340	+	6	434	-	Fix gap; pseudogene (5)
Gr61	-	5018	64118-66290	+	6	395	-	New gene model
Gr62	-	5018	66742-68931	+	6	395	-	New gene model
Gr63PSE	-	5018	69895-72074	+	6	389	-	Pseudogene (6)
Gr64	-	5018	74382-76560	+	6	395	-	New gene model
Gr65	-	5018	77020-79207	+	6	394	-	New gene model
Gr66	-	5018	79693-81862	+	6	390	-	New gene model
Gr67FIX	-	5018	84168-86845	+	6	394	-	Fix assembly gap
Gr68PSE	-	5018	87331-89514	+	6	389	-	Pseudogene (2)
Gr69FP	-	5018	90544->93088	+	6	388	-	Fix gap; pseudogene (3)
Gr70FIX	-	5018	<94170-96200	+	6	390	-	Fix assembly gaps
Gr71	-	5018	98532-101533	+	6	393	-	New gene model
Gr72	-	5018	102616-106230	+	6	389	-	New gene model
Gr73	-	5018	106853-109006	+	6	394	-	New gene model

Gr74CTE	-	5018	109888->112823	+	6	397	-	Fix assembly gap
Gr75	-	5018	113372-116116	+	6	391	-	New gene model
Gr76PSE	-	5018	116614-119360	+	6	392	-	Pseudogene (1)
Gr77	-	5018	119767-122613	+	6	398	-	New gene model
Gr78	-	5018	122998-125880	+	6	391	-	New gene model
Gr79	-	5018	126377-129200	+	6	395	-	New gene model
Gr80	-	5018	129654-132607	+	6	395	-	New gene model
Gr81	-	5018	133063-135916	+	6	392	-	New gene model
Gr82	-	5018	137000-139100	+	6	403	-	New gene model
Gr83	-	5018	139865-141999	+	6	389	-	New gene model
Gr84	-	4985	1994747-1997275	+	6	396	-	New gene model
Gr85	-	4985	1998234-2000866	+	6	392	-	New gene model
Gr86	-	4985	2002272-2004901	+	6	392	-	New gene model
Gr87	-	4985	2005927-2008474	+	6	391	-	New gene model
Gr88	-	4985	2009559-2012080	+	6	396	-	New gene model
Gr89PSE	-	4985	2013204-2015808	+	6	396	-	Pseudogene (5)
Gr90	-	4985	2016791-2019367	+	6	394	-	New gene model
Gr91	-	4985	2021453-2024016	+	6	398	-	New gene model
Gr92	LH20185	4985	2025125-2027700	+	6	402	-	Multiple changes
Gr93	-	4985	2030013-2032601	+	6	402	-	New gene model
Gr94	LH20184	4985	2033094-2035730	+	6	420	-	First part of model
Gr95	LH20184	4985	2036168-2039332	+	6	402	-	Second part of model
Gr96	LH20186	4985	2039837-2042487	+	6	398	-	First part of model
Gr97	LH20186	4985	2043004-2045399	+	6	394	-	Second part of model
Gr98	-	4985	2046134-2048806	+	6	403	-	New gene model
Gr99	-	4985	2049957-2052760	+	6	405	-	New gene model
Gr100	-	4985	2053920-2057216	+	6	406	-	New gene model
Gr101PSE	-	4985	2058443-2061142	+	6	405	-	Pseudogene (1)
Gr102	-	4985	2062677-2065778	+	6	402	-	New gene model
Gr103FIX	-	4985	2067579-2070567	+	6	400	-	Fix frameshift and stop codon
Gr104	-	4985	2071876-2075542	+	6	403	-	New gene model
Gr105FIX	-	4985	2076825-2079996	+	6	394	-	Fix assembly gap
Gr106FIX	-	4985	2081509-2084186	+	6	398	-	Fix assembly gap
Gr107	-	4985	2085098-2087820	+	6	397	-	New gene model
Gr108INT	-	4985	2091454-2094263	+	6	399	-	Fix assembly gap
Gr109	-	4985	2095436-2098097	+	6	396	-	New gene model
Gr110FIX	-	4985	2099310-2101152	+	6	398	-	Fix assembly gap
Gr111	-	4940	1732466-1735058	+	6	394	-	New gene model
Gr112PSE	-	4940	1735556-1738101	+	6	400	-	Pseudogene (1)
Gr113	LH18148	4940	1739673-1742228	+	6	391	-	Multiple changes
Gr114	-	3999	23409-25655	+	6	397	-	New gene model

Table S15. Details of LhOBP family genes and proteins. Columns are: Gene – the gene and protein name we are assigning (suffixes are: NTE – N-terminus missing; FIX – assembly was repaired) ; OGS – the official gene number in the 16,177 proteins in OGS1.1; Scaffold – the V4 genome assembly scaffold ID (preceded by scf18000100 in full name); Coordinates – the nucleotide range from the first position of the start codon to the last position of the stop codon in the scaffold; Strand – + is forward and - is reverse; Introns – number of introns; AAs – number of encoded amino acids in the protein; ESTs – number of ESTs (amongst 532,809 454 reads); Isotig – isotig number in EST assembly; Comments – comments on the OGS gene model and repairs to the genome assembly.

Gene	OGS	Scaffold	Coordinate	Strand	Introns	AAs	ESTs	Isotig	Comments
OBP1	LH21629	5010	285632-287	+	5	139	25	04013	Needs C-terminus
OBP2FIX	LH12959	4659	219626-222	-	4	156	13	03709	Fix frameshift
OBP3	LH12963	4659	214403-218	-	4	155	0	-	Fine as is
OBP4	LH12958	4659	211309-213	-	4	149	113	03012	Fine as is
OBP5	LH12960	4659	233686-235	-	4	144	8	01909	Fine as is
OBP6	LH12962	4659	229707-231	-	5	146	4	-	Fine as is
OBP7	LH23112	5043	21919-2327	+	4	133	33	03397	Fine as is
OBP8	LH12961	4659	205438-207	-	4	156	3	-	Fine as is
OBP9NTE	LH16671	4922	26398-2721	-	3	120	0	-	N-terminus missing
OBP10	LH15020	4838	1117240-11	+	5	146	27	03482	Fine as is
OBP11FIX	LH15023	4838	1120846-11	+	5	146	4	-	Fix assembly gap
OBP12	LH19059	4958	850368-851	-	5	173	15	03490	Needs N-terminus

Table S11. Details of LhOr family genes and proteins. Columns are: Gene – the gene and protein name we are assigning (suffixes are: PSE – pseudogene; NTE – N-terminus missing; CTE – C-terminus missing; INT – internal region missing; FIX – assembly was repaired; JOIN – gene model spans scaffolds; multiple suffixes are abbreviated) ; OGS – the official gene number in the 16,177 proteins in OGS1.1; Scaffold – the V4 genome assembly scaffold ID (preceded by scf718000100 in full name); Coordinates – the nucleotide range from the first position of the start codon to the last position of the stop codon in the scaffold; Strand – + is forward and - is reverse; Introns – number of introns; AAs – number of encoded amino acids in the protein; ESTs – number of ESTs (amongst 532,810 Roche/454 reads); Comments – comments on the OGS gene model, repairs to the genome assembly, and pseudogene status (numbers in parentheses are the number of pseudogenizing mutations). Superscript [a] – this gene lost one intron and gained another relative to the other 46 genes in this subfamily. Superscript[b] – these two genes have an additional intron shared with orthologous genes in *Nasonia* and *Apis*. Note that Or60-70 and Or171-203 have short first exons that cannot be confidently identified in the absence of EST evidence, therefore they are all NTE, and coordinates start from the start of the first codon after a phase 1 intron (and this intron is included in the intron count even though it is not in the range coordinates of the CDS).

Gene	OGS	Scaffold	Coordinates	Strar	Intro	AAs	ESTs	Comments
Or1JF	LH19204	4964	533215-536431	-	7	480	-	Join across two scaffolds;
	LH11309	4453	170456-172130	-				fix frameshift
Or2	LH25976	5020	110477-112233	-	4	405	-	Part of long model
Or3	LH25976	5020	107251-109112	-	4	406	-	Part of long model
Or4	LH25976	5020	103453-105313	-	4[a]	404	-	Part of long model
Or5	-	5020	100481-102698	-	4	397	-	New gene model
Or6	-	5020	98184-99899	-	4	409	-	New gene model
Or7	LH22493	5020	91596-93866	-	4	400	-	Part of long model

Or8	LH22493	5020	87345-89634	-	4	396	-	Part of long model
Or9	LH22493	5020	82824-86499	-	4	399	-	Part of long model
Or10	LH22493	5020	79304-81300	-	4	399	-	Part of long model
Or11	LH22493	5020	76185-77967	-	4	399	-	Part of long model
Or12	LH22493	5020	72178-73850	-	4	409	-	Part of long model
Or13	LH22493	5020	68896-71197	-	4	399	-	Part of long model
Or14FIX	LH22493	5020	65770->67903	-	4	400	-	Fix assembly gap
Or15	LH25980	5020	62073-65077	-	4	400	-	First half of model
Or16	LH25980	5020	59604-61360	-	4	399	-	Second half of model
Or17	-	5020	57484-59072	-	4	400	-	New gene model
Or18	-	5020	51309-53188	-	4	409	-	New gene model
Or19	LH22492	5020	47177-49471	-	4	408	-	Multiple changes
Or20	-	5020	43752-45471	-	4	407	-	New gene model
Or21	-	5020	39525-41775	-	4	415	-	New gene model
Or22PSE	-	5020	34590-35808	-	2	301	-	Pseudogene (3)
Or23	-	5020	32093-33886	-	4	406	-	New gene model
Or24PSE	-	5020	30072-31435	-	2	281	-	Pseudogene (2)
Or25	LH25978	5020	26693-28486	-	4	406	-	Multiple changes
Or26	-	5020	23515-26092	-	4	407	-	New gene model
Or27	-	5020	20967-22987	-	4	403	-	New gene model
Or28PSE	-	5020	15793-17635	-	4	370	-	Pseudogene (11)
Or29	-	5020	13718-15569	-	4	407	-	New gene model
Or30	-	5020	10481-12404	-	4	402	-	New gene model
Or31PSE	LH25977	5020	1753-3539	-	4	292	-	Pseudogene (1)
Or32	LH25400	4633	242188-244333	-	4	414	-	Part of long model
Or33	LH25400	4633	237193-239341	-	4	412	2	Part of long model
Or34	LH25400	4633	232737-234730	-	4	410	-	Part of long model
Or35	-	4633	226424-228518	-	4	406	-	New gene model
Or36PSE	-	4633	224002-225997	-	4	408	-	Pseudogene (3)
Or37	LH25400	4633	221387-223511	-	4	409	-	Part of long model
Or38	LH25401	4633	217472-219484	-	4	403	-	Multiple changes
Or39	-	4633	213972-215937	-	4	427	-	New gene model
Or40FIX	-	4633	210785-212699	-	4	411	-	Fix frameshift
Or41	-	4633	205894-207912	-	4	410	-	New gene model
Or42	LH12715	4633	201840-204335	-	4	411	-	Multiple changes
Or43	LH12714	4633	198657-201324	-	4	400	-	Multiple changes
Or44PSE	-	4633	194452-196107	-	4	371	-	Pseudogene (8)
Or45	LH12711	4633	190992-193463	-	5[b]	406	-	Fine as is
Or46	LH12712	4633	187141-190462	-	5[b]	406	-	Different final exon
Or47FIX	-	5082	797933-800054	+	4	394	-	Fix frameshift
Or48	-	5082	801408-803265	+	4	400	-	New gene model
Or49	-	5082	808411-810316	+	4	399	-	New gene model
Or50	-	5082	812264-814336	+	4	392	-	New gene model
Or51	-	5082	816066-818143	+	4	394	-	New gene model
Or52	-	5082	820197-822168	+	4	398	-	New gene model
Or53PSE	-	5082	823913-825877	+	4	397	-	Pseudogene (2)
Or54	LH26112	5082	827276-829195	+	4	398	-	Part of long model
Or55	LH26112	5082	830852-832813	+	4	399	-	Part of long model
Or56	LH26112	5082	834250-836133	+	4	395	-	Part of long model
Or57	LH24938	5082	837963-840334	+	4	402	-	First half of model
Or58	LH24938	5082	841401-843460	+	4	398	-	Second half of model
Or59	LH26113	5082	845883-848519	+	4	399	-	Multiple changes
Or60NTE	-	4955	118033-120675	+	6	392	-	New gene model
Or61NTE	-	4955	122500-124586	+	6	392	-	New gene model
Or62NP	-	4955	130515-133155	+	6	392	-	Pseudogene (1)
Or63NTE	-	4955	134974-137065	+	6	392	-	New gene model
Or64NTE	-	4955	143488-145641	+	6	392	-	New gene model
Or65NP	-	4955	150320-153703	+	6	393	-	Pseudogene (4)
Or66NTE	-	4955	156018-158117	+	6	393	-	New gene model
Or67NP	-	4955	174009-176235	+	6	392	-	Pseudogene (2)
Or68NTE	-	4955	179558-181789	+	6	393	1	New gene model
Or69NTE	-	4955	187483-190513	+	6	399	-	New gene model
Or70NTE	-	4955	192632-195896	+	6	386	-	New gene model
Or71	LH16353	4912	359883-361915	-	5	386	-	One exon missing
Or72	LH25609	4912	357098-358951	-	5	387	-	Multiple changes
Or73	LH25606	4912	351613-356208	-	5	376	-	Multiple changes

Or74	LH16358	4912	347629-350556	-	5	394	-	First half of model
Or75	LH16358	4912	344957-346862	-	5	393	-	Second half of model
Or76	-	4912	342301-344206	-	5	395	-	New gene model
Or77	-	4912	336581-338420	-	5	387	-	New gene model
Or78	-	4912	333600-335554	-	5	378	1*	New gene model
Or79	LH25607	4912	330692-332832	-	5	377	-	Multiple changes
Or80	LH25605	4912	327495-329656	-	5	381	-	Multiple changes
Or81	LH16362	4912	324338-326378	-	5	386	-	Part of long model
Or82	LH16362	4912	319111-321197	-	5	385	-	Part of long model
Or83	LH16362	4912	315873-318204	-	5	385	-	Part of long model
Or84	LH16362	4912	311006-313142	-	5	385	-	Part of long model
Or85	LH16360	4912	307780-310128	-	5	382	-	Part of long model
Or86	LH16360	4912	304727-306893	-	5	384	-	Part of long model
Or87	LH16360	4912	301614-303679	-	5	386	-	Part of long model
Or88PSE	LH16360	4912	299196-300662	-	4	315	-	Pseudogene (9)
Or89	LH16360	4912	295780-298063	-	5	385	-	Fix sequence error
Or90PSE	LH16360	4912	292260-294781	-	5	382	-	Pseudogene (2)
Or91	LH16360	4912	288873-291222	-	5	386	-	Part of long model
Or92	LH16360	4912	285885-287918	-	5	387	-	Part of long model
Or93PSE	-	4912	279773-284881	-	5	387	-	Pseudogene (6)
Or94	LH25610	4912	276779-278823	-	5	384	-	Multiple changes
Or95	-	4912	273792-275848	-	5	387	-	New gene model
Or96	LH16352	4912	269853-272829	-	5	388	-	Multiple changes
Or97	LH25598	4912	267035-268898	-	5	385	-	Multiple changes
Or98	LH25597	4912	263352-265925	-	5	381	-	Multiple changes
Or99	LH25596	4912	259949-262145	-	5	385	-	Multiple changes
Or100	-	4912	256657-258770	-	5	384	-	New gene model
Or101	-	4912	253185-255497	-	5	385	-	New gene model
Or102	LH16356	4912	250070-252441	-	5	387	-	Multiple changes
Or103	LH25603	4912	246289-248157	-	5	380	-	Multiple changes
Or104	LH25611	4912	241017-242914	-	5	389	-	Multiple changes
Or105FIX	-	4912	236946-239186	-	5	386	-	Fix frameshift
Or106FIX	-	4912	<234924-236241	-	5	386	-	Fix assembly gap
Or107FIX	-	4912	233332-236241	-	5	386	-	Fix assembly gap
Or108	LH16357	4912	230197-232323	-	5	386	-	Multiple changes
Or109	-	4912	226817-229070	-	5	386	1	New gene model
Or110	LH16363	4912	223676-225988	-	5	386	-	Multiple changes
Or111	LH16359	4912	220465-222753	-	5	387	-	Needs earlier start
Or112	LH16361	4912	217437-219758	-	5	385	-	First half of model
Or113	LH16361	4912	214429-216498	-	5	394	-	Second half of model
Or114	LH16365	4912	211642-213719	-	5	396	1*	Needs earlier start
Or115	LH25604	4912	208861-210936	-	5	396	-	Needs earlier start
Or116	LH16368	4912	205263-207897	-	5	386	-	Multiple changes
Or117	LH21671	5011	29975-32006	-	4	370	-	Multiple changes
Or118	LH25955	5011	26858-29009	-	4	373	-	Multiple changes
Or119	LH25956	5011	23654-25896	-	4	374	-	Multiple changes
Or120FIX	LH21668	5011	13777-15606	-	4	368	-	Fix frameshift
Or121	LH21670	5011	10319-12352	-	4	370	-	Multiple changes
Or122	LH21669	5011	7492-9358	-	4	368	-	Multiple changes
Or123FIX	-	5011	4077-6550	-	4	379	-	Fix assembly gap
Or124	-	5011	695-2591	-	4	369	-	New gene model
Or125	-	2461	15-1902	+	4	362	-	New gene model
Or126	LH10129	2461	3173-5141	+	4	369	-	First half of model
Or127	LH10129	2461	6473-8227	+	4	370	-	Second half of model
Or128	-	2461	9407-11138	+	4	366	-	New gene model
Or129	-	2461	12144-14190	+	4	370	-	New gene model
Or130	-	2461	15241-17360	+	4	370	-	New gene model
Or131	-	2461	18430-20985	+	4	367	-	New gene model
Or132	-	2461	22133-24258	+	4	372	-	New gene model
Or133	-	2461	25587-27983	+	4	368	-	New gene model
Or134FIX	-	2461	29445-31440	+	4	368	-	Fix assembly gap
Or135	-	2461	32441-34492	+	4	368	-	New gene model
Or136	-	2461	36463-38194	+	4	369	-	New gene model
Or137	LH18458	4949	134810-136258	+	4	384	-	New gene model
Or138	LH18459	4949	138197-141767	+	4	382	-	Different C-terminus
Or139	LH25728	4949	176458-178148	-	4	383	-	Multiple changes

Or140FIX	LH25730	4949	171052-175190	-	4	381	-	Fix frameshift
Or141	LH25730	4949	167683-169647	-	4	382	-	Second half of model
Or142	-	4949	163826-165836	-	4	382	-	New gene model
Or143	LH18464	4949	160306-162494	-	4	380	-	Part of long model
Or144	LH18464	4949	156408-158667	-	4	385	-	Part of long model
Or145	LH18464	4949	152289-154977	-	4	380	-	Part of long model
Or146	LH25711	4940	3541813-3545045	+	2	382	-	Multiple changes
Or147	LH25713	4940	3546152-3549378	+	2	398	-	Needs C-terminus
Or148PSE	-	4940	3550363-3551822	+	2	367	-	Pseudogene (12)
Or149	LH25716	4940	3553310-3555054	+	3	402	-	Different C-terminus
Or150	LH18292	4940	3556356-3558239	+	2	396	-	Different C-terminus
Or151	-	4940	3559106-3561273	+	3	397	-	New gene model
Or152	LH25712	4940	3561859-3563873	+	3	396	-	Multiple changes
Or153	LH25717	4940	3565417-3567456	+	3	396	-	Multiple changes
Or154	LH25718	4940	3570241-3572758	+	3	396	-	Multiple changes
Or155	-	4940	3575226-3577207	+	3	396	-	New gene model
Or156	-	4940	3578108-3581091	+	2	391	-	New gene model
Or157	LH18291	4940	3583053-3585281	+	3	395	1*	First half of model
Or158	LH18291	4940	3586321-3588009	+	2	403	-	Second half of model
Or159	LH18288	4940	3588544-3591573	+	3	398	-	Multiple changes
Or160	LH18289	4940	3593820-3596738	+	3	391	-	Internal exon missing
Or161	LH25648	4926	2390040-2392769	+	3	392	-	Multiple changes
Or162	LH25649	4926	2393694-2395798	+	3	392	-	Internal exon needed
Or163	LH25651	4926	2396458-2398610	+	3	392	-	Multiple changes
Or164PSE	-	4926	2400386-2402130	+	3	389	-	Pseudogene (13)
Or165	LH25644	4926	2402660-2404541	+	3	392	-	Internal exon needed
Or166PSE	-	4926	2405109-2406946	+	3	318	-	Pseudogene (5)
Or167	LH25652	4926	2408094-2410470	+	3	396	-	Part of long model
Or168	LH25652	4926	2412430-2414567	+	3	397	-	Part of long model
Or169PSE	LH25652	4926	2416771-2418631	+	3	378	-	Pseudogene (2)
Or170	LH25652	4926	2419700-2421337	+	3	392	-	Part of long model
Or171NP	LH17512	4929	<935128-939745	+	6	390	-	Pseudogene (3)
Or172NTE	LH17511	4929	<941424-943717	+	6	389	-	Multiple changes
Or173NTE	LH11296	4452	<171937-174311	+	6	389	-	First half of model
Or174NTE	LH11296	4452	<175936-177891	+	6	389	-	Second half of model
Or175NTE	-	4452	<179243-181435	+	6	389	-	New gene model
Or176NTE	-	4452	<182850-186350	+	6	391	-	New gene model
Or177NTE	-	4452	<188590-191353	+	6	391	-	New gene model
Or178FN	-	4452	<192805-195239	+	6	391	-	Fix assembly gap
Or179JFN	-	4452	<197237->200640	+	6	391	-	Join across two scaffolds
		4923	<1->1156	+	6			fix assembly gap
Or180FN	LH25636	4923	<4718-8245	+	6	391	-	Fix frameshift
Or181NTE	LH25636	4923	<9989-12608	+	6	391	-	Part of long model
Or182NTE	LH25636	4923	<14005-16496	+	6	388	-	Part of long model
Or183NTE	LH25633	4923	<18307-20886	+	6	390	-	Multiple changes
Or184NTE	-	4923	<22562-24957	+	6	389	-	New gene model
Or185NTE	-	4923	<26035-28104	+	6	387	-	New gene model
Or186NTE	-	4923	<29261-31275	+	6	387	-	New gene model
Or187FN	-	4923	<32617-35067	+	6	388	-	Fix frameshift
Or188PSE	-	4923	<35558-37114	+	5	297	-	Pseudogene (5)
Or189NP	-	4923	<38213-40758	+	6	388	-	Pseudogene (1)
Or190PSE	LH10470	4923	<41240-42762	+	5	297	-	Pseudogene (5)
Or191FN	-	4923	<43902-46044	+	6	389	-	Fix assembly gap
Or192NTE	-	4923	<48941-50970	+	6	390	-	New gene model
Or193NTE	-	4923	<52302-54821	+	6	389	-	New gene model
Or194NTE	LH25635	4923	<56088-58153	+	6	389	-	First half of model
Or195NTE	LH25635	4923	<59550-61791	+	6	387	-	Second half of model
Or196NTE	LH25637	4923	<62853-66150	+	6	387	-	Multiple changes
Or197FNC	-	4923	<68391->70673	+	6	371	-	Partially fix assembly gap
Or198FN	-	4923	<72508-75897	+	6	387	-	Fix assembly gap
Or199FN	LH25634	4923	<78150-81002	+	6	388	-	Fix assembly gap
Or200NTE	LH25632	4923	<82501-85235	+	6	387	-	Multiple changes
Or201NTE	-	4923	<87449-90341	+	6	388	-	New gene model
Or202NTE	LH16750	4923	<95442-98926	+	6	388	-	Multiple changes
Or203NTE	LH13656	4923	<2419045-2421433	+	6	388	-	Multiple changes
Or204PSE	-	4909	664407-667584	-	6	333	-	Pseudogene (12)

Or205	LH23982	5070	27167-34800	-	5	387	-	Fuse two gene models;
	LH23984							across a 5 kb intron
Or206NTE	LH19170	4964	320440-323154	+	6	384	-	N-terminal exon unidenti
Or207	LH19170	4964	325502-329195	+	6	389	-	Part of long model
Or208	LH19170	4964	330187-334399	+	6	393	-	Part of long model
Or209	LH22725	5033	101866-109632	+	7	399	1*	Multiple changes
Or210	LH23858	5066	863837-867843	+	5	438	-	Fine as is
Or211JOI	LH20522	4989	<1-1197	-	4	401	-	Join across two scaffolds;
		4923	152493-153827	-				assembly problem?
Or212	LH12905	4653	737578-739768	-	5	402	-	First half of model
Or213	LH12905	4653	731987-734515	-	5	403	-	Second half of model
Or214	LH25733	4950	40394-42536	-	4	408	-	Multiple changes
Or215	LH23980	5070	76078-176164	-	5	376	-	Needs a C-terminus
Or216	LH18732	4956	20162-22703	-	5	379	-	Multiple changes
Or217FIX	LH18727	4956	<25380-28349	+	6	373	-	Fix assembly gap
Or218	LH21199	5005	1587704-1592738	-	5	378	-	Multiple changes
Or219FIX	-	5005	1579650-1584773	-	5	378	-	Fix assembly gap
Or220	LH11487	4465	9057-84984	+	5	380	-	Multiple changes
Or221IC	LH23895	5068	<60692-107121	-	5	322	-	Exons 3 and 6 missing
Or222	LH19011	4958	263992-268751	-	5	372	-	Fine as is
Or223JOI	LH15447	4861	4635->25360	+	5	370	-	Join across three scaffold
	LH15442	4963	<1->33715	+				awkward because implies
		4843	93514->105292	-				assembly problem in 486
Or224	LH15148	4856	233563-236416	+	5	402	2	Fine as is
Or225	LH24139	5073	44540-46128	-	4	387	-	Fine as is
Or226	LH11096	4431	80014-83806	+	4	388	-	Needs a different C-termi
Or227	-	5018	2294078-2296134	-	5	386	-	New gene model
Or228	LH22142	5018	2287166-2288982	-	4	376	-	First part of model
Or229	LH22142	5018	2283805-2286406	-	5	384	-	Second part of model
Or230	LH22143	5018	2281480-2283208	-	5	380	-	Multiple changes
Or231	LH22141	5018	2277756-2280176	-	5	381	-	Needs a N-terminus
Or232	LH23776	5065	608871-611426	+	8	400	-	Multiple changes
Or233	LH23496	5057	215473-218709	+	8	389	-	Multiple changes
Or234	LH26046	5057	219045-221760	-	8	400	-	Second part of model
Or235	LH26046	5057	222750-225624	-	8	401	-	First part of model
Or236PSE	-	5057	226670-229312	-	8	318	-	Pseudogene (8)
Or237PSE	LH26038	5057	230035-232201	-	8	383	-	Pseudogene (1)
Or238	LH26038	5057	232736-235196	-	8	395	-	First part of model
Or239	-	5057	237949-240493	+	8	413	-	New gene model
Or240	LH23495	5057	244925-247502	+	8	415	-	Multiple changes
Or241	LH24047	5057	248687-251094	-	8	398	-	Multiple changes
Or242	LH26045	5057	252884-255224	-	8	400	-	Second part of model
Or243	LH26045	5057	256193-258665	-	8	403	-	First part of model
Or244	LH26048	5057	261164-263610	-	8	402	-	Multiple changes
Or245	LH23507	5057	268035-270962	+	8	407	-	Part of long model
Or246	LH23507	5057	271874-274568	+	8	408	-	Part of long model
Or247PSE	LH23507	5057	277157-279514	+	8	415	-	Pseudogene (2)
Or248PSE	LH23507	5057	280606-283007	+	8	404	-	Pseudogene (1)
Or249	LH23507	5057	283796-286444	+	8	398	-	Part of long model
Or250	-	5057	288418-290845	+	8	392	-	New gene model
Or251PSE	LH26052	5057	291690-294483	+	8	411	-	Pseudogene (3)
Or252	-	5057	296590-299137	+	8	390	-	New gene model
Or253	LH23505	5057	301113-303729	+	8	388	-	Multiple changes
Or254FIX	-	5057	305338-307469	+	8	398	-	Fix two frameshifts
Or255	-	5057	308634-311124	+	8	400	-	New gene model
Or256	LH23506	5057	313127-315644	+	8	397	-	Multiple changes
Or257	LH26051	5057	316253-318934	+	8	397	-	Multiple changes
Or258IP	-	5057	320217-322372	+	8	361	-	Pseudogene (3) with gap
Or259	LH26050	5057	324472-326878	+	8	403	-	Part of long model
Or260FIX	LH26050	5057	332210-334589	+	8	402	-	Fix frameshift and stop
Or261	LH26050	5057	336289-338710	+	8	403	-	Part of long model
Or262	LH23509	5057	339869-343193	-	8	395	-	Multiple changes
Or263	LH23511	5057	343991-346895	-	8	388	-	Multiple changes
Or264	-	5057	56423-59089	-	8	395	-	New gene model
Or265FPC	-	5057	52757-54376	-	5	281	-	Pseudogene (3); partial fi
Or266FIX	-	5057	46495-50025	-	8	390	1	Fix assembly gap

Or267	-	5057	37221-40640	-	8	386	-	New gene model
Or268	-	5057	32512-36018	-	8	390	-	New gene model
Or269	-	5057	27865-31313	-	8	390	-	New gene model
Or270JC	-	5057	23590-26617	-	8	376	-	Join across two scaffolds
		4638	7249-7787	+				final exon still missing
Or271	-	5057	13165-22039	-	8	392	-	New gene model
Or272	-	5057	8640-12102	-	8	390	-	New gene model
Or273	-	5057	3706-6628	-	8	391	-	New gene model
Or274FIX	-	5057	<1-2515	-	8	392	1	Extend scaffold
Or275	-	4662	1202-7933	-	8	391	-	New gene model
Or276FIX	-	4929	1946592->1953169	-	8	393	-	Extend scaffold
Or277	-	4929	1941424-1944919	-	8	391	-	New gene model
Or278	-	4929	1936681-1939788	-	8	391	-	New gene model
Or279	-	4929	1931553-1935324	-	8	391	-	New gene model
Or280	-	4929	446258-449028	+	8	395	-	New gene model
Or281	-	5009	149207-151964	-	8	393	-	New gene model
Or282	-	5009	145337-148253	-	8	392	-	New gene model
Or283NTE	-	5009	140198->142633	-	8	344	-	First exon missing in gap
Or284	-	5009	136062-138799	-	8	391	-	New gene model
Or285	-	5009	131750-135255	-	8	393	-	New gene model
Or286	-	5009	126818-129918	-	8	394	-	New gene model
Or287PSE	-	5009	118037-121437	-	8	385	-	Pseudogene (3)
Or288FIX	-	5009	112610-115680	-	8	395	-	Fix frameshift
Or289FIX	-	5009	108623-111706	-	8	393	-	Fix frameshift
Or290FIX	-	5009	104623-107823	-	8	393	-	Fix frameshift
Or291	-	5009	100326-103828	-	8	393	-	New gene model
Or292	-	5009	95481-99527	-	8	393	-	New gene model
Or293	-	5009	91624-94594	-	8	392	-	New gene model
Or294PSE	-	5009	85329-89059	-	8	388	-	Pseudogene (5)
Or295PSE	-	5009	82701-84535	-	6	254	-	Pseudogene (2)
Or296	-	5009	78929-81758	-	8	392	-	New gene model
Or297	-	5009	75500-78334	-	8	395	-	New gene model
Or298	-	5009	72059-74920	-	8	393	-	New gene model
Or299PSE	-	5009	67244-70407	-	8	394	-	Pseudogene (1)
Or300	-	5009	62860-65850	-	8	393	-	New gene model
Or301	-	5009	55954-59354	-	8	389	-	New gene model
Or302	-	5009	47774-51801	-	8	391	-	New gene model
Or303FIX	-	5009	40472-42833	-	8	392	-	Fix assembly gap
Or304	-	5009	36353-38951	-	8	393	-	New gene model
Or305	-	5009	32857-35268	-	8	395	-	New gene model
Or306	-	5009	29824-32239	-	8	396	-	New gene model
Or307	-	5009	26845-29211	-	8	396	-	New gene model
Or308	-	5009	23409-26247	-	8	394	-	New gene model
Or309	-	5009	16837-19690	-	8	394	-	New gene model
Or310	-	5009	10813-14257	-	8	391	-	New gene model
Or311	-	5009	7339-9966	-	8	394	-	New gene model
Or312	-	5009	3218-5985	-	8	390	-	New gene model
Or313	-	4834	802002-804791	+	8	392	-	New gene model
Or314	-	4834	805822-809087	+	8	385	-	New gene model
Or315	-	4834	809874-812579	+	8	390	-	New gene model
Or316	-	4834	813276-815887	+	8	394	-	New gene model
Or317	-	4834	817365-819805	+	8	393	-	New gene model
Or318	-	4834	824259-827620	+	8	393	-	New gene model
Or319	-	4834	829215-832227	+	8	392	1	New gene model
Or320	-	4834	833252-835944	+	8	401	-	New gene model
Or321PSE	-	4834	837085-840541	+	8	392	-	Pseudogene (1)
Or322	-	4834	845792-848693	+	8	400	-	New gene model
Or323	-	4834	852461-854980	+	8	387	-	New gene model
Or324	LH14860	4834	856325-859263	+	8	393	-	Part of long model
Or325	LH14860	4834	860022-863192	+	8	394	-	Part of long model
Or326	LH14860	4834	865887-868954	+	8	395	-	Part of long model
Or327	-	4834	871234-874432	+	8	392	-	New gene model
Or328	-	4834	875452-878103	+	8	391	-	New gene model
Or329	-	4834	879383-882352	+	8	393	-	New gene model
Or330	-	4834	883786-886665	+	8	392	-	New gene model
Or331	-	4834	888406-891218	+	8	394	-	New gene model

Or332	-	4834	892015-894763	+	8	393	-	New gene model
Or333	-	4834	895693-898387	+	8	397	-	New gene model
Or334	-	4834	900226-902455	+	8	394	-	New gene model
Or335PSE	-	4834	904449-906702	+	8	378	-	Pseudogene (4)
Or336	-	4834	907637-910019	+	8	398	-	New gene model
Or337	LH14219	4756	10772-13560	-	8	391	-	Multiple changes
Or338	LH22780	5036	13642-15694	-	8	395	-	Multiple changes
Or339FIX	LH19029	4958	437869->443156	+	8	392	-	Fix frameshift and gap
Or340FIX	-	4958	444610->446886	+	8	392	-	Fix two assembly gaps
Or341	LH19031	4958	451425-453999	+	8	391	-	Multiple changes
Or342	LH20416	4985	4586498-4588513	+	8	392	-	Multiple changes
Or343	LH24326	5077	127035-129001	+	8	391	-	Multiple changes
Or344PSE	LH17565	4930	35250-37618	+	8	390	-	Pseudogene (1)
Or345	LH18671	4953	564223-566505	+	8	402	-	First half of model
Or346	LH18671	4953	567889-570720	+	8	402	-	Second half of model
Or347	LH18672	4953	571637-574299	+	8	399	-	Multiple changes
Or348	LH18673	4953	575619-578012	+	8	399	-	Multiple changes
Or349	LH18722	4956	29253-33422	+	8	396	-	First part of large model
Or350	LH26058	5065	721047-717277	-	8	394	-	Multiple changes
Or351FP	-	4938	334243->336846	+	8	397	-	Pseudogene (3)
Or352FN	-	4938	<337671-339474	+	8	344	-	Fix gap; first exon missin
Or353JP	LH24060	4938	340465->342740	+	8	399	-	Join across two scaffolds
		5071	1760818->1765287	-				pseudogene (2)
Or354	LH24060	5071	1757467-1759776	-	8	398	-	Second half of model
Or355	LH20606	4989	1352963-1355444	-	8	406	-	Multiple changes
Or356	LH20597	4989	1356329-1358794	+	8	403	-	Multiple changes
Or357	LH20607	4989	1362107-1364546	-	8	406	-	Part of long model
Or358	LH20607	4989	1368393-1370801	-	8	406	-	Part of long model
Or359PSE	LH20607	4989	1380313-1382798	-	8	407	-	Pseudogene (1)
Or360FIX	LH25885	4989	1383695-1386154	+	8	401	-	Fix frameshift
Or361	LH25885	4989	1387893-1390055	+	8	403	-	Second part of model
Or362FIX	LH20614	4989	1391714-1394069	+	8	402	-	Fix three frameshifts
Or363	LH20614	4989	1395227-1398138	+	8	404	-	Second part of model
Or364FIX	-	4989	1417400-1423818	+	8	402	-	Fix two assembly gaps
Or365	LH18177	4940	1935928-1938616	+	8	403	-	First part of model
Or366	LH18177	4940	1939585-1942816	+	8	402	-	Second part of model
Or367	LH10827	4321	201492-203583	-	8	371	-	Multiple changes

Ionotropic Receptors (IRs). We annotated 32 Ionotropic Receptors in *L. humile* (Table S12). Phylogenetic tree of *L. humile* (blue), *A. mellifera* (green) and *N. vitripennis* (red) iGluRs and IRs, as well as representative fruit fly (*D. melanogaster*, black) orthologs (113). Two ant-specific expansions of IRs are highlighted with a blue vertical line. Protein sequences were aligned with PROBCONS, and the tree was built with RaxML under the WAG model of substitution with 1000 bootstrap replicates. Bootstrap values for each branch are indicated on the tree. The scale bar represents the number of substitutions per site. IR8a and IR25a have been proposed to derive from a non-NMDA iGluR, but in this tree these IR clades group with NMDA receptors with low bootstrap values, most likely due to the number of sequences analyzed.

Table S12. Details of Ionotropic Receptor (IR) annotation.

Name	AED	Scaffold	Strand	Start	Stop	Length	Introns	Comments	Notes
LineAMPA01	0.130991810806196	scf7180001005069	-	498669	481482	861	14		
LineIR25a	0.0613037123648057	scf7180001004995	-	760056	755488	843	4		Added N-term and C-term
LineIR307	0.0157284768211921	scf7180001004929	+	748008	749816	603	0		
LineIR308	0.0461658841940532	scf7180001004978	+	59264	61177	638	0		
LineIR309	novel	scf7180001004978	-	56030	54594	386	3	NTE	No ATG
LineIR310	0.400442708333333	scf7180001005033	-	22640	20895	281	3	NTE	No ATG, modified N-term and C-term
LineIR311.1	novel	scf7180001005018	+	4462665	4464479	605	0		
LineIR311.2	novel	scf7180001005018	+	4466164	4466943	260	0	NTE	No ATG
LineIR311.3	novel	scf7180001005018	+	4468697	4469494	266	0	NTE	No ATG
LineIR311.4	novel	scf7180001005018	+	4473679	4474477	266	0	NTE, PSE	No ATG, 1 frameshift
LineIR311.5	novel	scf7180001005018	+	4471196	4471994	266	0	NTE, PSE	No ATG, 1 frameshift
LineIR311.6	novel	scf7180001005018	+	4476225	4477019	265	0	NTE	No ATG
LineIR311.7	novel	scf7180001005018	+	4461188	4461985	266	0	NTE	No ATG
LineIR312	0.209175493149354	scf7180001004934	+	829250	833940	501	8		
LineIR313.1	0.372203887055372	scf7180001004574	-	72860	70934	367	5	NTE	No ATG. Modified N-term, added C-term
LineIR313.2	novel	scf7180001004574	-	103275	101307	367	5	NTE	No ATG
LineIR315	0.272507435431526	scf7180001004958	+	762376	765039	481	7		
LineIR316	0.10371278140886	scf7180001004922	+	10137	14473	637	3		
LineIR317.1	novel	scf7180001004838	+	18658	21233	581	4		No ATG
LineIR317.2	novel	scf7180001004838	+	6870	8359	245	1	NTE	No ATG
LineIR317.3	novel	scf7180001004838	+	15992	17264	245	1	NTE	No ATG
LineIR318	0.150796538994745	scf7180001004548	+	64685	70553	783	8		
LineIR319	0.314074595355384	scf7180001004995	-	202290	195262	473	8	NTE, INT	No ATG
LineIR68a	0.120852335084016	scf7180001004957	-	104667	100948	501	5		
LineIR75f.1	0.334689153439153	scf7180001005073	-	1429582	1426592	625	9		
LineIR75f.2	novel	scf7180001005073	-	1420314	1414369	610	6	PSE	1 frameshift
LineIR75f.3	0.319230769230769	scf7180001005073	-	1424598	1420762	621	6	PSE	No ATG, added N-term, 1 frameshift
LineIR75u.1	novel	scf7180001004421	+	561351	564853	586	7		No ATG
LineIR75u.2	novel	scf7180001004421	+	570315	573111	460	6	NTE	No ATG
LineIR75u.3	novel	scf7180001004421	+	578230	581254	576	7		No ATG
LineIR76b	0.0525244802146211	scf7180001004861	-	1305417	1303067	546	6		
LineIR8a	0.15557773157923	scf7180001004803	-	583159	576756	918	15		Added C-term
LineIR93a	novel	scf7180001005005	+	685891	691304	860	14		
LineKA01	0.470534586666534	scf7180001004868	-	604919	570511	829	12		No ATG, added N-term and C-term
LineKA02	0.130523604680125	scf7180001004985	-	4420607	4414044	902	14		
LineKA03	0.408257627375274	scf7180001005071	+	1471256	1494318	731	10		Added N-term and C-term
LineKA04	novel	scf7180001005071	+	1513227	1520004	838	13		No ATG
LineKA05	0.300944854602471	scf7180001005071	+	1503518	1510940	906	14		Removed C-term
LineNMDAR01	0.0816666666666667	scf7180001003344	-	47477	41922	899	14		
LineNMDAR02	0.159104710054835	scf7180001004877	-	591329	582044	544	9	NTE	Modified C-term
LineNMDAR03	0.0612734286453341	scf7180001004434	-	102556	95528	1367	7		Modified C-term

IRs	**32**	NTE	Missing N-terminal end
AMPA	**1**	CTE	Missing C-terminal end
NMDA	**3**	INT	Internal gap
Kainate	**5**	PSE	Pseudogene
TOTAL	**41**		

Delta-9 Desaturase Genes

An intricate system of communication is a distinct feature of social insects, indeed all social animals exhibit complex communicative behaviors through a variety methods and mediums. In social insects, colony recognition is an essential aspect of communication, which allows individuals to distinguish colony members from non-members in order to deter foreigners from entering another nest (73, 114, 115). In *L. humile* and other ant species, there is abundant evidence that colony recognition cues are largely based on cuticular hydrocarbons (CHC) (116-118). CHCs are produced by the queen and workers and can be influenced by the environment, resulting in a Gestalt odor for the colony (119).

Approximately 1,000 CHC compounds have been described in the 78 species of ants studied (120). Studies of CHC components in *D. melanogaster* show that carboxylases, elongases and desaturases each influence CHC biosynthesis (121). The desaturases (*desat1*, *desat2*, and *desatF* (syn. *Fad2*)), which are the best studied among these, insert carbon-carbon double bonds into *n*-alkanes to form monoenes and dienes (122, 123). These three desaturase genes have been shown to contribute to CHC alkene variability in *Drosophila* and affect mate recognition behavior (124). In *L. humile*, queens and workers produce variable amounts of four CHC alkenes (125), thus making the three *desaturase* genes, *D. melanogaster desat1*, *desat2*, and *desatF*, choice genome query candidates for determining genes for *L. humile* alkene synthesis.

For all three *D. melanogaster desat1*, *desat2*, and *desatF* query genes, we found the same thirty-three predicted desaturase genes/partial genes (*Main Text*, Figs. 3*D* and S15). These thirty-three Δ9 desaturase genes were distributed across fifteen scaffold regions, with no more than four predicted genes grouping in one scaffold (Fig. S15). This arrangement appears to be somewhat similar to the distribution of the seven Δ9 desaturase genes in *D. melanogaster*, although in *D. melanogaster* they are all grouped on the third chromosome (Fig. S15). Reciprocal BLAST analyses of the *L. humile* Δ9 desaturase genes against *D. melanogaster* found that eleven were most similar to the *D. melanogaster desat1* gene, twenty to the *D. melanogaster* gene CG9747, one to the *D. melanogaster* gene CG9743, one to the *D.*

Figure S15. Summary of *desaturase* gene annotations. Arrangement of the sixteen Δ9 *desaturase* genes and seventeen partial/fragmentary Δ9 *desaturase* genes found in *L. humile*, which are dispersed among fifteen scaffolds of the genome (a.i-xv). The seven Δ9 *desaturase* genes of *D. melanogaster* are also distributed across multiple regions, but are situated on one chromosome (b). Note the *D. melanogaster* chromosome is drawn to a different scale. Predicted genes are indicated by boxes with points representing direction of transcription and span of the genome, and are color coded according to the size of the gene model based on amino acid sequence length found. Asterisks next to *L. humile* gene names signify genes with EST evidence.

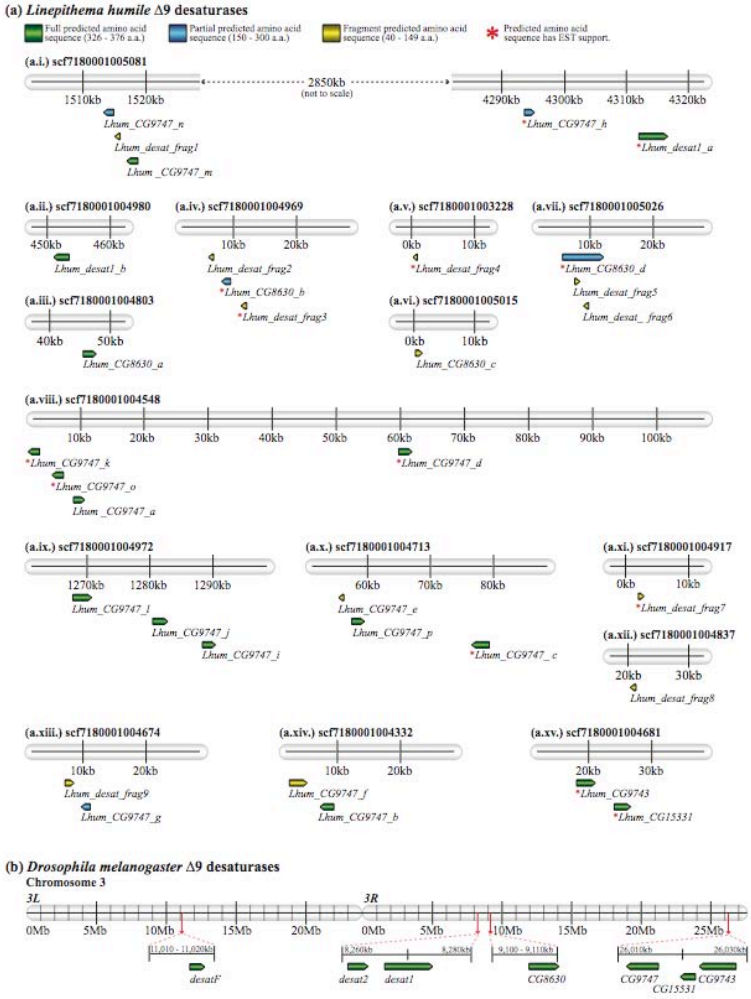

melanogaster gene CG15531, and none were found to be most similar to *D. melanogaster desat2, desatF* or CG8630.

To better elucidate the relationships between the desaturase genes of *L. humile* and several other insects, we performed a phylogenetic analysis using most of the Δ9 desaturase genes found in *L. humile* and six other insect taxa with completed genome sequences. Because of the relatively small size of the nine fragmentary fragmentary Δ9 genes in *L. humile*, these genes, as well as two partial *A. mellifera* desaturase genes, one similar to CG15531 and another to CG8630, were excluded from the analysis. Given this, the amino acid sequences of 85 homologous genes were aligned using the L-INS-i algorithm implemented in MAFFT v6 (12). Gblocks (126) was then used with low stringency parameter settings in order to eliminate positions that were poorly aligned. This resulted in a final trimmed dataset comprising 227 amino acid positions. CpREV+G, was found to be the best evolutionary model for the dataset as determined by ProtTest (127) according to the Akaike Information Criterion corrected for small sample size (we did not consider the LG model since it is not implemented in the phylogenetic software used). According to the best model, a maximum likelihood tree was reconstructed using RAxML v7.0.4 (128), and nodal support values were obtained by a 500-replicate rapid bootstrap analysis (BS).

Our phylogenetic analysis shows the existence of five major clades within the gene family of Δ9 desaturases in insects (Fig. 3*D*). Two clades, clade D and clade E, are each strongly supported (BS=100) and are comprised of single-copy genes, although losses appear to have occurred in some lineages. Clade C, moderately supported (BS = 72), is distinguished by a gene expansion in *N. vitripennis*, but is absent in the aculeates,

L. humile and *A. mellifera*. Furthermore, since the respective gene is also missing in *D. melanogaster*, reciprocal BLAST searches based on this taxon incorrectly identify members of this clade as orthologs of various other *D. melanogaster* genes, which shows that this method alone can be misleading when evaluating homology relations. In clade B, all CG9747 desaturases form a well-supported (BS = 98) monophyletic group, which shows several gene expansion events in *L. humile* and *N. vitripennis*, and seem to have occurred both before and after the split of these lineages. Notably, *A. mellifera* genes are not found in this clade. The remainder of the Δ9 desaturases are represented in clade A, a large and weakly supported (BS=50) group that is reduced in internal resolution and contains multiple genes in all represented taxa. However, it appears to be split into two sub-clades that include *D. melanogaster* CG8630 and *desatF* on the one hand, and *desat1* and *desat2* on the other. Homology relations between *L. humile* and *D. melanogaster* CG8630 and *desatF* cannot be identified reliably, and with the exception of two *A. pisum* and one *T. castaneum* gene, all other genes that are more closely related to CG8630 according to the phylogenetic reconstruction are deemed orthologous to *desat1* according to the best reciprocal BLAST criterion. For four *L. humile* genes this inconsistency also applies. Finally, two *L. humile* genes, *Lhum_desat1_a and Lhum_desat1_b*, can be considered orthologs of the *D. melanogaster desat1* according to both the phylogenetic and reciprocal BLAST analysis, and would be excellent candidate genes for experimental study of *L. humile* CHC alkenes.

Cytochrome P450s

We deduced P450 amino acid sequences for *N. vitripennis*, *A. mellifera*, *D. melanogaster*, and *T. castaneum* (http://drnelson.utmem.edu/CytochromeP450.html) and aligned the with *L. humile* P450s using CLUSTALW Version 2.0.10 (129) after removal of pseudogenes and sequences less than 50% complete. A neighbor joining tree was created using PHYLIP (Version 3.68) with 100 bootstrap replicates (Fig S13). Distances were corrected for multiple substitutions using TREE-PUZZLE Version 5.2 with the BLOSUM62 matrix as the model of substitution (107).

Figure S13. Neighbor-joining tree with four P450 clades highlighted and rooted with P450cam from *Pseudomonas putida*. All putatively functional P450 genes from *L. humile* (Lh, blue), *N. vitripennis* (Nv), *A. mellifera* (Am), *T. castaneum* (Tc), and *D. melanogaster* (Dm) are included as well as CYP3A4 and CYP2J2 from *Homo sapiens* (Hs). Species-specific gene radiations were collapsed into triangles with the number of P450s and family name listed. Nodes with greater than 50% support in 100 bootstrap replications is indicated (*).

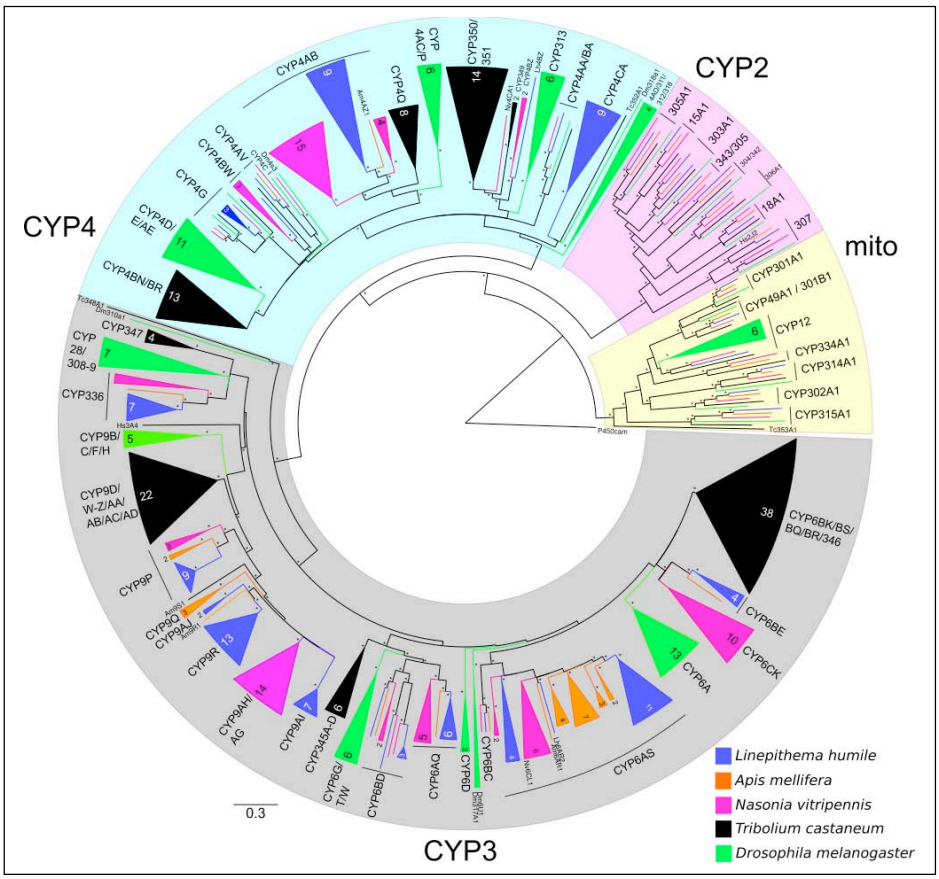

Hox genes

Hox genes are homeodomain-containing transcription factors, very conserved in sequence and expression across arthropods and other animals (130). They play an important role in cell-fate determination and embryonic development, have been identified in all bilateral animal phyla examined to date and are known to determine the positional specification of the anterior-posterior axis (131). Mutations in Hox genes lead to transformations in body-segments and organ identities along this axis and are known as homeotic mutations. This homeotic capability is conserved among arthropods and vertebrates, which diverged more than 600 million years ago (131).

It is speculated that the Early Cambrian ancestor of present-day arthropod groups had a complex containing ten Hox genes (130), which are expressed in Hox-like patterns in chelicerates and myriapods. In the insects, however, homologs of *Hox3* (*zerknullt –zen, zerknullt2 – zen2, bicoid – bcd*) and of *Hox6* (*fushi tarazu – ftz*) do not play a Hox-like role in determining segmental identity.

Hox genes are found in single clusters in a number of invertebrates including amphioxus, sea urchins, and several insects such as mosquitoes, beetles and locusts. In *D. melanogaster*, the cluster is divided in two sections. The Antennapedia Complex (ANT-C) contains genes required for the development of the mouth, head and thoracic segments – *labial* (*lab*), *proboscipedia* (*pb*), *deformed* (*dfd*), *Sex combs reduced* (*Scr*), and *Antennapedia* (*Antp*) –, and the genes in the Ultrabithorax Complex (BX-C), *Ultrabithorax* (*Ubx*), *Abdominal-A* (*abd-A*), and *Abdominal-B* (*abd-B*), are responsible for the development of the fly's abdomen and telson. These portions are separated by approximately 7.5Mb, and the split is thought to be fairly recent in origin. In addition to

the eight genes with traditional Hox-like function, *zen*, *zen2*, *bcd* and *ftz*, the *D. melanogaster* cluster also inlcudes eight cuticle genes, five lysine tRNA genes, and *amalgam* (*Ama*, member of the immunoglobulin superfamily). All other insect genomes studied to date, e.g: *Anopheles gambiae*, *T. castaneum*, *A. mellifera* and *N. vitripennis*, have a contiguous cluster of Hox genes.

The *L. humile* genome has one single gene associated with each of the ten Hox groups of orthology mentioned above, constituting a single Hox cluster in which all transcription occurs in the same direction (Fig. S18; Table S2). The cluster is found in two separate scaffolds (7180001004429 and 7180001004972) of the current assembly. Because of this, it is difficult to assess whether the cluster has been divided in two complexes as it occurs in *D. melanogaster*, or remains a compact cluster of genes. Given that Hox genes are arranged in compact, single clusters in all other hymenopteran genomes studied to date (132) it is possible to assume that the *L. humile* cluster is also found as a single, compact group of genes. Further analyses are necessary to test this

Figure S18. *L. humile* HOX genes, compared to *D. melanogaster*, and *A. mellifera*. *L. humile* HOX genes, compared to *D. melanogaster*, and *A. mellifera*. Figure modeled after Dearden et al (2006). The complex spans approximately 0.8Mb (ruler for intergenic distances is not drawn to scale). *The sequence of the *L. humile* Hox cluster is split across scaffolds 7180001004429 and 7180001004972.

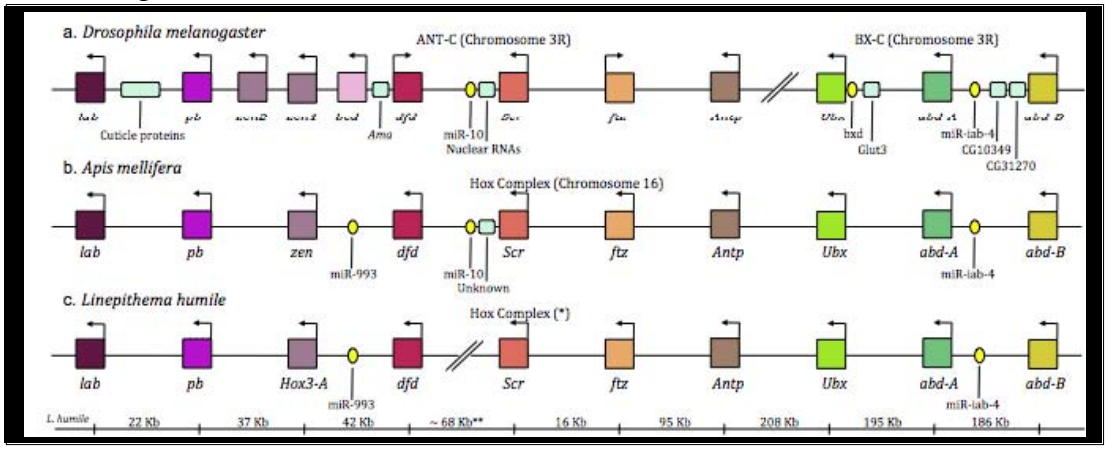

assumption.

We identified two microRNAs within the *L. humile* Hox cluster (Fig. S18). *miR-iab-4* is located in a conserved position compared to *A. mellifera* and *D. melanogaster* (132). The location of *miR-993* is conserved relative to *A. mellifera* and *N. vitripennis* (42) and has not been identified in other Arthropod Hox clusters. A third miRNA conserved throughout currently sequenced Hymenoptera, *mir-10* (42, 132) was not found within the *L. humile* cluster. This could be due to he fact that the current sequence assembly split the cluster in two different scaffolds in the area comprised between genes *dfd* and *Scr*, where *mir-10* is located in other insects where it has been described. No additional gene models were identified within the *L. humile* Hox cluster.The partition of the cluster onto two scaffolds also affects the estimated total size of the cluster. The distance from *Scr* to the end of scf7180001004429 is approximately 44Kb, and the distance from *dfd* to the end of scf7180001004972 is approx. 24Kb. Thus, the estimated distance between the two genes according to the current assembly is about 68Kb. We then estimate the total size of the *L. humile* cluster at approximately 0.8Mb, which is comparable to that of *D. melanogaster* and *T. castaneum* (approx. 0.7Mb), and about half the size of the clusters in the other two hymenopterans sequenced to date (1.68Mb for *N. vitripennis* and 1.37 Mb in *A. mellifera*). Intergenic distances are comparatively smaller than those of *N. vitripennis* and *A. mellifera* (132).

Immune response

Insect humoral immune responses include several signaling pathways that produce effector proteins for the elimination infectious microbes. Genome-wide characterization of insect immune genes has indicated that these pathways are conserved in most insects,

and differences between genomes stem from differences in gene family sizes (Table S16). For example, the honeybee and Nasonia have significantly fewer immune genes than *D. melanogaster* and *Anopheles gambiae* (42, 133-135). In honeybees this finding contrasts with the expectations since the characteristics of sociality (e.g. living in colonies and cooperation) presumably expose them to increased pathogen transmission. However, honeybees also have multitude of social defenses (136) and these may play a more important role than the innate immune responses (133).

Table S16. *L. humile* immune genes.

Apis-blast	Droso-blast	Nasonia-blast	Other copies	ANNOTATED	NOTE	Flybase ID/Apis ID	Gene name in Drosophila/Apis	Symbol
1				lhum_18w		GB15177	18-wheeler	18-w
1				lhum_armi		FBgn0041164	armitage	armi
	1			lhum_Ago2			Argonaute-2	
1				lhum_aub		FBgn0000146	aubergine	aub
1				lhum_Atg5		Fbgn0029943	Autophagy-specific gene 5	Atg5
1				lhum_Atg7		FBgn0034366	Autophagy-specific gene 7	Atg7
	1			lhum_Atg12		Fbgn0036255	Autophagy-specific gene 12	Atg12
1				lhum_cactin		Fbgn0031114	cactin	cactin
1				lhum_cact1a	CG:02184972	GB10655	NF-kappa-B inhibitor cactus 1	cact1a
			1	lhum_cact1b	CG:02184980	GB10655	NF-kappa-B inhibitor cactus 1	cact1b
1				lhum_casp		Fbgn0034068	caspar	casp
	1			lhum_Dcr-2		Fbgn0034246	Dicer-2	Dcr-2
	1			lhum_dredd		Fbgn0020381	death related ced-3/Nedd2-like protein	Dredd
1				lhum_def		Fbgn0010385	defensin	Def
	1			lhum_dome		FBgn0043903	domeless	dome
1				lhum_dl		Fbgn0260632	dorsal	dl
1				lhum_Duox		FBgn0031464	dual oxidase	Duox
1				lhum_egr		Fbgn0033483	eiger	egr
	1			lhum_FADD		FBgn0038928	FADD	FADD
1				lhum_galectin1		GB10026	Galectin 1	galectin1
1				lhum_galectin2		GB18324	Galectin 2	galectin2
	1			lhum_galectin		CG11372	Galectin	galectin
1				lhum_GNBP1-1	CG:02183786,	Fbgn0040323, GB19961	Gram-negative bacteria-binding protein 1	GNBP1-1
			1	lhum_GNBP1-2_like1	shorter than others; no functional domain; still has EST support.	Fbgn0040323, GB19961	Gram-negative bacteria-binding protein 1-2	GNBP1-2_like1
1				lhum_GNBP1-2	CG:02183974	Fbgn0040323, GB19961	Gram-negative bacteria-binding protein 1-2	GNBP1-2
			1	lhum_GNBP1-	shorter than	Fbgn0040323,	Gram-negative	GNBP1-

				2_like2	others; no functional domain; still has EST support.	GB19961	bacteria-binding protein 1-2	2_like2
		1		lhum_Hisnavicin-3		XP_001607730	Hisnavicin-3	Hisnavicin-3
1				lhum_hop		Fbgn0004864	hopscotch	hop
1				lhum_hymenoptaecin		GB17538-PA	hymenoptaecin preproprotein	LOC406142
1				lhum_imd		FBgn0013983	immune deficiency	imd
1				lhum_Iap2		Fbgn0015247	inhibitor of apoptosis 2	Iap2
1				lhum_IKKgamma	poor blast match	GB17106-PA	inhibitor of kappaB kinase gamma	IKKgamma
1				lhum_bsk		GB16401-PA	JNK MAP kinase basket	bsk
1				lhum_Jra		GB12004-PA	Jun-related antigen	Jra
1				lhum_kay		Fbgn0001297	kayak	kay
1				lhum_Lys-3		GB19988-PA	Lysozyme 3	Lys-3
1				lhum_Lys-2		GB15106	Lysozyme-2	Lys-2
1				lhum_MyD88	CG:02184700	GB12344-PA	myeloid differentiation primary response factor 88	Myd88
1				lhum_Rel		GB13742-PA	NF-kappaB transcription factor relish	Rel
		1		lhum_Naickin-1		XP_001600083	Naickin-1	Naickin-1
		1		lhum_Naickin-2a		XP_001599718	Naickin-2	Naickin-2a
			1	lhum_Naickin-2b		XP_001599718	Naickin-2	Naickin-2b
1				lhum_NimA		GB12883-PA	nimrod A	NimA
1				lhum_Atg7		FBgn0034366	Autophagy-specific gene 7	Atg7
1				lhum_NimC		GB14645-PA	nimrod C1	NimC1
1				lhum_NOS		GB18010-PA	nitric oxide synthase	NOS
1				lhum_Pli		Fbgn0025574	Pellino	Pli
1				lhum_PGRP-LC		GB17188-PA	Peptidoglycan recognition protein LC	PGRP-LC
1				lhum_PGRP-S2a		GB19301	peptidoglycan recognition protein S2	PGRP-S2a
			1	lhum_PGRP-S2b		GB19301	peptidoglycan recognition protein S2	PGRP-S2b
1				lhum_PGRP-S1		GB15371	peptidoglycan recognition protein S1	PGRP-S1
			1	lhum_PGRP-LC_like		GB17188-PA	peptidoglycan-recognition protein LC	PGRP-LC_like
1				lhum_PGRP-SA		GB17879-PA	peptidoglycan-recognition protein SA	PGRP-SA
1				lhum_PPO		GB18313-PA	prophenoloxidase	PPO
1				lhum_Rpn3		GB12827-PA	regulatory particle non-ATPase 3	Rpn3
1				lhum_SCR-B10		GB19683	scavenger receptor class B, type 10	SCR-B10
1				lhum_SCR-B2		GB11743-PA	scavenger receptor class B, type 2	SCR-B2
1				lhum_SCR-B5		GB13813-PA	scavenger receptor class B, type 5	SCR-B5
1				lhum_SCR-B9		GB19916	scavenger receptor class B, type 9	SCR-B9
1				lhum_SCR-C	Missing 5’	GB19925-PA	scavenger receptor	SCR-C

					end		class C	
1				lhum_SP14		GB14044-PA	serine protease 14	SP14
1				lhum_SP1b		GB16147	serine protease 1	SP1
			1	lhum_SP1a		GB16147	serine protease 1	SP1
1				lhum_SP2		GB14247	serine protease 2	SP2
1				lhum_SP30		GB19649-PA	serine protease 30	SP30
1				lhum_SP46		GB16367-PA	serine protease 46	SP46
1				lhum_SP49		GB15317-PA	serine protease 49	SP49
1				lhum_Serpin-1		GB17012-PA	serine protease inhibitor 1	serpin-1
1				lhum_Serpin-3		GB30307-PA	serine protease inhibitor 3	Serpin-3
1				lhum_Serpin-5		GB19582-PA	serine protease inhibitor 5	serpin-5
	1			lhum_Serpin-4		FBgn0028985	serine protease inhibitor 4	serpin-4
1				lhum_pll		GB16397-PA	serine/threonine-protein kinase pelle	pll
1				lhum_Stat92E		Fbgn0016917	Signal-transducer and activator of transcription protein at 92E	Stat92E
		1		lhum_spz1		Fbgn0003495	Spatzle 1	spz1
				lhum_spz2		Fbgn0261526	Spatzle 2	spz2
				lhum_spz4		FBgn0032362	Spatzle 4	spz4
				lhum_spz5		Fbgn0035379	Spatzle 5	spz5
				lhum_spz6		Fbgn0035056	Spatzle 6	spz6
1				lhum_Tab2		FBgn0086358	Tak1-associated binding protein 2	Tab2
1				lhum_Tak1		GB14664	TGF-beta activated kinase 1	Tak1
1				lhum_TepIII		Fbgn0041181	thiolester containing protein III	TepIII
1				lhum_TEP7		GB12605-PA	thiolester-containing protein 7	TEP7
1				lhum_TEPA		GB18789-PA	thiolester-containing protein A	TEPA
1				lhum_Traf6		GB10539-PA	TNF-receptor-associated factor 6	Traf6
1				lhum_Traf1		GB10394	TNF-receptor-associated factor 1	Traf1
1				lhum_Toll-1a		GB18520	toll like receptor 1	Toll-1a
			1	lhum_Toll-1b		GB18520	toll like receptor 1	Toll-1b
			1	lhum_Toll-1_like1	no start codon	GB18520	toll like receptor 1	Toll-1_like1
			1	lhum_Toll-1_like2		GB18520	toll like receptor 1	Toll-1_like2
			1	lhum_Toll-1d		GB18520	toll like receptor 1	Toll-1d
1				lhum_Toll-10		GB16299	toll like receptor 10	Toll-10
1				lhum_Toll-6		GB17781	toll like receptor 6	Toll-6
1				lhum_Toll-8		GB10640-PA	toll like receptor 8	Toll-8
1				lhum_tub		Fbgn0003882	tube	tub
67	8	4	11					
				lhum_GNBP	Pseudogene?			
				lhum_Toll-1	Pseudogene?			

Opsins

Opsins are transmembrane, G-protein coupled receptors that, when coupled with a chromophore, form visual pigments. In insects, the number of opsin genes varies from

two, in *Tribolium*, to seven, in *D. melanogaster*, and in some cases the number of opsins has evolved in tandem with distinctive wing coloration. Although Argentine ants are less visually-oriented foragers than honeybees, they have still retained the same four visual opsins that are present in the honeybee genome: *ultraviolet*, *blue*, *long wavelength opsin 1* and *long wavelength opsin 2* (Table S2). The Argentine ant genome also contains a *pteropsin*-like non-visual opsin, as has been reported for *A. mellifera*.

Behavior

The unusual unicolonial social structure of introduced Argentine ant populations has made them an attractive model system for studies of colonymate recognition and social behaviors. We manually annotated >75 genes associated with important behaviors that are related to Argentine ant sociality, including genes implicated in learning, memory, aggression, and circadian cycles. The ability to distinguish between colonymates and ants from foreign colonies requires the production of colony-specific labels, the ability to recognize these labels, and elements of learning and memory.

Learning and memory. Many animals possess the ability to gain and process information about the environment (learning) and store and retrieve information over time (memory). Insects, in particular, often rely on olfaction for a variety of behaviors such as foraging, mating, and predator avoidance (137-139). Candidate genes implicated in learning and memory have been most well studied in *Drosophila*, and this functional group includes a diverse array of genes, including some involved in neurotransmitter production (140-142), cell adhesion molecules (143, 144), cAMP signaling cascade molecules (145, 146), CaMKII proteins (147-149), and RNA transport and translation molecules (150).

Drosophila melanogaster and *A. mellifera* have been well studied in the last four decades, becoming widely used models for studying olfactory learning and memory. The learning and memory functional group is composed genes that when absent or altered are known to affect learning and memory.

Most of the insect genes that have been implicated in olfactory learning and memory have been described and studied in *D. melanogaster*. We selected genes for annotation based on the gene ontology terms "learning or memory" in *D. melanogaster*. We found 106 genes, investigated the 69 genes with annotation records in other species, and manually annotated the 59 found in Argentine ants (Table S2). Only two of these genes were found in *L. humile*, but not *N. vitripennis* or *A. mellifera*. Social insects, like *L. humile*, rely heavily on olfactory learning and memory for activities such as nest mate recognition. This data set will provide a rich resource for further studies in learning and memory within ant species.

Aggression. As with most ants, nestmate recognition in Argentine ants has often been studied by examining the behavior of workers towards non-colonymates (151-153). Aggression involves the direct action, interaction and regulation of several genes that results in a complex behavioral phenotype.

Several studies on the genetics of aggression in mammals and invertebrates have focused on bioamines, major chemical substances involved in the neurobiology of animals that appear to have clear effects on the aggression (154, 155). However, recent studies in *D. melanogaster* suggest that genes involved in basic biological and molecular functions also play a role in aggression (156-158). These include genes involved in

processes such as cell communication, metabolic processes and electron transport. While the role of these genes in aggression have been discovered in the context of intraspecific male aggression in *D. melanogaster*, similar gene categories have also been implicated in the honey bee colony defense (159). Moreover, some of the genes involved in aggressive behavior in fruit flies appear to have evolutionary conserved orthologous also found in humans (160).

Animals display both intraspecific and interspecific aggression in a variety of different contexts. Aggression is particularly common in ants, often because colonies must defend local resources from neighboring ant colonies. We identified five genes in *L. humile* that are similar to those associated with interspecific male aggression in *D. melanogaster* including *ade5*, *eclair*, *echinoid, no occelli,* and *sugarless* (Table S2). The ontology of these genes varies from cell communication and intracellular protein transport to sensory organ development. Additionally, all five of these genes appear to have pleiotropic effects on other male *D. melanogaster* phenotypes including number of sensory bristles, sleep patterns, and starvation stress resistance (158). All five aggression genes in *L. humile* had significant matches to *A. mellifera* indicating possible orthology while only two such gene similarities were found in *N. vitripennis*.

Circadian rhythms. In insects, daily cycles of activity are controlled by one of three different transcriptional regulation systems: those governed by the expression of *cryptochrome 1* (*cry1*), those driven by the expression of *cryptochrome 2* (*cry2*), and those in which both *cry1* and *cry2* are present. Butterflies and mosquitoes possess both *cry1*and *cry2*; *Drosophila* only has *cry1*. Unlike many other insects, *L. humile* does not

exhibit a strong daily activity pattern. Instead, workers typically forage during both the day and night, often along enormous foraging trails. Argentine ants, like *Apis* and *Tribolium*, do not possess a copy of the *cry1* gene (Table S2).

Model for human disease. Insect models, particularly *D. melanogaster*, have been invaluable systems for studies of human processes and diseases. Recent studies suggest that social insects may also prove to be useful for as model systems for some human diseases. *A. mellifera*, for example, exibits a behavioral response to cocaine that is similar to that of humans (161), raising the intriguing possibility that ant genomes could be also be a useful invertebrate models of human behavioral diseases. Indeed, our KEGG and OrthoMCL analysis of the *L. humile* genome identified over 1400 genes involved in over 30 pathways implicated in human diseases ranging from diabetes, to multiple cancers, to neurological disorders such as Alzheimer's, Parkinson's disease, and William's Beuren Syndrome (Table S5).

Figure S14. *Major royal jelly protein* genes in the three Hymenoptera with sequenced genomes, *L. humile* (green), *N. vitripennis* (blue), *and A. mellifera* (red).

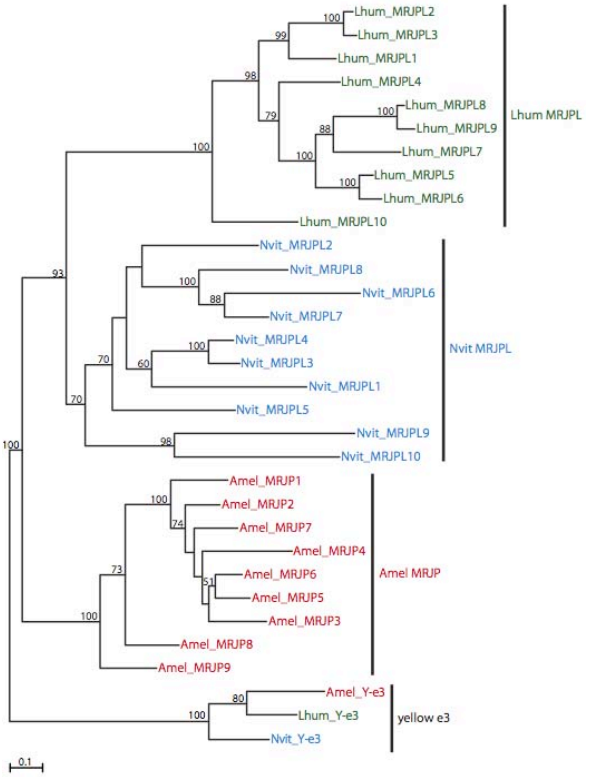

Yellow/Major royal jelly proteins
To identify and retrieve genes belonging to the yellow and major

royal jelly protein (MRJP) gene family in *L. humile*, we employed a standardized BLAST strategy. The members of the focal gene family in D. melanogaster were selected from FlyBase (http://flybase.org) and served as reference genes; in the case of the major royal jelly protein and major royal jelly protein-like genes, reference sequences were retrieved from the *A. mellifera* and *N. vitripennis* assemblies of the Hymenopteran Genome Database (http://genomes.arc.georgetown.edu/drupal/). The BLAST package (133) was then used to identify regions and gene models from the L. humile OGS v1.1 produced by MAKER.

To understand the evolutionary history and homology relations of the yellow/MRJP gene family in the Argentine ant, we performed two phylogenetic analyses: The first analysis included all yellow and MRJP genes of the focal taxa mentioned above and *Tribolium castaneum*. The amino acid sequences of these 94 genes were aligned with MAFFT v6 and the L-INS-i algorithm (30). Positions that were aligned ambiguously were removed using Gblocks (96) with low stringency parameters. This resulted in a final dataset containing 169 amino acid positions. The evolutionary model with the best fit to this dataset, LG+G, was determined by ProtTest (97) according to the Akaike Information Criterion corrected for small sample size. Based on this model, a maximum likelihood tree was reconstructed using RAxML version 7.2.6 (98). Nodal support values were obtained by the rapid bootstrap algorithm as implemented in RAxML (500 replicates). A yellow gene from the bacterium *Dienococus radiodurans* was used as the outgroup for the analysis.

The maximum likelihood tree of this analysis reveals six clades, here termed yellow g and g2, yellow x1, yellow core group (b/c/f/h/y), yellow e, yellow

e3/x2 and MRJP (includes MRJP-like) (Fig. 3 *C*). Several of these clades provide strong support for orthologous relationships between *L. humile* genes and those of similarly named genes from the other four focal taxa (see clades yellow g and g2, x1, e, and e3/x2, Fig. 3*C*). The yellow core group (named because it contains the originally described *yellow-y* of *D. melanogaster*) contains well-supported yellow b and y groups but the relationships of the *yellow-h, -c,* and *-f* genes are less resolved in this analysis.

The second analysis focused exclusively on the 29 members of the MRJP gene subfamily retrieved from the hymenopteran taxa, as well as 3 hymenopteran *yellow-e3* genes which comprised the outgroup (Fig. S14). Except for the alignment algorithm, which was E-INS-i, the same methods were used as described above. After removing ambiguously aligned positions, the dataset encompassed 284 positions, which indicates that a larger amount of informative sites were retained due to decreased sequence diversity in the dataset. Consequently, higher confidence values support this tree, which is topologically identical to the comprehensive tree with respect to the MRJP gene subfamily. The topology strongly indicates that the radiation of the MRJP genes in each taxon took place after the evolutionary split of their respective lineages (see main text). Except for the production of royal jelly in *Apis,* the functions of these genes are unknown but may share similarities between *Nasonia*, *Apis* and *L. humile* and may have evolved in response to similar selective pressures.

Insulin signaling

The insulin signaling pathway is highly conserved among animals and is a major regulator of growth, reproduction, and aging (162). In *A. mellifera*, it is also known to be involved in developmental differentiation of the queen and worker castes (163-167).

Appropriate allocation of carbohydrates to lipids is an important process in social insects as stored lipids are a stored "communal resource" that can be tapped into if incoming food supplies decrease (168). Ants with high carbohydrate intake, such as those feeding on homopteran honeydew, may face challenges in coping with such high carbohydrate intake. Interestingly, introduced populations of *L. humile* commonly tend Homoptera, and thus occupy a lower trophic position than the more carnivorous populations in the native range (169), suggesting that there may be associated differences in insulin signaling between the two ranges.

We annotated a complete and apparently functional insulin signaling pathway (22 genes annotated) in the Argentine ant (Table S2).). Initiation of cell growth is likely induced by this pathway, with the detection of growth factor receptors by the *Pi3K* complex (*Lhum_Pi3K21B, Lhum_Pi3K59F, Lhum_Pi3K68D, and Lhum_Pi3K92E*) which activates *PDK-1* and *AKT* (*Lhum_PDK1*; *Lhum_AKT*). *AKT* can then phosphorylate *mTor* (*Lhum_TOR*), which in turn can phosphorylate *4EBP* (*Lhum_4EBP*), leading to the downstream activation of *EIF-4B* (*Lhum_EIF4B*) and *RPS6* (*Lhum_RPS6*). This can result in the initiation of translation and contributes to overall cell growth. Most of the proteins in this pathway are highly conserved and have only minor variation compared to even mammalian orthologs (e.g., *target of rapamycin*, *Lhum_Tor*, has 61% identity to its ortholog in humans, *mTor*, across 2538 amino acid positions). The general exceptions to sequence conservation are the insulin-like peptides (*Ilp*, also referred to as insulin related peptides, *Irp*), which are short, ~100 a.a., and have few highly conserved residues (162). Furthermore, the number of insulin-like peptides varies across taxa; *Drosophila melanogaster* has seven *Ilp* genes while *A. mellifera* only two (one of which

is described as an Insulin-like growth factor peptide, *Igf*). Similarly, the number of insulin receptor genes (*InR*) varies across taxa, with *D. melanogaster* having only one while *A. mellifera* two. In *L. humile* we found two *Ilp* and two *InR* genes. One of the *L. humile* insulin peptides is more similar to typical insect Ilp (*Lhum_Ilp1*) while the other to insulin growth factor (*Lhum_Ilp2*). A search of the *Lhum_InR1-2* predicted proteins in NCBI is similarly complicated with hits of both insulin receptors and insulin-like growth factor receptors. Thus, it is currently unclear whether there is a one to one relationship of the peptides and receptors, and in mammals both peptides bind to both receptors, but with differing affinities.

Relative Evolutionary Rates Analysis

To analyze the rate of evolution of *L. humile*, we compared the amino acid composition of Argentine ant OGS1.1 proteins and their predicted orthologs in *Apis mellifera*, *Nasonia vitripennis*, and *Drosophila melanogaster*. Evolutionary comparisons between distantly related species can be skewed if more than one mutation, on average, occurs per synonymous codon site. Since Diptera and Hymenoptera are separated by >300MYA, we focused on non-synonymous substitutions in highly conserved regions of orthologous proteins.

Predicted orthologs were identified with OrthoMCL (53) to group annotated proteins into putative orthologous sets. Each set was required to have a single gene copy from each species with no species being unrepresented in the set. Proteins from of each set were aligned to each other using Clustalw (170) and further processed using Gblocks (126) to extract only conserved blocks found in all four species. The final alignments were measured to estimate the distribution of amino acid substitution rates. We then

concatenated the multiple alignments from each orthologous set together to estimate the average substitution rate for the coding portion of he genome using the program PROML (http://evolution.genetics.washington.edu/phylip.html). PROML was constrained by the tree topology corresponding to the known phylogenic relationship of the species studied. Branch lengths were allowed to vary to best fit the multiple alignments to the constrained tree topology. The branch lengths produced by PROML are proportional to the expected amino acid substitutions, and provides a simple means to calculate the substitution rates between different nodes of the tree. Each tree was rooted using *D. melanogaster* as the out-group, which allowed us to calculate the number of amino acid substitutions per site occurring in the remaining three species relative to their last shared common ancestor (Figure S19).

Figure S19. A tree of the phylogenetic relationships for different species of insects related to *L. humile*. Amino acid substitution rates in orthologous proteins were estimated for organisms in the orange box (A). The average number of amino acid substitutions estimated to have occurred per site in a concatenated, multiple seqence alignment of orthologous proteins compared to the last common ancestor of the organisms from (A) and *D. melanogaster* is shown (B). The distribution of substitution rates for all orthologous protein sets when calculated independently, rather than as part of the concatenated alignments are indicated for *L. humile* (red), *N. vitripennis* (green), and *A. mellifera* (blue) (C).

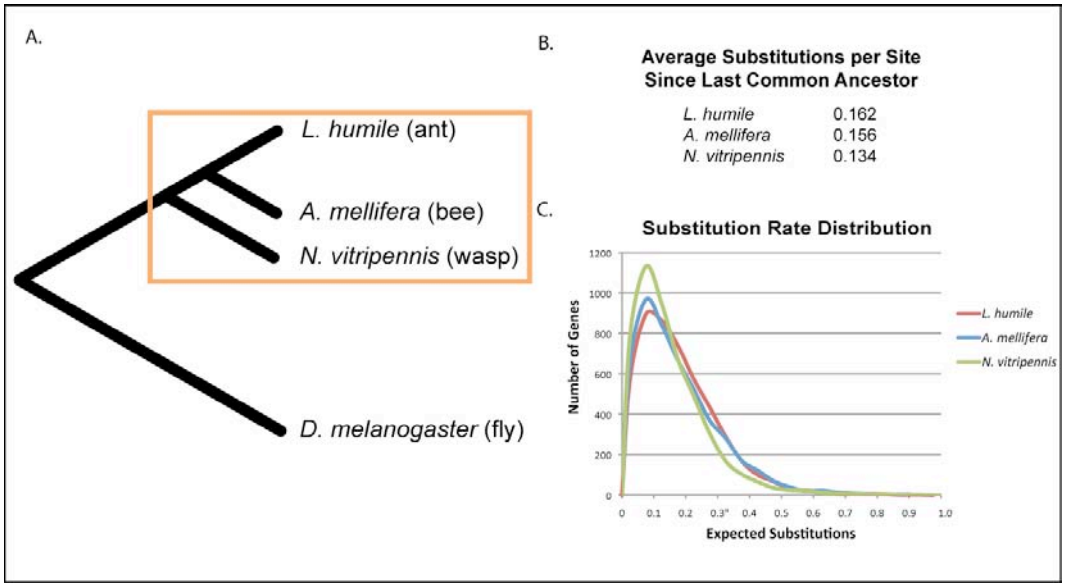

Foraging Gene qPCR

The resources presented here will accelerate and facilitate molecular studies of Argentine ants. Using the transcriptome and genomic data presented here, we annotated the *foraging* gene (LH17994/LH24060), designed primers for quantitiative PCR, and quantified expression levels of this gene across several developmental stages.

Using the *L. humile* transcriptome dataset we matched contigs to the *foraging* gene sequence of *D. melanogaster, A. mellifera*, *N. vitripennis*, and *P. barbatus*. We selected primers using Primer3 (171) then purchased them from Elim Biopharmaceuticals, Inc. (Hayward, CA). We extracted RNA from workers, larvae and

pupae raised in the lab and gathered in the field using Qiagen RNeasy Mini kit (Catalog #74104). Residual DNA was removed using Turbo DNAse from Ambion (AM2238). cDNA was made using the Invitrogen SuperScript III First-Strand Synthesis System for RT-PCR kit (Catalog Number 18080-051) using oligo d(T).

Quantitative reverse-transcriptase real-time PCR was performed using the Invitrogen kit, SYBR GreenER qPCR SuperMix Universal (Catalog number 11762-100). Each sample was diluted to contain the same volume of starting RNA and run in triplicate. The average of the CT value as well as the standard deviations were calculated. The housekeeping gene *glyceraldehyde 3-phosphate dehydrogenase* (GAPDH) was used as the reference gene and the primers were tailored to the Argentine ant by using the EST dataset.

During the larval stage, expression is similar to that of the workers however, the pupae stage increases almost 6 fold higher than both the larval and worker stages (Fig. S20). We standardized all of the data to values obtained from samples of workers giving the following results for fold change: 1, 6.39, 2.23 for worker, pupae and larvae, respectively. The following results are fold changes for field samples: 1, 6.14, 1.39 for worker, pupae and larvae, respectively. The fold changes for lab samples: 1, 6.68, 2.00 for worker pupae and larvae, respectively. Our data compares gene expression of a section of the 3' end of the *foraging* gene in developmental stages of the Argentine ant. We looked at larvae, pupae, and workers. We compared samples that were taken directly from the field and samples that had been reared in the laboratory colonies to confirm that there is no variation in gene expression between these two environments (Fig. S20). We used *GAPDH* as a control gene for every sample taken to insure uniformity across

samples and no contaminates or variants were present. There is no significant difference between field and lab samples, with only a slight increase in expression of the *foraging* gene in the field samples (Fig. S20). In comparison to other organisms we see that expression increasing in developmental stages but in the harvester ant regulation is down regulated. Importantly, the harvester ant data was taken only from callows and workers while our data was taken from early developmental stages (larvae and pupae) as well as workers. The differences seen in regulation of the *foraging* gene between these two organisms could be due to the limited developmental stages tested.

Figure S20. Quantitative PCR data of the *foraging* gene. A comparison between larva, pupae, and adult workers from lab and field samples. Results are normalized to worker expression, which is set at 1.

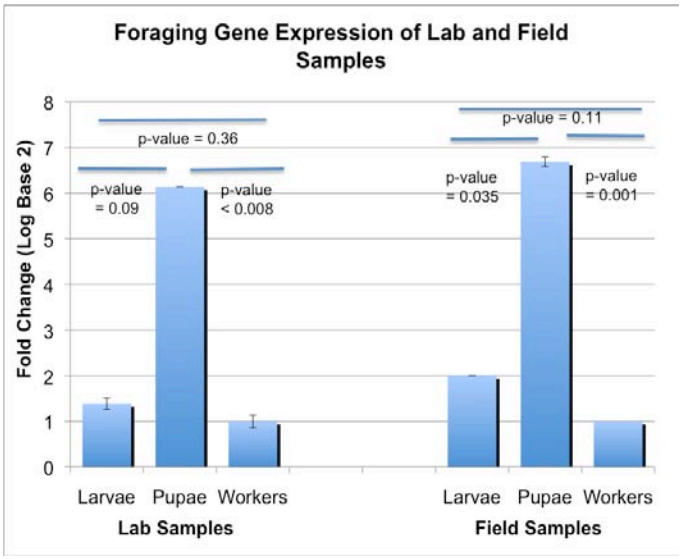

Annotation of the *L. humile* genome as a teaching tool

The undergraduate Evolutionary Genomics class at Earlham College (students: H. Albers, M. Bahnick, T. Carter, K. Clay, P. Hallowell, J. Hood, S. McGuire, A. Miller, M. Naughton, K. O'Rourke-Owens, K. Paine, J. Pillow, P. Raines, and C. Wertman) used the *L. humile* genome as a tool for students to learn gene structure, orthology, and annotation. Each student in the class chose five genes to annotate. The choice of genes varied from those involved in basic cellular processes (e.g., the cell cycle) to heat shock proteins, but

was entirely student driven. More than 50 genes were annotated by the class. After selecting their genes, students researched the literature on the genes and found gene models in insects (principally *D. melanogaster* and *A. mellifera*). Students identified the location of genes in the *L. humile* genome, and used basic BLAST tools to assess whether the *ab initio* gene predictors used by Maker had computationally predicted a gene. Using all available evidence the students reviewed the gene models and, in the process, learned basic elements of gene structure (intron/exon boundaries, conserved domains, etc.) and the process of refining gene models. As a quality control step, the students turned in their revised gene model and detailed evidence for any changes they made to the *ab initio* prediction; once approved the students uploaded their revisions to the genome server. At the conclusion of the course students responded very positively (4.7 on a 1-5 scale) in a survey about how influential working on a real, unpublished genome was in the material learned in the course.

ACKNOWLEDGEMENTS

We thank G. Anderson for providing the ants used in this project, A. Smith for assistance with transcriptome sequencing, L. Tonkin and the V. Coates Genomic Sequencing Facility (UC Berkeley) and the Center for High Performance Computing (University of Utah) for assistance and use of facilities, G. Robinson for support, M. Wong for script support, M. Goodisman for valuable discussion, B. Hunt and S. Yi for generously sharing useful data, and B. Moore for assistance with SNP analysis. Infrastructure for this work was supported in part by NHGRI NIH grant 1R01HG004694 (MY) , NIMH NIH grant 5SC2MH086071 (CDS) and the UIUC Romano Professorial Scholarship (HMR).

REFERENCES

1. van Wilgenburg E, Torres CW, & Tsutsui ND (2010) The global expansion of a single ant supercolony. Evolutionary Applications 3(2):136-143.
2. Krieger MJB & Keller L (1997) Polymorphism at dinucleotide microsatellite loci in fire ant *Solenopsis invicta* populations. Molecular Ecology 6:997-999.
3. Suarez AV, Tsutsui ND, Holway DA, & Case TJ (1999) Behavioral and genetic differentiation between native and introduced populations of the Argentine ant. Biological Invasions 1(1):43-53.
4. Tsutsui ND, Suarez AV, Holway DA, & Case TJ (2000) Reduced genetic variation and the success of an invasive species. Proceedings of the National Academy of Sciences of the United States of America 97(11):5948-5953.
5. Nei M (1987) Molecular evolutionary genetics (Columbia University Press, New York).
6. Suarez AV, Holway DA, Liang D, Tsutsui ND, & Case TJ (2002) Spatiotemporal patterns of intraspecific aggression in the invasive Argentine ant. Animal Behaviour 64:697-708.
7. Miller JR, *et al*. (2008) Aggressive assembly of pyrosequencing reads with mates. Bioinformatics 24(24):2818-2824.
8. Cantarel BL, *et al*. (2008) MAKER: An easy-to-use annotation pipeline designed for emerging model organism genomes. Genome Res 18(1):188-196.
9. Edgar RC & Myers EW (2005) PILER: identification and classification of genomic repeats. Bioinformatics 21 Suppl 1:i152-158.
10. Korf I, Yandell M, & Bedell J (2003) BLAST (O'Reilly Media, Sebastopol, CA) p 368.
11. Slater GS & Birney E (2005) Automated generation of heuristics for biological sequence comparison. Bmc Bioinformatics 6:31.
12. Benson DA, Karsch-Mizrachi I, Lipman DJ, Ostell J, & Wheeler DL (2005) GenBank. Nucleic Acids Res 33(Database issue):D34-38.
13. Anonymous (The Universal Protein Resource (UniProt) in 2010. Nucleic Acids Res 38(Database issue):D142-148.
14. Korf I (2004) Gene finding in novel genomes. Bmc Bioinformatics 5:-.
15. Stanke M, Tzvetkova A, & Morgenstern B (2006) AUGUSTUS at EGASP: using EST, protein and genomic alignments for improved gene prediction in the human genome. Genome Biol 7 Suppl 1:S11 11-18.
16. Lukashin AV & Borodovsky M (1998) GeneMark.hmm: new solutions for gene finding. Nucleic Acids Res 26(4):1107-1115.
17. Eilbeck K, Moore B, Holt C, & Yandell M (2009) Quantitative measures for the management and comparison of annotated genomes. Bmc Bioinformatics 10:67.
18. Quevillon E, *et al*. (2005) InterProScan: protein domains identifier. Nucleic Acids Research 33:W116-W120.
19. Smith CD, *et al*. (2007) Improved repeat identification and masking in Dipterans. Gene 389(1):1-9.
20. Mungall CJ & Emmert DB (2007) A Chado case study: an ontology-based modular schema for representing genome-associated biological information. Bioinformatics 23(13):i337-346.

21. Lewis SE, *et al*. (2002) Apollo: a sequence annotation editor. Genome Biol 3(12):RESEARCH0082.
22. Waterhouse AM, Procter JB, Martin DM, Clamp M, & Barton GJ (2009) Jalview Version 2--a multiple sequence alignment editor and analysis workbench. Bioinformatics 25(9):1189-1191.
23. Ryter JM & Schultz SC (1998) Molecular basis of double-stranded RNA-protein interactions: structure of a dsRNA-binding domain complexed with dsRNA. Embo J 17(24):7505-7513.
24. Kenmochi N, *et al*. (1998) A map of 75 human ribosomal protein genes. Genome Res 8(5):509-523.
25. Brodersen DE & Nissen P (2005) The social life of ribosomal proteins. Febs J 272(9):2098-2108.
26. Sengupta J, *et al*. (2004) Identification of the versatile scaffold protein RACK1 on the eukaryotic ribosome by cryo-EM. Nat Struct Mol Biol 11(10):957-962.
27. Nilsson J, Sengupta J, Frank J, & Nissen P (2004) Regulation of eukaryotic translation by the RACK1 protein: a platform for signalling molecules on the ribosome. EMBO Rep 5(12):1137-1141.
28. Wool IG, Chan YL, & Gluck A (1995) Structure and evolution of mammalian ribosomal proteins. Biochem Cell Biol 73(11-12):933-947.
29. Marygold SJ, *et al*. (2007) The ribosomal protein genes and minute loci of *Drosophila melanogaster*. Genome Biol 8(10):R216.
30. Zhang Z, Harrison P, & Gerstein M (2002) Identification and analysis of over 2000 ribosomal protein pseudogenes in the human genome. Genome Res 12(10):1466-1482.
31. Uechi T, Tanaka T, & Kenmochi N (2001) A complete map of the human ribosomal protein genes: assignment of 80 genes to the cytogenetic map and implications for human disorders. Genomics 72(3):223-230.
32. Katoh K, Misawa K, Kuma K, & Miyata T (2002) MAFFT: a novel method for rapid multiple sequence alignment based on fast Fourier transform. Nucleic Acids Res 30(14):3059-3066.
33. Wall DP, Fraser HB, & Hirsh AE (2003) Detecting putative orthologs. Bioinformatics 19(13):1710-1711.
34. Porcelli D, Barsanti P, Pesole G, & Caggese C (2007) The nuclear OXPHOS genes in insecta: a common evolutionary origin, a common cis-regulatory motif, a common destiny for gene duplicates. Bmc Evol Biol 7:215.
35. Rand DM, Haney RA, & Fry AJ (2004) Cytonuclear coevolution: the genomics of cooperation. Trends in Ecology & Evolution 19(12):645-653.
36. D'Elia D, *et al*. (2006) The MitoDrome database annotates and compares the OXPHOS nuclear genes of *Drosophila melanogaster*, *Drosophila pseudoobscura* and *Anopheles gambiae*. Mitochondrion 6(5):252-257.
37. Smit AFA, Hubley R, & Green P (1996-2004) Repeatmasker open-3.0).
38. Bao Z & Eddy SR (2002) Automated de novo identification of repeat sequence families in sequenced genomes. Genome Res 12(8):1269-1276.
39. Benson G (1999) Tandem repeats finder: a program to analyze DNA sequences. Nucleic Acids Research 27(2):573-580.
40. Price AL, Jones NC, & Pevzner PA (2005) De novo identification of repeat

families in large genomes. Bioinformatics 21 Suppl 1:i351-358.
41. Weinstock GM, *et al*. (2006) Insights into social insects from the genome of the honeybee *Apis mellifera*. Nature 443(7114):931-949.
42. Werren JH, *et al*. (2010) Functional and evolutionary insights from the genomes of three parasitoid *Nasonia* species. Science 327(5963):343-348.
43. Robertson HM (1993) The mariner transposable element is widespread in insects. Nature 362(6417):241-245.
44. Kojima KK & Fujiwara H (2005) Long-term inheritance of the 28S rDNA-specific retrotransposon R2. Mol Biol Evol 22(11):2157-2165.
45. Valles SM, *et al*. (2004) A picorna-like virus from the red imported fire ant, *Solenopsis invicta*: initial discovery, genome sequence, and characterization. Virology 328(1):151-157.
46. Valles SM, Strong CA, & Hashimoto Y (2007) A new positive-strand RNA virus with unique genome characteristics from the red imported fire ant, *Solenopsis invicta*. Virology 365(2):457-463.
47. Genersch E & Aubert M (2010) Emerging and re-emerging viruses of the honey bee (*Apis mellifera* L.). Vet Res 41(6):54.
48. Durbin R, Eddy S, Krogh A, & Mitchison G (1998) Biological sequence analysis: probabilistic models of proteins and nucleic acids (Cambridge University Press).
49. Zdobnov EM & Apweiler R (2001) InterProScan--an integration platform for the signature-recognition methods in InterPro. Bioinformatics 17(9):847-848.
50. Moriya Y, Itoh M, Okuda S, Yoshizawa AC, & Kanehisa M (2007) KAAS: an automatic genome annotation and pathway reconstruction server. Nucleic Acids Research 35:W182-W185.
51. Boyle EI, *et al*. (2004) GO::TermFinder--open source software for accessing Gene Ontology information and finding significantly enriched Gene Ontology terms associated with a list of genes. Bioinformatics 20(18):3710-3715.
52. Ashburner M, *et al*. (2000) Gene ontology: tool for the unification of biology. Nat Genet 25(1):25-29.
53. Li L, Stoeckert CJ, Jr., & Roos DS (2003) OrthoMCL: identification of ortholog groups for eukaryotic genomes. Genome Res 13(9):2178-2189.
54. Tweedie S, *et al*. (2009) FlyBase: enhancing *Drosophila* gene ontology annotations. Nucleic Acids Res 37(Database issue):D555-559.
55. Boore JL (1999) Animal mitochondrial genomes. Nucleic Acids Research 27(8):1767-1780.
56. Crozier RH & Crozier YC (1993) The mitochondrial genome of the honeybee *Apis mellifera* complete sequence and genome organization. Genetics 133(1):97-117.
57. Oliveira DCSG, Raychoudhury R, Lavrov DV, & Werren JH (2008) Rapidly evolving mitochondrial genome and directional selection in mitochondrial genes in the parasitic wasp *Nasonia* (Hymenoptera : Pteromalidae). Molecular Biology and Evolution 25(10):2167-2180.
58. Bernardi G (2000) Isochores and the evolutionary genomics of vertebrates. Gene 241(1):3-17.
59. Lander ES, *et al*. (2001) Initial sequencing and analysis of the human genome. Nature 409(6822):860-921.

60. Elhaik E, Graur D, & Josi K (2010) Identifying compositionally homogeneous and nonhomogeneous domains within the human genome using a novel segmentation algorithm. Nucleic Acids Research in press.
61. Cohen N, Dagan T, Stone L, & Graur D (2005) GC composition of the human genome: in search of isochores. Mol Biol Evol 22(5):1260-1272.
62. Elhaik E, Graur D, & Josic K (2010) Comparative testing of DNA segmentation algorithms using benchmark simulations. Mol Biol Evol 27(5):1015-1024.
63. Clauset A, Shalizi CR, & Newman MEJ (2007) Power-law distributions in empirical data.).
64. Sokal RR & Rohlf FJ (1995) Biometry: the principles and practice of statistics in biological research (W. H. Freeman and Company, New York) 3rd edition Ed.
65. Griffiths-Jones S (2004) The microRNA Registry. Nucleic Acids Res 32(Database issue):D109-111.
66. Griffiths-Jones S, Grocock RJ, van Dongen S, Bateman A, & Enright AJ (2006) miRBase: microRNA sequences, targets and gene nomenclature. Nucleic Acids Res 34(Database issue):D140-144.
67. Griffiths-Jones S, Saini HK, van Dongen S, & Enright AJ (2008) miRBase: tools for microRNA genomics. Nucleic Acids Res 36(Database issue):D154-158.
68. Pearson WR (1990) Rapid and sensitive sequence comparison with FASTP and FASTA. Methods Enzymol 183:63-98.
69. Larkin MA, *et al*. (2007) Clustal W and clustal X version 2.0. Bioinformatics 23(21):2947-2948.
70. Hofacker IL, *et al*. (1994) Fast folding and comparison of RNA secondary structures. Monatshefte f. Chemie 125:167-188.
71. Weaver DB, *et al*. (2007) Computational and transcriptional evidence for microRNAs in the honey bee genome. Genome Biol 8(6):R97.
72. Tran T, Havlak P, & Miller J (2006) MicroRNA enrichment among short 'ultraconserved' sequences in insects. Nucleic Acids Res 34(9):e65.
73. Hölldobler B & Wilson EO (1990) The ants (Belknap Press, Cambridge, Massachusetts) p 733.
74. Moreau CS, Bell CD, Vila R, Archibald SB, & Pierce NE (2006) Phylogeny of the ants: Diversification in the age of angiosperms. Science 312(5770):101-104.
75. Brady SG, Schultz TR, Fisher BL, & Ward PS (2006) Evaluating alternative hypotheses for the early evolution and diversification of ants. Proceedings of the National Academy of Sciences, USA 103:18172-18177.
76. Abouheif E & Wray GA (2002) Evolution of the gene network underlying wing polyphenism in ants. Science 297(5579):249-252.
77. Khila A & Abouheif E (2008) Reproductive constraint is a developmental mechanism that maintains social harmony in advanced ant societies. Proceedings of the National Academy of Sciences of the United States of America 105(46):17884-17889.
78. Tsutsui ND & Suarez AV (2003) The colony structure and population biology of invasive ants. Conservation Biology 17(1):48-58.
79. Passera L, Keller L, & Suzzoni JP (1988) Control of brood male production in the Argentine ant *Iridomyrmex humilis* (Mayr). Insectes Sociaux 35(1):19-33.
80. Elango N, Hunt BG, Goodisman MAD, & Yi SV (2009) DNA methylation is

widespread and associated with differential gene expression in castes of the honeybee, *Apis mellifera*. Proceedings of the National Academy of Sciences of the United States of America 106(27):11206-11211.
81. Sameshima S, Miura T, & Matsumoto T (2004) Wing disc development during caste differentiation in the ant Pheidole megacephala (Hymenoptera: Formicidae). Evolution and Development 6:336-341.
82. Gibson MC & Perrimon N (2005) Extrusion and death of DPP/BMP-compromised epithelial cells in the developing *Drosophila* wing. Science 307(5716):1785-1789.
83. Klattenhoff C, *et al*. (2007) *Drosophila* rasiRNA pathway mutations disrupt embryonic axis specification through activation of an ATR/Chk2 DNA damage response. Dev Cell 12(1):45-55.
84. Robertson HM, Gadau J, & Wanner KW (2010) The insect chemoreceptor superfamily of the parasitoid jewel wasp *Nasonia vitripennis*. Insect Molecular Biology 19:121-136.
85. Robertson HM, Warr CG, & Carlson JR (2003) Molecular evolution of the insect chemoreceptor gene superfamily in *Drosophila melanogaster*. Proceedings of the National Academy of Sciences of the United States of America 100:14537-14542.
86. Kent LB, Walden KK, & Robertson HM (2008) The Gr family of candidate gustatory and olfactory receptors in the yellow-fever mosquito Aedes aegypti. Chem Senses 33(1):79-93.
87. Foret S & Maleszka R (2006) Function and evolution of a gene family encoding odorant binding-like proteins in a social insect, the honey bee (Apis mellifera). Genome Res 16(11):1404-1413.
88. Gotzek D & Ross KG (2009) Current status of a model system: the gene Gp-9 and its association with social organization in fire ants. PLoS One 4(11):e7713.
89. Su CY, Menuz K, & Carlson JR (2009) Olfactory perception: receptors, cells, and circuits. Cell 139(1):45-59.
90. Touhara K & Vosshall LB (2009) Sensing odorants and pheromones with chemosensory receptors. Annu Rev Physiol 71:307-332.
91. Jones WD, Cayirlioglu P, Kadow IG, & Vosshall LB (2007) Two chemosensory receptors together mediate carbon dioxide detection in Drosophila. Nature 445(7123):86-90.
92. Kwon JY, Dahanukar A, Weiss LA, & Carlson JR (2007) The molecular basis of CO2 reception in Drosophila. Proc Natl Acad Sci U S A 104(9):3574-3578.
93. Lu T, *et al*. (2007) Odor coding in the maxillary palp of the malaria vector mosquito Anopheles gambiae. Curr Biol 17(18):1533-1544.
94. Benton R, Vannice KS, Gomez-Diaz C, & Vosshall LB (2009) Variant ionotropic glutamate receptors as chemosensory receptors in *Drosophila*. Cell 136(1):149-162.
95. Kirkness EF, *et al*. (2010) Genome sequences of the human body louse and its primary endosymbiont provide insights into the permanent parasitic lifestyle. Proc Natl Acad Sci U S A 107(27):12168-12173.
96. Nozawa M & Nei M (2007) Evolutionary dynamics of olfactory receptor genes in Drosophila species. Proc Natl Acad Sci U S A 104(17):7122-7127.
97. Hill CA, *et al*. (2002) G protein coupled receptors in *Anopheles gambiae*. Science

298(5591):176-178.
98. Bohbot J, *et al*. (2007) Molecular characterization of the Aedes aegypti odorant receptor gene family. Insect Mol Biol 16(5):525-537.
99. Wanner KW, *et al*. (2007) Female-biased expression of odourant receptor genes in the adult antennae of the silkworm, Bombyx mori. Insect Mol Biol 16(1):107-119.
100. Tanaka K, *et al*. (2009) Highly selective tuning of a silkworm olfactory receptor to a key mulberry leaf volatile. Curr Biol 19(11):881-890.
101. Smadja C, Shi P, Butlin RK, & Robertson HM (2009) Large gene family expansions and adaptive evolution for odorant and gustatory receptors in the pea aphid, Acyrthosiphon pisum. Mol Biol Evol 26(9):2073-2086.
102. Engsontia P, *et al*. (2008) The red flour beetle's large nose: an expanded odorant receptor gene family in Tribolium castaneum. Insect Biochem Mol Biol 38(4):387-397.
103. Robertson HM & Wanner KW (2006) The chemoreceptor superfamily in the honey bee, *Apis mellifera*: Expansion of the odorant, but not gustatory, receptor family. Genome Res 16(11):1395-1403.
104. Kelber C, Rossler W, & Kleineidam CJ (2006) Multiple olfactory receptor neurons and their axonal projections in the antennal lobe of the honeybee Apis mellifera. J Comp Neurol 496(3):395-405.
105. Nakanishi A, Nishino H, Watanabe H, Yokohari F, & Nishikawa M (2010) Sex-specific antennal sensory system in the ant Camponotus japonicus: glomerular organizations of antennal lobes. J Comp Neurol 518(12):2186-2201.
106. Swofford DL (2003) PAUP*. Phylogenetic Analysis Using Parsimony (*and other methods). Version 4. (Sinauer Associates, Sunderland, Massachusetts).
107. Schmidt HA, Strimmer K, Vingron M, & von Haeseler A (2002) TREE-PUZZLE: maximum likelihood phylogenetic analysis using quartets and parallel computing. Bioinformatics 18(3):502-504.
108. Wanner KW, *et al*. (2007) A honey bee odorant receptor for the queen substance 9-oxo-2-decenoic acid. Proc Natl Acad Sci U S A 104(36):14383-14388.
109. Ozaki M, *et al*. (2005) Ant nestmate and non-nestmate discrimination by a chemosensory sensillum. Science 309(5732):311-314.
110. Brandt M, van Wilgenburg E, Sulc R, Shea KJ, & Tsutsui ND (2009) The scent of supercolonies: the discovery, synthesis and behavioural verification of ant colony recognition cues. Bmc Biology 7:-.
111. Bray S & Amrein H (2003) A putative Drosophila pheromone receptor expressed in male-specific taste neurons is required for efficient courtship. Neuron 39(6):1019-1029.
112. Ebbs ML & Amrein H (2007) Taste and pheromone perception in the fruit fly Drosophila melanogaster. Pflugers Arch 454(5):735-747.
113. Croset V, *et al*. (2010) Ancient protostome origin of chemosensory ionotropic glutamate receptors and the evolution of insect taste and olfaction. Plos Genet 6(8):e1001064.
114. Tsutsui ND (2004) Scents of self: The expression component of self/nonself recognition systems. Ann Zool Fenn 41(6):713-727.
115. Payne CM, Tillberg CV, & Suarez AV (2004) Recognition systems and biological

invasions. Ann Zool Fenn 41(6):843-858.
116. Hefetz A, Errard C, Chambris A, & LeNegrate A (1996) Postpharyngeal gland secretion as a modifier of aggressive behavior in the myrmicine ant *Manica rubida*. Journal of Insect Behavior 9(5):709-717.
117. Torres CW, Brandt M, & Tsutsui ND (2007) The role of cuticular hydrocarbons as chemical cues for nestmate recognition in the invasive Argentine ant (*Linepithema humile*). Insectes Sociaux 54(4):363-373.
118. Lahav S, Soroker V, Hefetz A, & Vander Meer RK (1999) Direct behavioral evidence for hydrocarbons as ant recognition discriminators. Naturwissenschaften 86(5):246-249.
119. Carlin NF & Hölldobler B (1986) The kin recognition system of carpenter ants (*Camponotus* spp.) I. Hierarchical cues in small colonies. Behavioral Ecology and Sociobiology 19:123-134.
120. Martin S & Drijfhout F (2009) A review of ant cuticular hydrocarbons. Journal of Chemical Ecology 35(10):1151-1161.
121. Gleason JM, Jallon JM, Rouault JD, & Ritchie MG (2005) Quantitative trait loci for cuticular hydrocarbons associated with sexual isolation between *Drosophila simulans* and *D. sechellia*. Genetics 171(4):1789-1798.
122. Dallerac R, *et al*. (2000) A Delta 9 desaturase gene with a different substrate specificity is responsible for the cuticular diene hydrocarbon polymorphism in *Drosophila melanogaster*. Proceedings of the National Academy of Sciences of the United States of America 97(17):9449-9454.
123. Lemieux C, Otis C, & Turmel M (2000) Ancestral chloroplast genome in Mesostigma viride reveals an early branch of green plant evolution. Nature 403:649-652.
124. Legendre A, Miao XX, Da Lage JL, & Wicker-Thomas C (2008) Evolution of a desaturase involved in female pheromonal cuticular hydrocarbon biosynthesis and courtship behavior in *Drosophila*. Insect Biochemistry and Molecular Biology 38(2):244-255.
125. Liang D (2001) Hydrocarbon-released nestmate aggression in the Argentine ant, *Linepithema humile*, following encounters with insect prey. Comparative Biochemistry and Physiology Part B 129:871-882.
126. Castresana J (2000) Selection of conserved blocks from multiple alignments for their use in phylogenetic analysis. Mol Biol Evol 17(4):540-552.
127. Abascal F, Zardoya R, & Posada D (2005) ProtTest: selection of best-fit models of protein evolution. Bioinformatics 21(9):2104-2105.
128. Stamatakis A (2006) RAxML-VI-HPC: maximum likelihood-based phylogenetic analyses with thousands of taxa and mixed models. Bioinformatics 22(21):2688-2690.
129. Thompson JD, Higgins DG, & Gibson TJ (1994) CLUSTAL W: improving the sensitivity of progressive multiple sequence alignment through sequence weighting, position-specific gap penalties and weight matrix choice. Nucleic Acids Res 22(22):4673-4680.
130. Hughes CL & Kaufman TC (2002) Hox genes and the evolution of the arthropod body plan. Evol Dev 4(6):459-499.
131. Lemons D & McGinnis W (2006) Genomic evolution of Hox gene clusters.

Science 313(5795):1918-1922.
132. Dearden PK, *et al*. (2006) Patterns of conservation and change in honey bee developmental genes. Genome Res 16(11):1376-1384.
133. Evans JD, *et al*. (2006) Immune pathways and defence mechanisms in honey bees *Apis mellifera*. Insect Molecular Biology 15(5):645-656.
134. Christophides GK, *et al*. (2002) Immunity-related genes and gene families in *Anopheles gambiae*. Science 298(5591):159-165.
135. Sackton TB, *et al*. (2007) Dynamic evolution of the innate immune system in *Drosophila*. Nat Genet 39(12):1461-1468.
136. Cremer S, Armitage SAO, & Schmid-Hempel P (2007) Social immunity. Current Biology 17(16):R693-R702.
137. Dukas R (2008) Evolutionary biology of insect learning. Annual Review of Entomology 53:145-160.
138. Skoulakis EMC & Grammenoudi S (2006) Dunces and da Vincis: The genetics of learning and memory in *Drosophila*. Cell Mol Life Sci 63(9):975-988.
139. Liu X & Davis RL (2006) Insect olfactory memory in time and space. Curr Opin Neurobiol 16(6):679-685.
140. Waddell S & Quinn WG (2001) Flies, genes, and learning. Annu Rev Neurosci 24:1283-1309.
141. Schwaerzel M, *et al*. (2003) Dopamine and octopamine differentiate between aversive and appetitive olfactory memories in *Drosophila*. J Neurosci 23(33):10495-10502.
142. Tempel BL, Livingstone MS, & Quinn WG (1984) Mutations in the dopa decarboxylase gene affect learning in *Drosophila*. P Natl Acad Sci-Biol 81(11):3577-3581.
143. Grotewiel MS, Beck CDO, Wu KH, Zhu XR, & Davis RL (1998) Integrin-mediated short-term memory in *Drosophila*. Nature 391(6666):455-460.
144. Cheng YZ, *et al*. (2001) *Drosophila fasciclin II* is required for the formation of odor memories and for normal sensitivity to alcohol. Cell 105(6):757-768.
145. Dudai Y, Jan YN, Byers D, Quinn WG, & Benzer S (1976) *Dunce*, a mutant of *Drosophila* deficient in learning. Proceedings of the National Academy of Sciences of the United States of America 73(5):1684-1688.
146. Acevespina EO, *et al*. (1983) Learning and memory in *Drosophila*, studied with mutants. Cold Spring Harb Sym 48:831-840.
147. Griffith LC, *et al*. (1993) Inhibition of calcium calmodulin-dependent protein-kinase in *Drosophila* disrupts behavioral plasticity. Neuron 10(3):501-509.
148. Joiner MLA & Griffith LC (1997) CaM kinase II and visual input modulate memory formation in the neuronal circuit controlling courtship conditioning. J Neurosci 17(23):9384-9391.
149. Mehren JE & Griffith LC (2004) Calcium-independent calcium/calmodulin-dependent protein kinase II in the adult *Drosophila* CNS enhances the training of pheromonal cues. J Neurosci 24(47):10584-10593.
150. Dubnau J, *et al*. (2003) The staufen/pumilio pathway is involved in *Drosophila* long-term memory. Current Biology 13(4):286-296.
151. Thomas ML, Payne-Makrisa CM, Suarez AV, Tsutsui ND, & Holway DA (2006) When supercolonies collide: territorial aggression in an invasive and unicolonial

social insect. Molecular Ecology 15(14):4303-4315.
152. Tsutsui ND, Suarez AV, & Grosberg RK (2003) Genetic diversity, asymmetrical aggression, and recognition in a widespread invasive species. Proceedings of the National Academy of Sciences of the United States of America 100:1078-1083.
153. Holway DA, Suarez AV, & Case TJ (1998) Loss of intraspecific aggression in the success of a widespread invasive social insect. Science (Washington D C) 283(5390):949-952.
154. Nelson RJ (2006) Biology of Aggression (Oxford University Press, New York).
155. Edwards AC & Mackay TF (2009) Quantitative trait loci for aggressive behavior in *Drosophila melanogaster*. Genetics 182(3):889-897.
156. Dierick HA & Greenspan RJ (2006) Molecular analysis of flies selected for aggressive behavior. Nat Genet 38(9):1023-1031.
157. Edwards AC, *et al*. (2009) A transcriptional network associated with natural variation in *Drosophila* aggressive behavior. Genome Biol 10(7):R76.
158. Edwards AC, Zwarts L, Yamamoto A, Callaerts P, & Mackay TF (2009) Mutations in many genes affect aggressive behavior in *Drosophila melanogaster*. BMC Biol 7:29.
159. Alaux C, *et al*. (2009) Honey bee aggression supports a link between gene regulation and behavioral evolution. Proc Natl Acad Sci U S A 106(36):15400-15405.
160. Edwards AC, Rollmann SM, Morgan TJ, & Mackay TFC (2006) Quantitative genomics of aggressive behavior in *Drosophila melanogaster*. Plos Genet 2(9):1386-1395.
161. Barron AB, Maleszka R, Helliwell PG, & Robinson GE (2009) Effects of cocaine on honey bee dance behaviour. J Exp Biol 212(Pt 2):163-168.
162. Claeys I, *et al*. (2002) Insulin-related peptides and their conserved signal transduction pathway. Peptides 23(4):807-816.
163. Wheeler DE, Buck N, & Evans JD (2006) Expression of insulin pathway genes during the period of caste determination in the honey bee, *Apis mellifera*. Insect Molecular Biology 15(5):597-602.
164. Evans JD & Wheeler DE (1999) Differential gene expression between developing queens and workers in the honey bee, *Apis mellifera*. Proceedings of the National Academy of Sciences of the United States of America 96(10):5575-5580.
165. Patel A, *et al*. (2007) The making of a queen: TOR pathway Is a key player in diphenic caste development. Plos One 2(6):-.
166. de Azevedo SV & Hartfelder K (2008) The insulin signaling pathway in honey bee (*Apis mellifera*) caste development - differential expression of insulin-like peptides and insulin receptors in queen and worker larvae. J Insect Physiol 54(6):1064-1071.
167. Smith CR, Toth AL, Suarez AV, & Robinson GE (2008) Genetic and genomic analyses of the division of labour in insect societies. Nat Rev Genet 9(10):735-748.
168. Smith CR (2007) Energy use and allocation in the Florida harvester ant, *Pogonomyrmex badius*: are stored seeds a buffer? Behavioral Ecology and Sociobiology 61(9):1479-1487.
169. Tillberg CV, Holway DA, Lebrun EG, & Suarez AV (2007) Trophic ecology of

invasive Argentine ants in their native and introduced ranges. Proc Natl Acad Sci U S A 104(52):20856-20861.
170. Chenna R, *et al*. (2003) Multiple sequence alignment with the Clustal series of programs. Nucleic Acids Res 31(13):3497-3500.
171. Rozen S & Skaleysky HJ (2000) Primer3 on the WWW for general users and for biologist programmers. Bioinformatics Methods and Protocols: Methods in Molecular Biology, eds Krawetz S & Misener S (Humana Press, Totowa, NJ), pp 365-386.